INTERACTIONS OF PYRROLIDINYL PEPTIDE NUCLEIC ACID WITH

OLIGODEOXYGUANOSINE AND BIOSENSING APPLICATIONS

Mr. Chayan Charoenpakdee

จุฬาลงกรณ์มหาวิทยาลัย

CHULALONGKORN UNIVERSITY

A Dissertation Submitted in Partial Fulfillment of the Requirements

for the Degree of Doctor of Philosophy in Chemistry

Department of Chemistry

FACULTY OF SCIENCE

Chulalongkorn University

Academic Year 2019

อันตรกิริยาของพิร์โรลิดินิลเพปไทด์นิวคลีอิกแอซิดกับออลิโกดีออกซีกัวโนซีน
และการประยุกต์ในการรับรู้ทางชีวภาพ

นายชญัญ เจริญภักดี

จุฬาลงกรณ์มหาวิทยาลัย
CHULALONGKORN UNIVERSITY

วิทยานิพนธ์นี้เป็นส่วนหนึ่งของการศึกษาตามหลักสูตรปริญญาวิทยาศาสตรดุษฎีบัณฑิต
สาขาวิชาเคมี ภาควิชาเคมี
คณะวิทยาศาสตร์ จุฬาลงกรณ์มหาวิทยาลัย
ปีการศึกษา 2562

Thesis Title	INTERACTIONS OF PYRROLIDINYL PEPTIDE NUCLEIC ACID
	WITH OLIGODEOXYGUANOSINE AND BIOSENSING
	APPLICATIONS
By	Mr. Chayan Charoenpakdee
Field of Study	Chemistry
Thesis Advisor	Professor TIRAYUT VILAIVAN, Ph.D.

Accepted by the FACULTY OF SCIENCE, Chulalongkorn University in Partial Fulfillment of the Requirement for the Doctor of Philosophy

.... Dean of the FACULTY OF SCIENCE

(Professor POLKIT SANGVANICH, Ph.D.)

DISSERTATION COMMITTEE

.... Chairman

(Associate Professor VUDHICHAI PARASUK, Ph.D.)

.... Thesis Advisor

(Professor TIRAYUT VILAIVAN, Ph.D.)

.... Examiner

(Professor THAWATCHAI TUNTULANI, Ph.D.)

.... Examiner

(Associate Professor VORAVEE HOVEN, Ph.D.)

.... External Examiner

(Assistant Professor Chittanon Buranachai, Ph.D.)

ชญัญ เจริญภักดี : อันตรกิริยาของพิร์โรลิดินิลเพปไทด์นิวคลีอิกแอซิดกับออลิโกดีออกซีกัวโนซีนและการประยุกต์ในการรับรู้ทางชีวภาพ. (INTERACTIONS OF PYRROLIDINYL PEPTIDE NUCLEIC ACID WITH OLIGODEOXYGUANOSINE AND BIOSENSING APPLICATIONS) อ.ที่ปรึกษาหลัก : ศ. ดร.ธีรยุทธ วิไลวัลย์

พิร์โรลิดินิลเพปไทด์นิวคลีอิกแอซิดเป็นสารเลียนแบบดีเอ็นเอที่ประกอบด้วยโพรลีน-2-อะมิโนไซโคลเพนเทนคาร์บอกซิลิกแอซิดเป็นโครงสร้างหลัก (เอซีพีซีพีเอ็นเอ, acpcPNA) ที่แสดงการจับยึดกับดีเอ็นเอได้อย่างแข็งแรงและจำเพาะเจาะจงกว่าดีเอ็นเอและพีเอ็นเอทั่วไป งานวิจัยนี้มุ่งเน้นพัฒนาระบบการตรวจวัดดีเอ็นเอหรือกลุ่มเป้าหมายด้วยการตรวจวัดเชิงแสงโดยอาศัยเอซีพีซีพีเอ็นเอโพรบ งานในส่วนแรกเป็นการใช้กราฟีนออกไซด์เป็นตัวระงับสัญญาณการเรืองแสง โดยพบว่ากราฟีนออกไซด์สามารถดับสัญญาณของฉลากฟลูออเรสซีนบนสายของพีเอ็นเอได้ และเมื่อเติมดีเอ็นเอเป้าหมายลงไปจะได้สัญญาณกลับคืนมา นอกจากนี้ยังได้นำระบบเอซีพีซีพีเอ็นเอ-กราฟีนออกไซด์ไปตรวจวัดการจับกันระหว่างพีเอ็นเอและดีเอ็นสายคู่และนำไปประยุกต์ใช้ในการตรวจวัดดีเอ็นเอแบบมัลพิเพล็กซ์ด้วยโพรบเรืองแสงหลากสี งานในส่วนที่สองได้แสดงการระงับสัญญาณการเรืองแสงของพีเอ็นเอโพรบที่ติดฉลากสารเรืองแสงด้วยออลิโกดีออกซีกัวโนซีน โดยอันตรกิริยาทางไฟฟ้าสถิตระหว่างประจุบวกบนสายพีเอ็นเอและประจุลบบนสายดีเอ็นเอที่แข็งแรงทำให้เกิดการดับสัญญาณผ่านกระบวนการถ่ายโอนอิเล็กตรอนที่กระตุ้นด้วยแสง การเติมดีเอ็นเอเป้าหมายทำให้เกิดการกลับคืนสัญญาณอย่างรวดเร็วและสมบูรณ์โดยไม่มีการหลุดออกของออลิโกดีออกซีกัวโนซีนจากพีเอ็นเอโพรบ ระบบที่พัฒนาขึ้นมานี้มีความจำเพาะเจาะจงในการตรวจวัดดีเอ็นเอเป้าหมายในระดับที่บ่งบอกความแตกต่างของลำดับเบสที่ผิดไปเพียงตำแหน่งเดียวได้และสามารถนำหลักการไปประยุกต์ใช้กับดีเอ็นเอที่มีลำดับเบสที่หลากหลาย นอกจากนี้สามารถนำระบบเอซีพีซีพีเอ็นเอ-โอลิโกดีออกซีกัวโนซีนนี้ไปประยุกต์ใช้สำหรับการตรวจวัดดีเอ็นเอแบบมัลติเพล็กซ์โดยใช้โพรบเรืองแสงหลากสี ตรวจวัด Hg^{2+} และติดตามปฏิกิริยาการเชื่อมต่อกันระหว่างพีเอ็นเอสองสาย งานในส่วนสุดท้ายได้ศึกษาความเป็นไปได้ในการพัฒนาระบบตรวจวัดดีเอ็นเอใหม่โดยอาศัยระบบเอซีพีซีพีเอ็นเอ-ออลิโกดีออกซีกัวโนซีน โดยอาศัยความสามารถในการเป็นดีเอ็นเอไซม์ ผลการทดลองเบื้องต้นแสดงให้เห็นว่าสามารถพัฒนาการตรวจดีเอ็นเอเชิงสีโดยใช้หลักการของโพรบที่ถูกแทนที่ได้ (strand displacement probe) กล่าวโดยสรุปคือการจับยึดระหว่างดีเอ็นเอที่ถูกดัดแปรด้วยออลิโกดีออกซีกัวโนซีนกับพีเอ็นเอโพรบจะทำลายความสามารถในการเลียนแบบเอนไซม์เพอร์ออกซิเดสของมันซึ่งความสามารถนี้จะกลับคืนมาเมื่อเติมดีเอ็นเอเป้าหมายเพื่อไปแทนที่ดีเอ็นเอไซม์

สาขาวิชา	เคมี	ลายมือชื่อนิสิต ....
ปีการศึกษา	2562	ลายมือชื่อ อ.ที่ปรึกษาหลัก ....

5671932523 : MAJOR CHEMISTRY

KEYWORD: peptide nucleic acid, oligodeoxyguanosine, DNA sensing, fluorescence, colorimetric, DNAzyme

Chayan Charoenpakdee : INTERACTIONS OF PYRROLIDINYL PEPTIDE NUCLEIC ACID WITH OLIGODEOXYGUANOSINE AND BIOSENSING APPLICATIONS. Advisor: Prof. TIRAYUT VILAIVAN, Ph.D.

Pyrrolidinyl peptide nucleic acid is a DNA mimic consisting of proline-2-aminocyclopentane carboxylic acid (acpcPNA) as a core structure. It binds to DNA to form a more stable hybrid while showing greater selectivity and affinity than the conventional DNA and PNA probes. In this study, we aim to develop novel DNA sensing systems based on the acpcPNA probe. In the first part, graphene oxide (GO) was used as an external quencher which could effectively quench the fluorescein-labeled PNA probe. A remarkable fluorescence restoration was achieved after the addition of a complementary DNA target. This acpcPNA-GO combination was successfully used to monitor the strand-invasion of the duplex DNA by acpcPNA, and to detect two DNA targets in a multiplex, multicolor detection. In the second part, we demonstrated the effective quenching of fluorescently labeled acpcPNA by using oligodeoxyguanosine as an external quencher. The electrostatic interaction between the positively-charged modification on the PNA probe and the phosphate backbone of the oligodeoxyguanosine (dGX) resulted in a strong association, resulting in an effective quenching of the fluorescence by photoinduced electron transfer. The addition of the complementary DNA strand rapidly and completely restored the fluorescence without detaching the dGX from the PNA probe. This sensing system could detect the complementary DNA target with single-base mismatch specificity and could be applied to detect various other DNA sequences. The acpcPNA-dGX platform has been used in the multiplex detection of two DNA sequences and to detect Hg^{2+} ion as well as to monitor the PNA ligation. In the last part, a new DNA sensing system based on the combination of acpcPNA-dGX in the context of DNAzyme was explored. Preliminary studies revealed a promising result from the colorimetric DNA detection employing a strand displacement probe strategy. In short, binding of the dGX-modified DNA strand to PNA diminished its peroxidase activity, which could be restored when the DNA target was added to displace the DNAzyme.

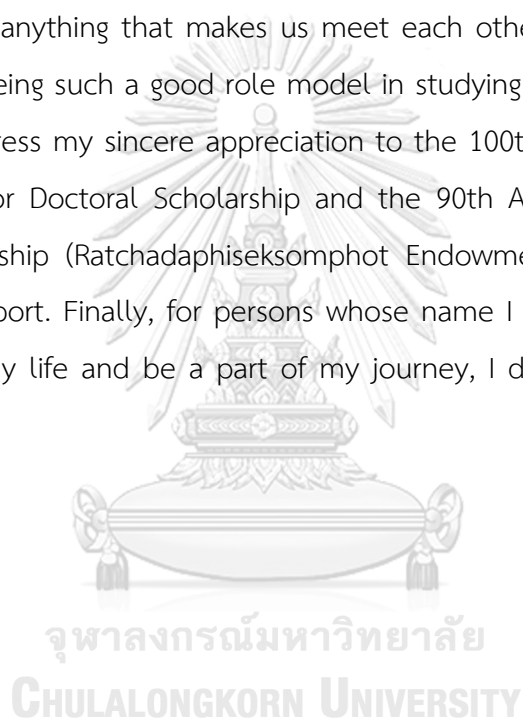|		
Field of Study:	Chemistry	Student's Signature ....
Academic Year:	2019	Advisor's Signature ....

ACKNOWLEDGEMENTS

Eventually, my PhD journey has come to an end. It is such a long, long journey, but everything is truly worth remembering.

First and foremost, I would like to express my sincere and heartfelt gratitude to Prof. Dr. Tirayut Vilaivan for everything he has done for me during my years at Chulalongkorn University as a PhD student under his supervision. Ajarn. Tirayut does not only academically supervise me, but also equips me with all necessary skills needed for my future career. Apart from my usual lab routines, Ajarn Tirayut also gives me chances to do various works that might not be related to my main thesis much but they are proved to be very beneficial for me since they tremendously help me improve my laboratory skills and gain experience in other fields of chemistry. Ajarn Tirayut's instructional and supervising methods are not like others. He is direct and doesn't give sugarcoated comments. I have to admit that his words and comments cut deep and sometimes bruise my feelings, but now I truly understand that those comments are not to harm but build me to be a better person who is worth the PhD degree, which I really do appreciate it. Thank you so much.

Secondly, I would like to thank my family: my mom, dad, grandma, aunties, and sister for all their unceasing mental supports and encouragement. Although they all live far away from me, I could sense their love and care around me and I am certain that they are with me every step I make. Whenever I am thrown to the ground, they are people who grab my hands and pull me up. There was time when I encountered difficulties and really wanted to give up, but my family is the thing that make me move forward and keeps me on this path. So, I would like to devote this dissertation and all the achievements I have received to be a beautiful present for them. An also another special one in my family, I would like to thank you from the bottom of my heart "my Sound" who is my everything and a part of my life. The guy who supports me in every possible way, encourages, and waits to see my success in this journey.

Well, I cannot forget to thank all TVLab senior members: P Kung, P Lin, P Beer, P Terk, P Wor, P Tew, P Mook, P Dew, P Tor, P Ton and P. A for devoting time to teach

me laboratory skills since I was in an undergraduate level and also for all useful suggestions and comments on reactions and life. In addition, my love goes to current TVLab members: Wa, Pong, Yong, NutNoi, Dear, Mints, and N' Duang. We have been through thick and thin together. You guys make my life in this lab memorable. The memories we have together will be with me for long. Also, I would like to thank you Peggy, my lovely and lively German friend. You are the one who inspires me and keep the fire inside my alight. I do appreciate your care and love you always send to me. Your words "everyone can cry, and then rise like a phoenix" are what keep me motivated. Thank anything that makes us meet each other. I would like to thank Yui and Michael for being such a good role model in studying for me. Last but not least, I would like to express my sincere appreciation to the 100th Anniversary Chulalongkorn University Fund for Doctoral Scholarship and the 90th Anniversary of Chulalongkorn University Scholarship (Ratchadaphiseksomphot Endowment Fund) for providing me with financial support. Finally, for persons whose name I forget to mention here who may come into my life and be a part of my journey, I don't know what to say, but thank you.

Chayan Charoenpakdee

TABLE OF CONTENTS

LIST OF FIGURES

จุฬาลงกรณ์มหาวิทยาลัย
CHULALONGKORN UNIVERSITY

LIST OF TABLES

LIST OF ABBREVIATIONS AND SYMBOLS

δ	chemical shift
μL	microliter
μmol	micromole
A	adenine
A^{Bz}	N^6-benzoyladenine
Ac	acetyl
Ac_2O	acetic anhydride
Boc	*tert*-butoxycarbonyl
Bz	benzoyl
c	concentration
C	cytosine
calcd	calculated
C^{Bz}	N^4-benzoylcytosine
CCA	α-cyano-4-hydroxy cinnamic acid
$CDCl_3$	deuterated chloroform
DMSO-d6	deuterated dimethyl sulfoxide
d	doublet
DBU	1,8-diazabicyclo[5.4.0]undec-7-ene
DCM	dichloromethane
dG_n	oligodeoxyguanosine
DIEA	diisopropylethylamine
DMF	*N,N'*-dimethylformamide
DNA	deoxyribonucleic acid
Dpm	diphenylmethyl
ds	double-stranded
equiv	equivalent (s)
Flu	5(6)-carboxyfluorescein
Fmoc	9*H*-fluoren-9-ylmethoxycarbonyl

FmocOSu	9*H*-fluoren-9-ylmethyl succinimidyl carbonate
FRET	Förster (fluorescence) resonance energy transfer
g	gram
G	guanine
GO	graphene oxide
h	hour
HATU	*O*-(7-azabenzotriazol-1-yl)-*N,N,N',N'*-tetramethyluronium hexafluorophosphate
HOAt	1-hydroxy-7-azabenzotriazole
HPLC	high performance liquid chromatography
Hz	hertz
J	coupling constant
K	lysine
m	multiplet
M	molar
MALDI-TOF	matrix-assisted laser desorption/ionization-time of flight
MeCN	acetonitrile
MeOH	methanol
mg	milligram
MHz	megahertz
min	minute
mL	milliliter
mM	millimolar
mmol	millimole
MS	mass spectrometry
m/z	mass to charge ratio
nm	nanometer
nM	nanomolar
NMR	nuclear magnetic resonance
°C	degree Celsius
PET	photo-induced electron transfer

Pfp	pentafluorophenyl
Ph	phenyl
Py	pyrene
PNA	peptide nucleic acid or polyamide nucleic acid
R_f	retention factor
RNA	ribonucleic acid
s	singlet
SPPS	solid phase peptide synthesis
ss	single-stranded
t	triplet
T	thymine
^{t}BuOH	*tert*-butanol
TBE	tris-borate-EDTA
TEMED	*N,N,N',N'*-Tetramethylethylenediamine
TFA	trifluoroacetic acid
THF	tetrahydrofuran
TLC	thin layer chromatography
TMR	5(6)-carboxytetramethylrhodamine
T_m	melting temperature
t_R	retention time
U	uracil or uridine
UV	ultraviolet

CHAPTER 1

INTRODUCTION

1.1 Nucleic acid biosensors

Nucleic acid sensors are one of the most widely used bioanalytical tools which have been continuously developed over the past decades since they can be applied in various fields. As opposed to the more resource-demanding DNA sequencing, these sensors offer a rapid, sensitive, and low-cost alternative so they are employed to diagnose genetic diseases, investigate biological processes, analyze samples in forensic science, detect metal in live cells, etc.[1-4] In general, a biosensor consists of a recognition element and a signal transducer (**Figure 1.1**).[5] For nucleic acid biosensors, an oligonucleotide probe is frequently used as the recognition element. The probe can hybridize with its target (either DNA or RNA) with a high binding affinity and specificity via the specific pairing between two complementary nucleobases (A-T, C-G) according to the Watson-Crick base pairing rules. The signal transduction element will then convert the binding interaction between the probe and the nucleic acid target into a measurable signals such as color, fluorescence, or electrical signals.
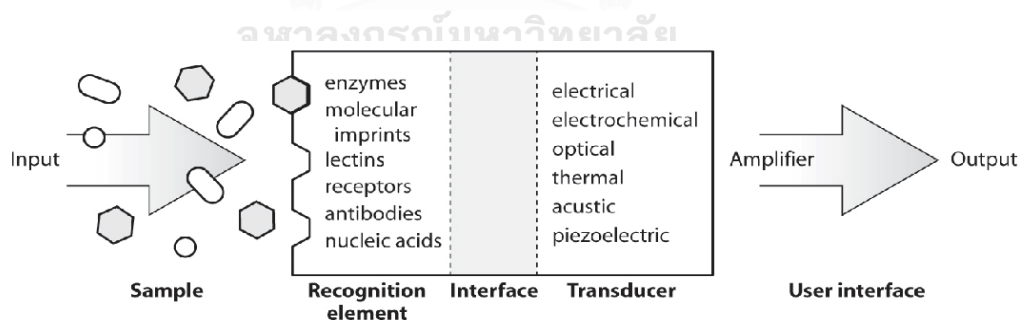
Figure 1.1 Concept of biosensors[6]

1.2 Fluorescent probes for nucleic acid sensing

Fluorescent technique is one of the powerful and effective signal transducers which can report the interaction between the recognition element and its target through the light emission of the fluorescent moiety or a "fluorophore". The use of

fluorescence technique can yield qualitative and quantitative information about biological and physiological properties of the nucleic biological samples.[7] Fluorescently labelled oligonucleotide probes are widely used in the investigation of a nucleic acid sequence.[8] The desirable fluorescent probe should selectively respond to the nucleic acid target in focus by giving a fluorescence change in a rapid, sensitive, and low-cost fashion. In addition, the ideal probe should be able to change the fluorescent signal in a signal-on mode, whereby the probe is non-fluorescence (turn-off) in the free state and strongly fluoresces (turn-on) in the presence of the correct nucleic acid target. Traditional fluorescent oligonucleotide probes[9] are designed to carry fluorophore and a quencher, or multiple fluorophores. The probes must be designed so that the interaction between the fluorophores or the fluorophore and the quencher such as fluorescence resonance energy transfer (FRET),[10] photo-induced electron transfer (PET),[11, 12] are modulated by the binding between the probe and the target.

Most fluorescent oligonucleotide probes contain a fluorophore and a quencher pair. These two components can be present in the same probe such as in molecular beacons.[13, 14] They can also exist as separated entities consisting of a fluorescently labeled oligonucleotide probe and an external quencher such as gold nanoparticles,[15, 16] graphene oxide,[17-20] nanoceria,[21] or perylene diimide.[22, 23]
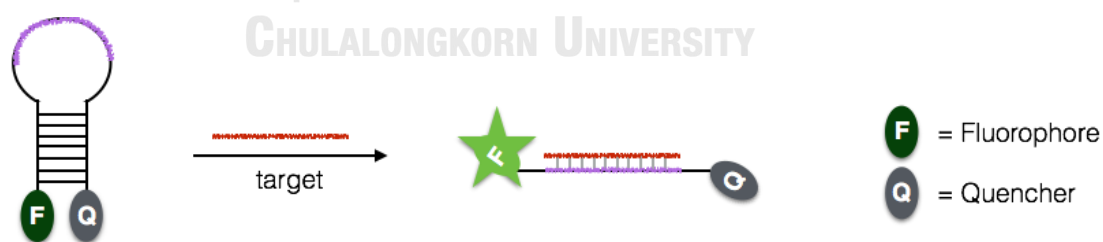
Figure 1.2 Molecular beacon structure and its principal

Molecular beacon (MB)[13, 14, 24, 25] is a typical example of fluorescent oligonucleotide probe in which both the fluorophore and the quencher are incorrorated in the same molecule. It is a single strand oligonucleotide designed to fold into a stem and loop structure in the absence of the DNA target (**Figure 1.2**).

The fluorophore and the quencher are placed at the opposite ends of the same probe molecule. In the free state, the duplex formation in the stem part will force the fluorophore and the quencher to be in a close proximity, which results in quenching of the fluorescence by various mechanisms such as contact quenching or FRET. The recognition sequence is placed in the loop region. Once the correct nucleic acid target hybridizes with the MB's loop, the stem part will separate because of the stiffening of the DNA duplex formed in the loop region. The change results in opening of the stem part, resulting in a restoration of the fluorescence due to the increased distance between the two labels. However, the major drawback of such beacon is the complicated probe design, especially in the stem region.[26] If the stem is too stable, it will not open up when the probe hybridizes with the target (false negative). On the other hand, too unstable stem will result in high fluorescence background and non-specific response (false positive). Moreover, it is synthetically difficult and costly to incorporate two labels in the same molecule. In addition, the fluorophore and quencher pair must be carefully chosen so that their interaction are maximized, resulting in high quenching efficiencies.
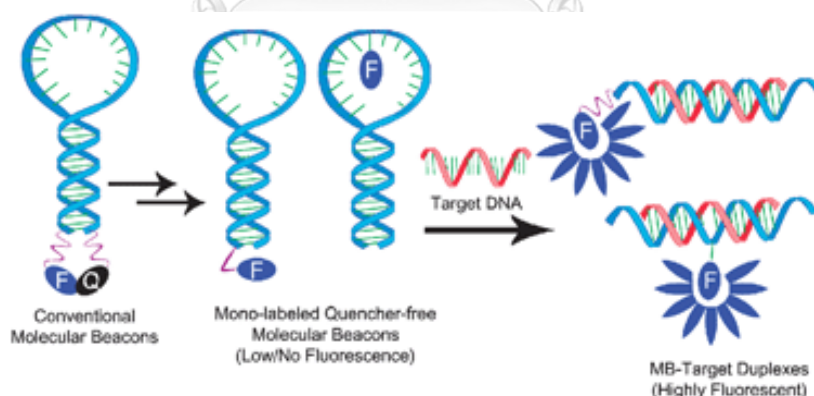
Figure 1.3 Conventional and modification of conventional molecular beacon[27]

To overcomes the limitation concerning the need for both the fluorophore and the quencher in the beacon probes, one approach is to omit the quencher from the molecular beacon altogether and use the nucleobase inside the probe as a quencher. Alternatively, the quencher-free probe may be designed to carry a fluorophore that can change it properties such as interaction with the nucleobases or

the conformational freedom upon the hybrid formation between the probe and the target.[28] The molecular beacon without the quencher is called the 'quencher free molecular beacon'.[27] Another design is the strand displacement probe, in which the fluorophore and quencher exist separately in two different probe strands.[29] The working principle is still based upon the same concept of the molecular beacon in the sense that, in the absence of the target (quenching state), the fluorophore and the quencher would be in close proximity through the hybridization of the fluorescent probe and a shorter sequences of oligonucleotide containing the quencher. In the presence of the target, the quencher probe is displaced by the target leading to the fluorescent signal enhancement.

1.3 Peptide nucleic acid probe

Although DNA oligonucleotides have been extensively used as the recognition element, over the past decades, there are needs for development of alternative probes that can improve the performance such as sensitivity and specificity, as well as biological stability.[30, 31] Peptide nucleic acid (PNA), an electrostatically neutral synthetic DNA analogue in which the sugar phosphate backbone is replaced by *N*-(2-aminoethyl) glycine (aegPNA), was introduced by Nielsen and co-workers since 1991.[32, 33] Not only PNA can bind to its complementary DNA specifically following the Watson-Crick base-pairing rules, the uncharged peptide backbone of PNA further contributes to its ability to pair with single-stranded nucleic acids with higher affinity. Despite of this, the hybridization between PNA and DNA surprisingly offers a higher sequence specificity than DNA-DNA hybridization. In addition, PNA is also resistant to nucleases and proteases.[34-36] These desirable properties makes PNA an ideal tools for diagnostics, molecular biology procedures, antisense therapies.[37]

The flexibility of aegPNA structure was thought to negatively affect the DNA binding due to the expected entropy loss upon hybridization with the DNA target. Hence, various new PNA systems have been developed over the past few decades in order to improve the binding properties. One of the most successful approaches involves rigidification of the PNA structure to minimize the entropy change upon the formation of PNA-DNA duplex.[38]

Pyrrolidinyl peptide nucleic acid (**Figure 1.4**) is a class of conformationally constrained PNA system developed by Vilaivan and co-workers since 2005.[39-42] This new PNA system consists of a nucleobases-modified proline and a cyclic β-amino acid spacer. The most extensively studied spacer is 2-amino-1-cyclopentabecarboxylic acid (ACPC), hence the name acpcPNA was adopted for the pyrrolidinyl PNA system carrying this particular spacer. Unlike aegPNA which can bind to DNA/RNA in both parallel and antiparallel directions, acpcPNA can bind to its complementary DNA only in the antiparallel direction similar to natural DNA-DNA duplexes. Moreover, the duplex of acpcPNA with its complementary target shows a higher thermal stability than the corresponding DNA-DNA and aegPNA-DNA duplexes. Furthermore, acpcPNA can distinguish its complementary DNA target from mismatched target better than aegPNA and even newer variants such as γPNA. Because of these advantages, acpcPNA have been extensively applied in DNA sensing applications[43] such as the development of self-reporting fluorescence acpcPNA probes.[44-46] In addition, the electrostatically neutral backbone of acpcPNA as well as other PNA allows the development of novel DNA sensing methods based on differential electrostatic properties of PNA and DNA.[47]
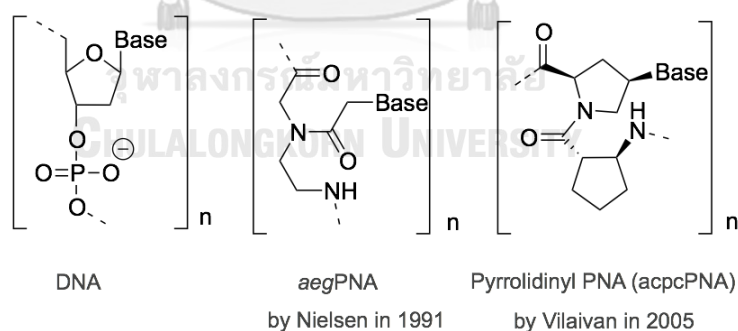
Figure 1.4 Structures of DNA, aegPNA, and acpcPNA

The first PNA-base molecular beacon probe was reported in 1998 by adopting the same concept of DNA molecular beacon whereby the fluorophore and the quencher were placed at the separate ends of the PNA strand.[48] Subsequently, there were several reports of other PNA beacon probes.[49] Our group have developed a kind of strand displacement probe employing acpcPNA. The fluorescent PNA probe

was labeled with fluorescein or TAMRA at the N-termini and a 3'-dabcyl-modified DNA was used as a quencher (**Figure 1.5**). The results showed that the fluorescence of the PNA stranded was quenched by the quencher after the hybridization with the quencher DNA and was restored upon the addition of its complementary target. However, the limitation of strategy is the slow kinetics of the strand displacement reaction.

PNA/   DNA   PNA/   DNAQ
DNAQ   target   DNA
                                  target
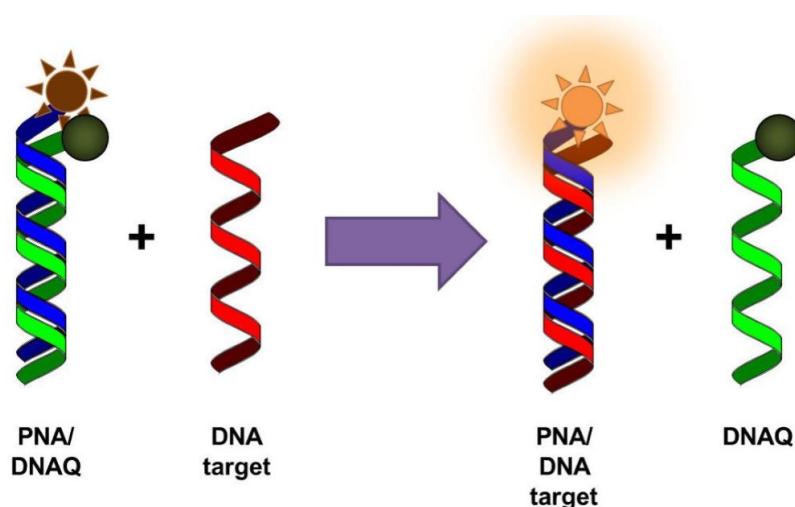
Figure 1.5 The concept of PNA displacement probe[50]

In another example, the fluorophore and the quencher were placed at the same end (N-terminus) of the acpcPNA probe. According to the principle shown in **Figure 1.6**, the free PNA displays a weak fluorescent signal due to a close contact between the fluorophore and the quencher. After the hybridization with the DNA target, the quencher with a stacking/intercalating ability would adhere to the final base pair formed in the duplex. This would destroy the interaction of the quencher and the fluorophore, leading to the observed increase in fluorescence. Although, this strategy was selective to the complementary target, labelling two molecules at the same end of PNA was complicated, time consuming and presented solubility issues.
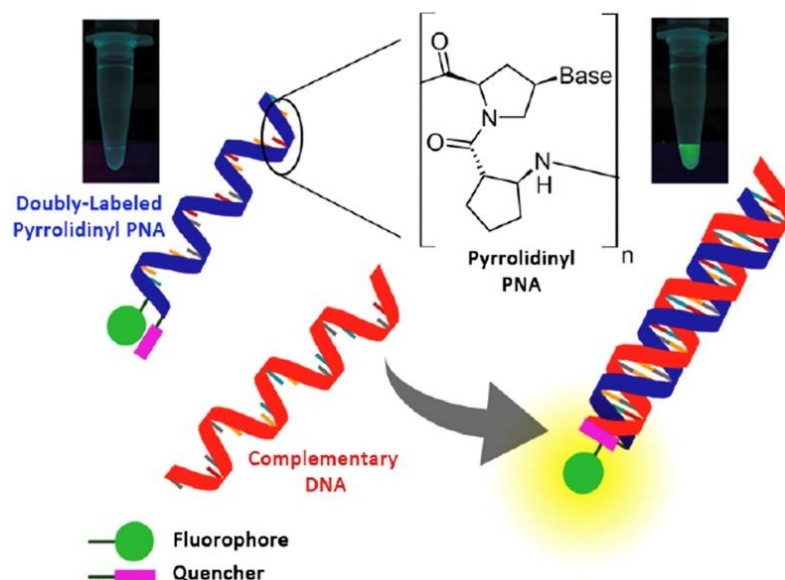
Figure 1.6 The PNA probe labeling with a pair of dyes and its concept[51]

In yet a few more studies, alternative fluorescent acpcPNA probes carrying only a single fluorescent label without the additional quencher were reported. This probe has been designed to carry an environment sensitive fluorescent dye such as pyrene, Nile red, or thiazole orange.[42] **Figure 1.7** shows the design of the fluorescent PNA probe labelled with a single fluorescent molecule.[42] The single-stranded PNA initially yielded a weak fluorescence, but the signal became stronger after the hybridization between the PNA probe and its complementary DNA target. The increase in the signal was a result of the changes in the environment around the fluorophore or the interaction between the fluorophore and nucleobase/duplex.
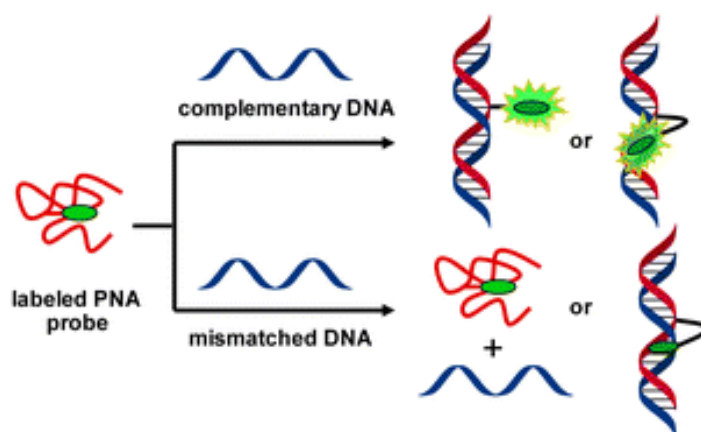
Figure 1.7 Various designs of self-reporting fluorescence acpcPNA probes[42]
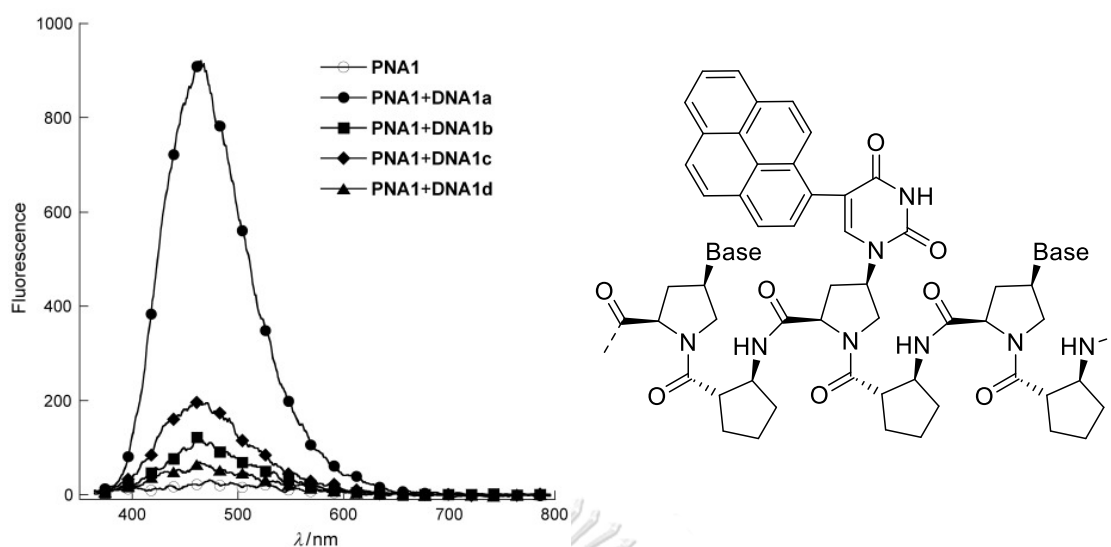
Figure 1.8 The selectivity of U^{Py}-PNA and U^{Py} [44]

In some singly-labeled acpcPNA probes, the labeled dyes had been incorporated as part of the nucleobase or attached to the PNA backbone. As an example (**Figure 1.8**), the fluorescence nucleobase 5-pyrene-1-yluracil (U^{py}) was incorporated into acpcPNA as a thymine base substitute.[44] The U^{Py}-PNA can act as a the hybridization-responsive fluorescence probe whereby specific pairing with adenine on the DNA strand provide a strong fluorescence enhancement. One disadvantage of this approach is that the PNA monomer must be individually synthesized and incorporated into the PNA probe at a specific site. Therefore, optimization of the fluorophore would not be straightforward.
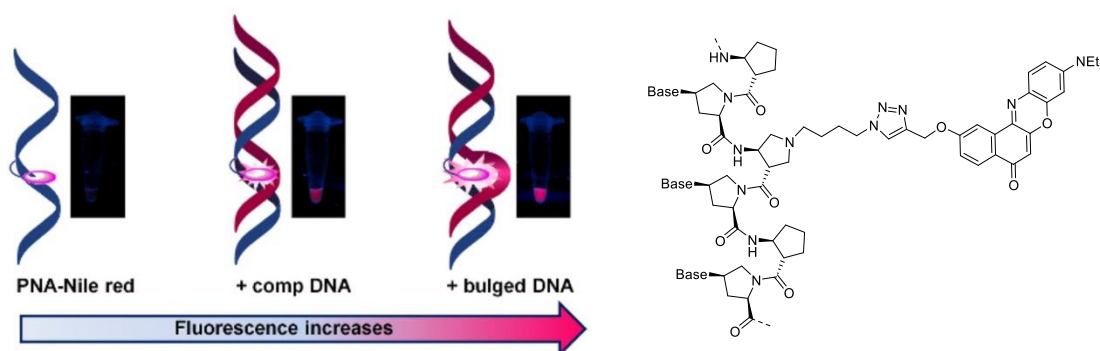
Figure 1.9 The fluorescence enhancement of Nile red-labeled acpcPNA probe in response to complementary and base-inserted DNA targets[46]

In another example of single-labeled self-reporting PNA probe (**Figure 1.9**), the environment sensitive dye Nile red was post-synthetically attached onto the acpcPNA backbone by click reaction.[46] The Nile red-modified acpcPNA probe showed a blue-shifted and enhanced fluorescent signal upon hybridization with the DNA target. Based on the enhanced fluorescence especially in the presence of bulge in the duplex, it was proposed that the Nile red label in the PNA-DNA duplex is located in a more hydrophobic environment than the single-stranded probe.
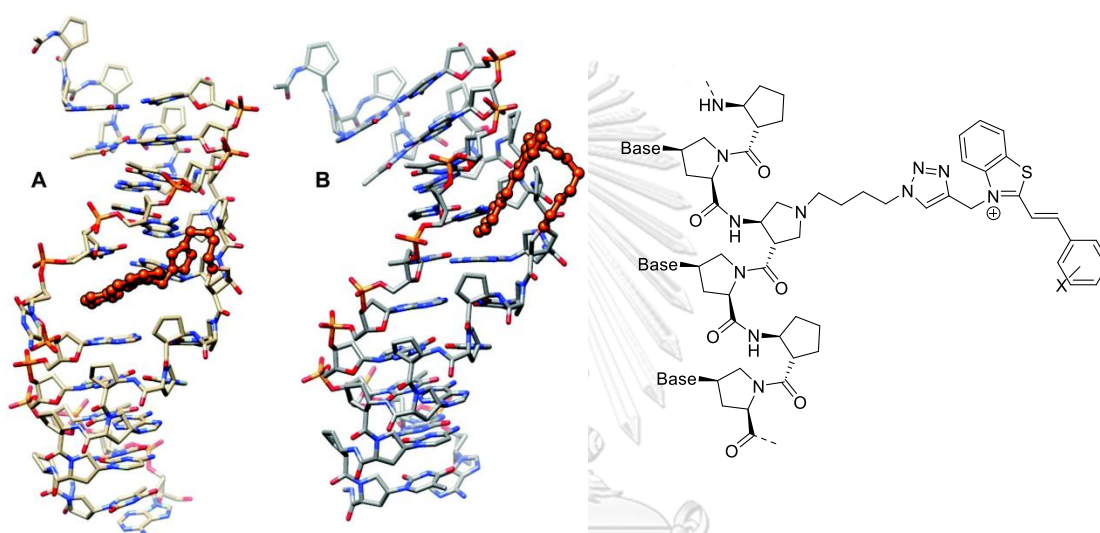
Figure 1.10 Averaged MD structures of styryl dye PNA binding to (A) base-inserted and (B) complementary DNA.[52]

Another related example of acpcPNA probe bearing an environment sensitive styryl dye combination is shown in **Figure 1.10**.[52] The free styryl dye-labeled PNA probe yielded a weak fluorescent signal in aqueous solution. The fluorescence increase was only marginal in the presence of complementary target. However, this probe fluoresced much more strongly upon binding to several uncommon DNA targets including mismatched, base-inserted, or abasic DNA. It was proposed that these defects in the duplex structure allow the hydrophobic dye to slip in, resulting in the conformational restriction and thus the observed fluorescence increase. Such labeled PNA probe may find some uses in certain circumstances but are not generally applicable for sensing of complementary DNA targets.

1.4 Graphene oxide and nucleic acid sensing

Recently, a new generation of fluorescent DNA sensing systems was developed whereby the fluorophore and the quencher can exist as separated entities. These are generally based on a fluorescently labeled oligonucleotide probe and an external quencher such as metal nanoparticles[53, 54] and graphene oxide (GO).[17, 55] Such systems have attracted much interest in the DNA sensing applications due to the simplicity of the design and high quenching ability of these material involving a surface energy transfer process.[56]

GO is a unique carbon-based nanomaterial that contains various types of oxygen species (epoxide, hydroxyl, and carboxyl groups) present on the monolayer of graphene. Unlike graphene, GO has an overall negative charge and is well dispersed in water.[57] Despite being negatively charged, GO can interact with single-stranded fluorescently labeled oligonucleotides (also negatively charged) via π-π stacking interaction of the graphene surface and the nucleobase (**Figure 1.11**).[58] This results in quenching of the fluorescent signal of the probe. Hybridization with its complementary DNA strand restores the fluorescence because the nucleobases became involved in the base pairing in the DNA duplex, and therefore are not available for the interaction with the GO. The repulsion between DNA's negatively charged backbone and GO's surface resulted in the detachment of the hybridized probe from the GO surface, resulting in the observed fluorescence increase.

In 2009, the first report on a DNA-graphene oxide platform demonstrated that it can be used as a rapid, sensitive and selective detection of biomolecules such as DNA and proteins.[17] In this study, it was revealed that the interaction between dye-labeled oligonucleotide and GO led to a strong fluorescence quenching. Addition of the target biomolecule resulted in the binding between the fluorescent oligonucleotide probe and its target, thus releasing it from the GO surface and thereby the fluorescent signal was restored.
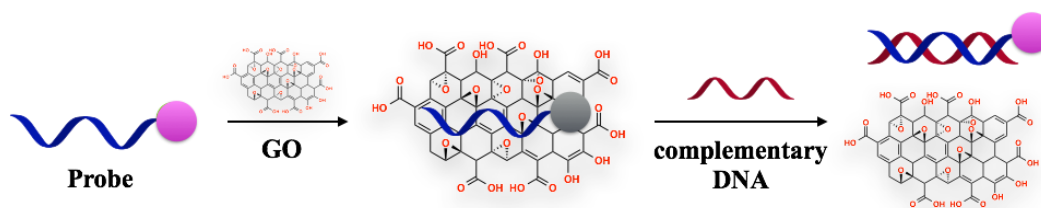
Figure 1.11 The principle for the detection of DNA sequence using nucleic acid probe and GO

In 2011, Wu and co-workers[59] reported that the adsorption of DNA on the graphene oxide depended on the length of the DNA probe, pH and salt concentration of the solution (**Figure 1.12**). This report further revealed some limitations of the DNA-GO based DNA sensing platform. Since the interactions between DNA and GO are non-specific in nature and are likely to be similar for many DNA sequences, the probe can be competitively displaced from the GO surface by other DNA sequences and can thus lead to false positive signals. In addition, the strong adsorption between the nucleobases and GO surface leads to the need for large excess of DNA target to restore the fluorescence signal, resulting in poor sensitivity.[60]
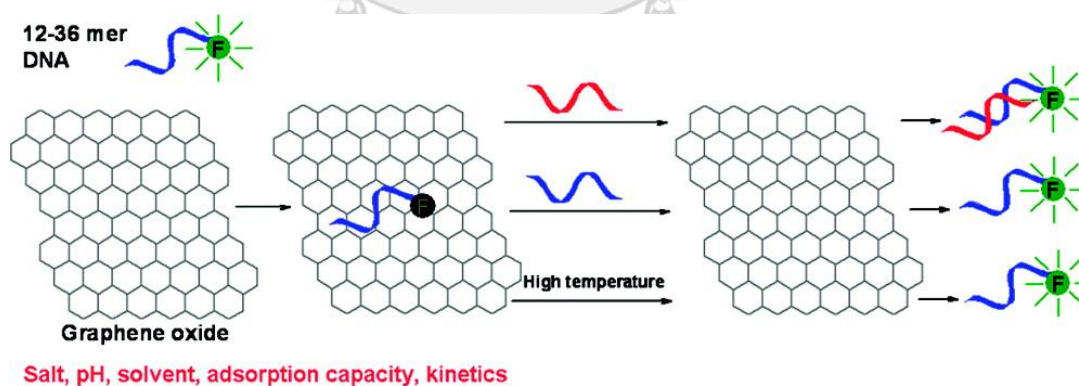
Figure 1.12 Possible mechanisms of the displacement of fluorescently labeled DNA probes from the GO surface[59]

A promising system for a fluorescence detection of DNA employing a singly-labeled PNA probe in combination with graphene oxide (GO) as a quencher was reported by Guo and co-workers in 2013 (**Figure 1.13**).[18] They reported that labeled

aegPNA in combination with GO outperformed DNA in terms of detection sensitivity, although the kinetics were rather slow and the fluorescence restoration was not complete. Furthermore, the fluorescence change was rather modest (ca 2.5 fold).[18] Nevertheless, the PNA-GO combination has been successfully employed for quantitative analysis and multiplex detection of miRNA in living cells.[61] Furthermore, the PNA-GO system was capable of detecting dsDNA directly without requiring denaturation due to the ability of PNA to invade into DNA duplexes.[62] The main advantage of these GO-based platforms is the simplicity since only one fluorophore was required on the probe, but there are still rooms for improvements as stated earlier.
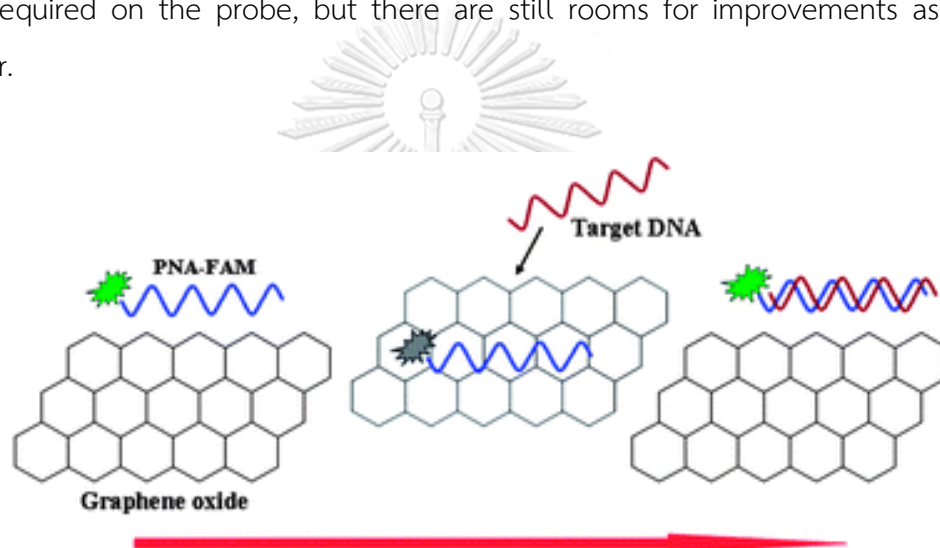
Figure 1.13 PNA probe in combination with graphene oxide[18]

1.5 Guanine rich sequence DNA as a quencher

Guanine is a nucleobase that can act as an effective quencher for many fluorophores typically used in biological applications[63-65] such as FAM, pyrene, rhodamine and oxazine dyes. Since its oxidation potential is the lowest among the naturally occurring four nucleobases (**Figure 1.14**), an electron from guanine can be easily donated to the singlet excited state of the fluorescent dye, leading to a non-radiative relaxation of the dye to its ground state.[64, 66] This quenching process has been referred to as photo-induced electron transfer (PET), which can occur from the close contact between the fluorophore and guanine via chemical bonding (H-bonding), π-π stacking interaction or other types of attraction.[67-69]
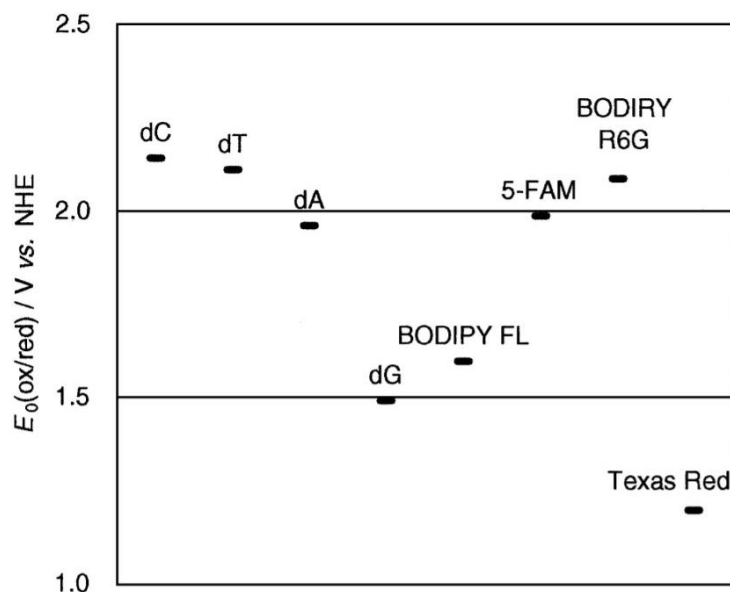
Figure 1.14 The reductive potentials of the fluorescent dyes and the oxidative potentials of nucleobases[66]
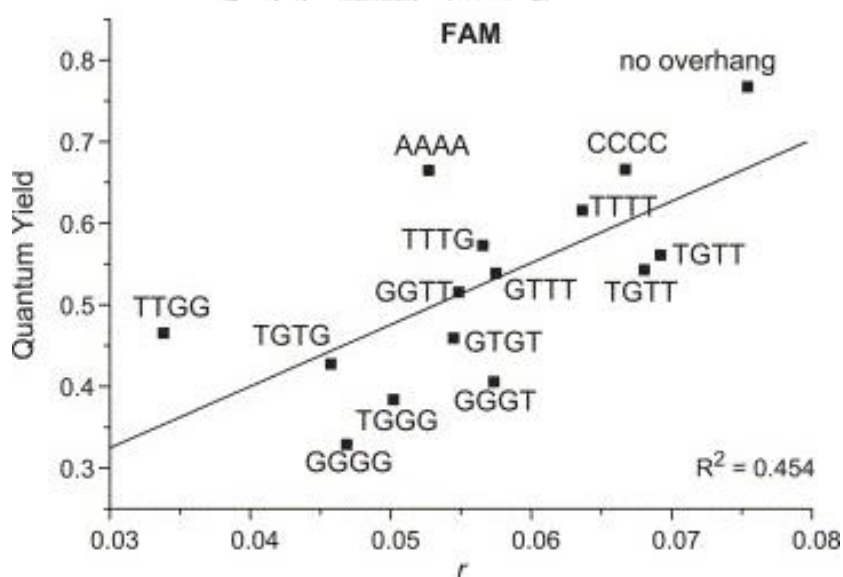
Figure 1.15 The relationship between fluorescence quantum yield and anisotropy for the hybridization reactions employing FAM-labelled probes[64]

Fluorescein is a xanthene dye that has been widely used as a fluorescent label in biological applications because of its strong fluorescence.[70] In 2005, Noble and co-workers determined the effect of the nucleobase overhangs on the

complementary strand on the fluorescent signal of the hybridization fluorescein-labelled probe (**Figure 1.15**).[71] The results showed the presence of guanine base overhangs in the close proximity to the fluorescein resulted in the highest fluorescence quenching.

In 2009, Qu and co-workers[72] examined the effect of free nucleotide monophosphates (dNMPs) on the inter- and intra-molecular PET quenching of TMR in aqueous solution. The results showed that only guanosine can quench TMR effectively, while the quenching by other nucleobases is not significant (**Figure 1.16**). Moreover, the effect of the fluorescence quenching by guanosine relied on the steric hindrance by nucleobases around the guanosine residue.
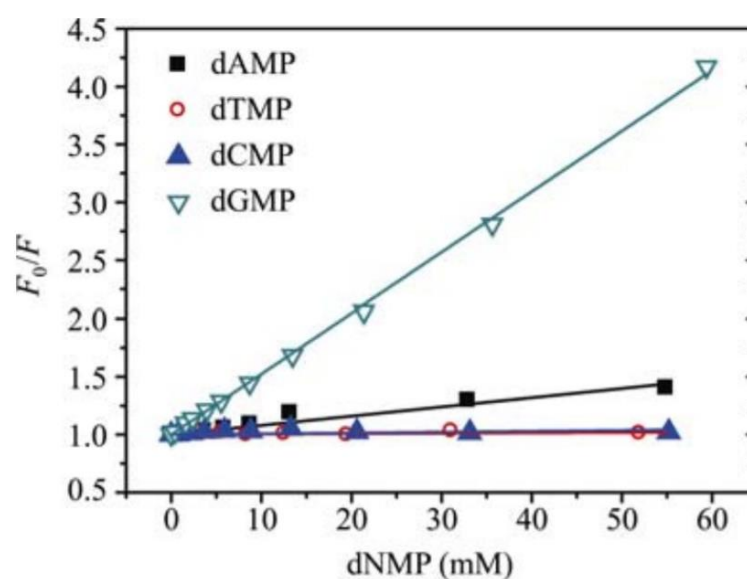
Figure 1.16 Steady-state bimolecular Stern-Volmer plots of TMR and the four nucleobase monophosphates (dNMP)[72]

In 2003, Heinlein and cowerkers[73] designed hairpin-shaped oligonucleotide probes with a stem-loop structure similar to MBs to detect the DNA target sequences. However, guanine was used as the quencher instead of dabcyl or other organic dyes typically used in conventional MBs. In the hairpin state, the dye attached at the 5'-end was quenched by the guanosine residues in the complementary stem. After the hybridization with its complementary target, a

conformational re-organization occurred, leading to the 20-fold increase of the fluorescence (**Figure 1.17**). Similarly, Misra and coworker[74] synthesized the molecular beacon in which the fluorophore was labelled at only the 5'-end and using extra overhung guanosines at 3'-end as a quencher (FAM-C3-*catc*AAAAAAAAAAAAAAAAAAAAA*gatggg*-3'). The fluorescence quenching occurred in the absence of DNA target due to the stacking between the fluorophore and the guanosine residue.
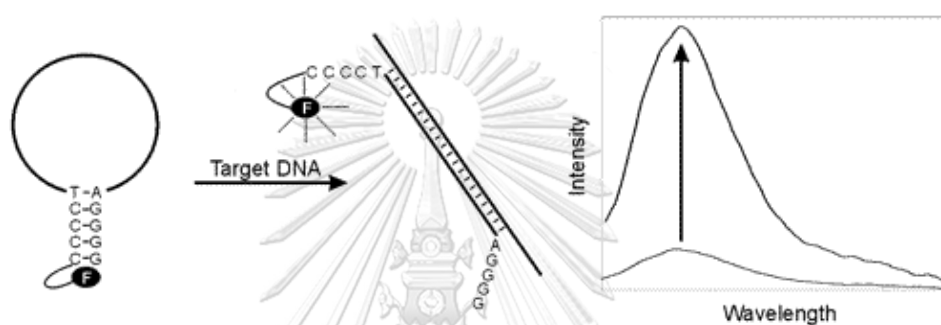
Figure 1.17 The molecular beacon design by using oligodeoxyguanosine as an internal quencher[73]

Instead of sensing a DNA target, Hu and coworked[75] applied the concept of the molecular beacon by using deoxyguanosine as a quencher for the detection of mercury(II) ion (Hg^{2+}). **Figure 1.18** showed that in the presence of mercury ions, the fluorescent probe was quenched when it folded into the duplex-like formation via Hg^{2+}-mediated formation of the T–Hg^{2+}–T base pairs. The folding positioned the guanine region near the fluorophore, leading to the observed fluorescence quenching.
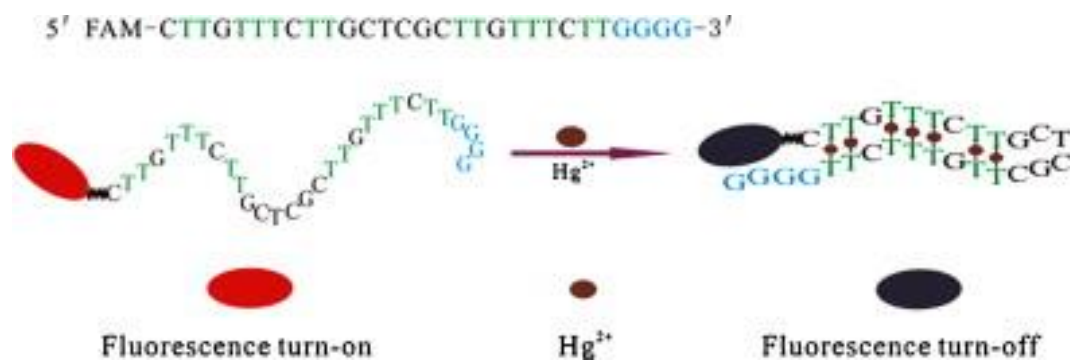
Figure 1.18 Sensitive detection of Hg²⁺ ions based on the G-quenching fluorescence.[75]

Zhou and co-workers reported a novel homogenous miRNA detection by using the quenching ability of guanine (**Figure 1.19**).[76] The circular DNA was used as a recognition probe for the hybridization with miRNA target, and then miRNA target primed an rolling circle amplification (RCA) reaction to generate a long dsDNA target with a tandem repeated sequence. The RCA product could be hybridized with thousands of FAM-labeled signal DNA probes to form double-stranded DNA (dsDNA), which induced the fluorophore to be positioned near the –GGG– base, leading to the quenching of the fluorophore through the PET mechanism. The drawback of this approach is the signal-off (fluorescence quenching) nature of the DNA sensing which is less desirable.
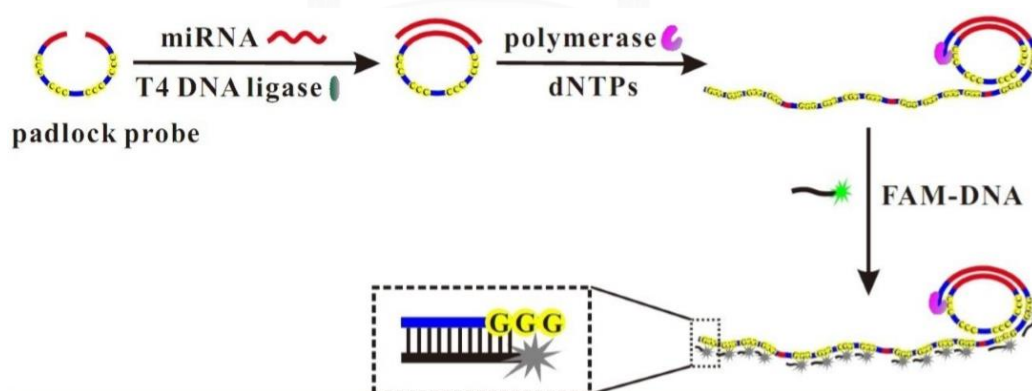
Figure 1.19 The strategy for PET-based RCA fluorescence detection of miRNA with linear DNA as signal probe.[76]

In addition, guanine-rich sequences of DNA can self-assemble and form a tetra-stranded structures known as G-quadruplexes (G4).[77, 78] This square planar

structure is formed by four guanine bases connected by four hydrogen bonds between each G residue (**Figure 1.20**). Each G4 quartet is further stabilized by stacking of one layer on top of another. Although the G4 structure is stabilized by hydrogen bonds, it can also be stabilized by an alkali metal ion that can accept the electrons from the guanine carbonyl oxygen.
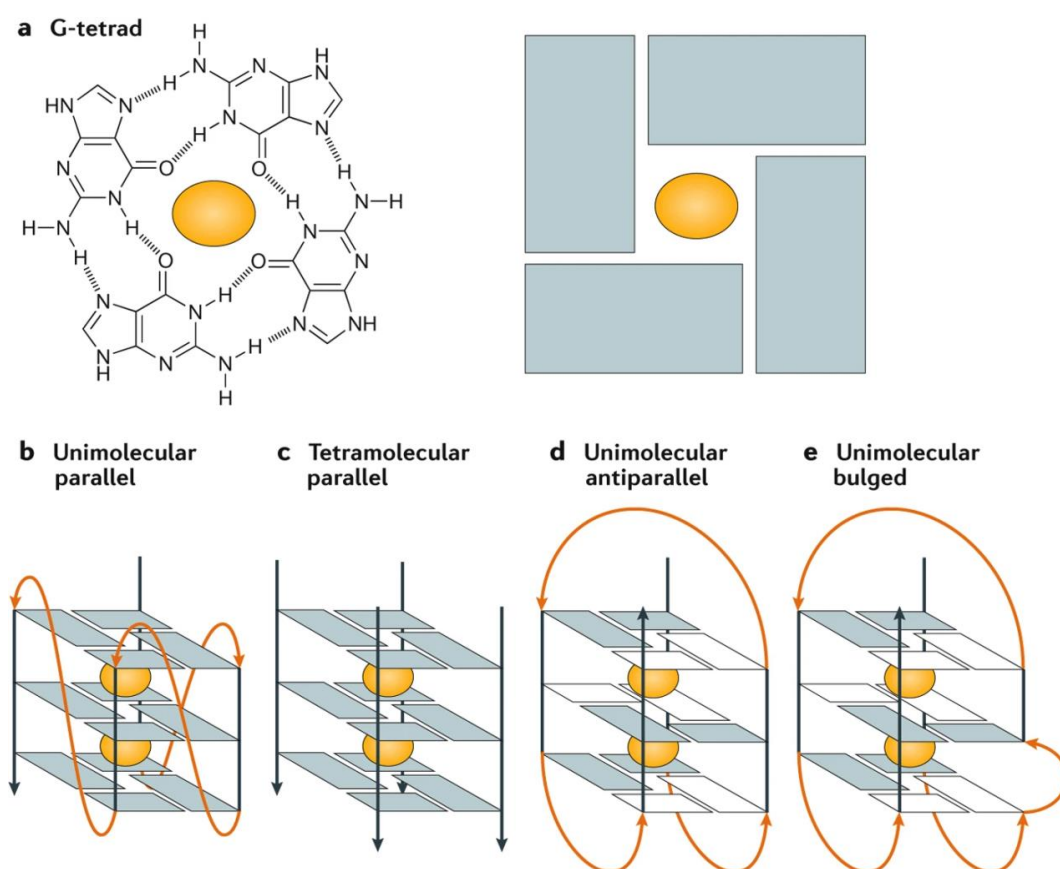
Figure 1.20 (a) The structure of G-quadruplex and (b-e) examples of G-quadruplex folding patterns[79]

Yang and co-workers developed a simple, sensitive and selective method using singly-labeled fluorescent DNA appended with a G-quadruplex as an intramolecular quencher for the detection of mercury and cysteine (**Figure 1.21**).[80] A selective binding between Hg^{2+} and two thymine DNAs can stabilize T-T mismatches to form a stable T-Hg^{2+}-T base pair.[81] The probe was designed to carry a thymine-rich sequence and a G-quadruplex forming sequence at the 5'-end and a FAM label at

the 3'-end. In the presence of Hg^{2+}, the T-rich sequence folded to form a hairpin structure which brought the FAM label to close contact with the G-quadruplex. Hence the FAM signal was quenched by the G-quadruplex in the presence of Hg^{2+}. When cysteine was added, the hairpin structure was unfolded, and the fluorescence signal was restored because of the strong binding between Hg^{2+} and cysteine. The same principle can be applied to sense Ag^+, which can stabilize these C-C mismatches to form a stable C-Ag^+-C base pair.[82]
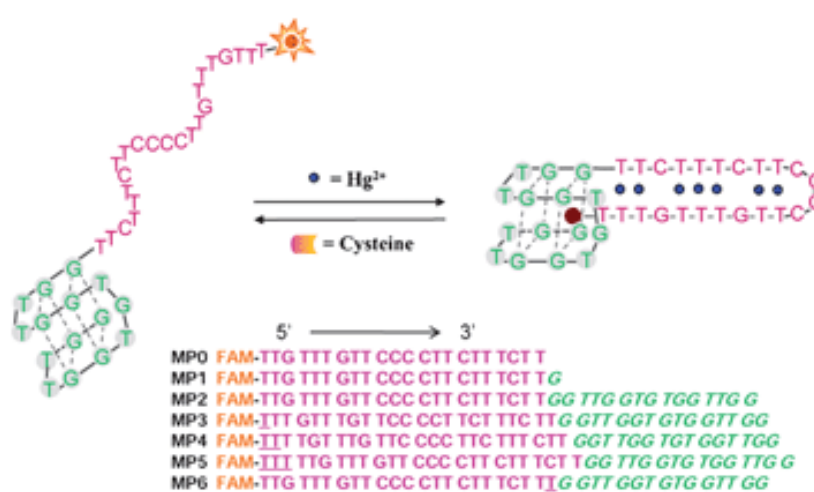
Figure 1.21 The detection of mercury(II) ion and cysteine using a fluorescent DNA probe bearing an internal G-quadruplex.[80]

Based upon the previous literature on the use of guanine-rich sequence as a quencher, the quenching would occur when the fluorophore was positioned near the guanine through the photoinduced electron transferred process. However, the design of the G-quenched probe is not universal because the G-rich sequences must be incorporated into the probe. This is considered as a disadvantage when compared to the use of graphene oxide, which could quench the fluorescent intensity of the reported probe without the need to incorporate into the sequence of the fluorescent probe.

1.6 G-quadruplex - hemin DNAzyme

In the previous section, the role of G-rich sequences in DNA sensing was discussed mainly as a fluorescence quencher. In this section, another role of the G-rich sequences as "DNAzyme" in the DNA sensing will be discussed. DNAzymes are specific nucleic acid sequences that can mimic the behavior of enzyme, i.e. catalyzing chemical reactions. Compared to conventional enzymes, DNAzymes are stable, inexpensive, and easy to synthesize and functionalize. These characteristics, in addition to due to its flexibility to code the recognition region in DNAzyme sequence,[83] make DNAzyme an excellent choice for biosensing applications. Nowadays, DNAzymes are widely used in various catalytic reactions for DNA sensing application, nanotechnology, and drug for treatment cancer.[84-86] This section will focus on only one particular type of DNAzyme involving the G-quadruplex-hemin complex that can act as a peroxidase mimic.

In 1998, Travascio and co-workers reported that hemin can form a complex with G-quadruplex by stacking onto the 5'-or 3' end of the G-quadruplex, and the resulting complex can act as a DNAzyme which exhibits a peroxidase-like activity.[87] Hemin itself possessed low peroxidase activity, but the complexation with the G-quadruplex substantially enhanced the activity, and thus it can be considered as a cofactor. Some reports suggested that the parallel G-quadruplex yielded greater activities than anti-parallel form.[88]
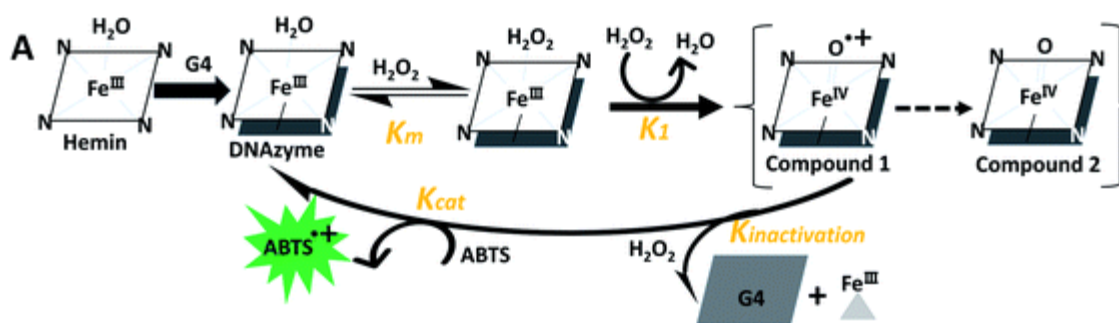
Figure 1.22 A proposed mechanism for the catalysis and inactivation of G-quadruplex-hemin DNAzyme.[88]

Figure **1.22** showed a proposed the mechanism of the G-quadruplex-hemin DNAzyme. First, the association between G-quadruplex and hemin (DNAzyme) would enhance the peroxidase activity. Then, H_2O_2 replaces the H_2O coordinating on the hemin and withdraws two electrons from hemin to form an intermediate. Finally, the intermediates withdraw electron from the substate or hydrogen peroxide.[89] Thus, the green solution would be observed caused from the presence of the oxidation form of ABTS substrate.
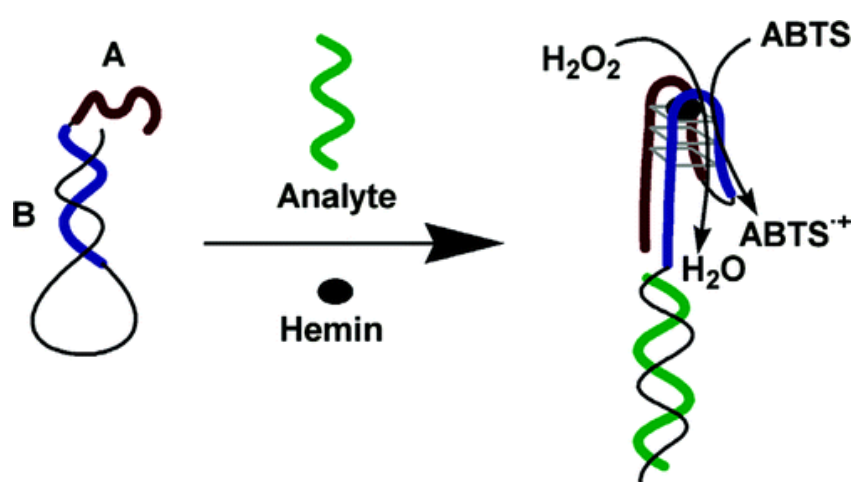
Figure **1.23** A G-quadruplex DNAzyme-based molecular beacon[90]

Figure **1.23** depicted a strategy of molecular beacon in which a guanine-rich region (black line) which could form a G-quadruplex formation with part of the stem region (blue line) was incorporated into the beacon.[90] Since the stem is preferentially formed in the absence of the DNA target, there was no G-quadruplex and the peroxidase activity was low. In the presence of the DNA target, the stem of the beacon would open up. Then, the G-quadruplex structure would form and associate with the hemin and thus act as the DNAzyme. Finally, the DNAzyme could catalyze the oxidation of the ATBS substrate to give a colored oxidized product. Shao and co-workers reported a related but distinctively approach for the DNA detection by using G-quadruplex-hemin DNAzyme.[91] The probe contains half G-quadruplex forming sequences at each end of the molecule. The G-quadruplex would form when both ends are positioned near each other as in the case of free probe which could act as DNAzyme when hemin was added. Accordingly, in the absence of target, or in the

presence of mismatched or non-complementary targets, the addition of hemin could generate the peroxidase activity (**Figure 1.24**). On the other hand, when the complementary DNA target was present, the hybridization between the probe and its target forces the two ends of the molecule apart, leading to the suppression of DNAzyme activity. The limitation of this approach is the signal-off nature of the detection. It should also be noted that 2,2′-azino-bis(3-ethylbenzothiazoline-6-sulfonic acid) diammonium salt (ABTS), which was widely used in various applications as a peroxidase substrate, is not stable after the oxidation and can rapidly decay and become colorless product in aqueous solution.[92]
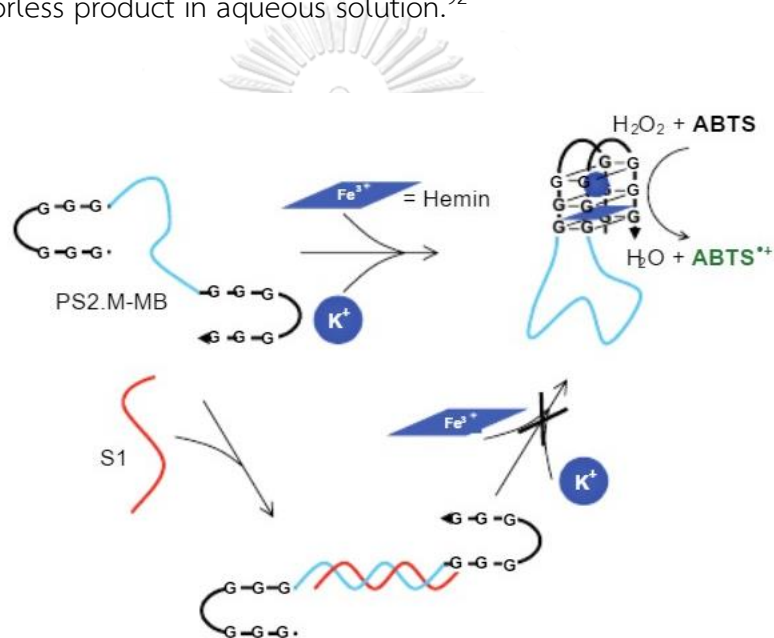
Figure 1.24 The modulation of peroxidase activity of a split G-quadruplex probe by the hybridization with DNA target[91]

In 2009, Li and coworker reported that 3,3',5,5'-tetramethylbenzidine sulfate (TMB) was an excellent chromogenic substrate for reporting peroxidase activities in the G-quadruplex-hemin DNAzyme system. Figure **1.25** revealed that the DNAzyme catalyzes the oxidation of TMB to produce two colored products in the presence of hydrogen peroxide. The first product was a blue complex of the TMB and its oxidation product (diamine) which showed the absorption wavelength at 370 and 652 nm, respectively. In the presence of acid, the blue product will be further oxidized to a stable yellow diimine with the absorption at 450 nm.
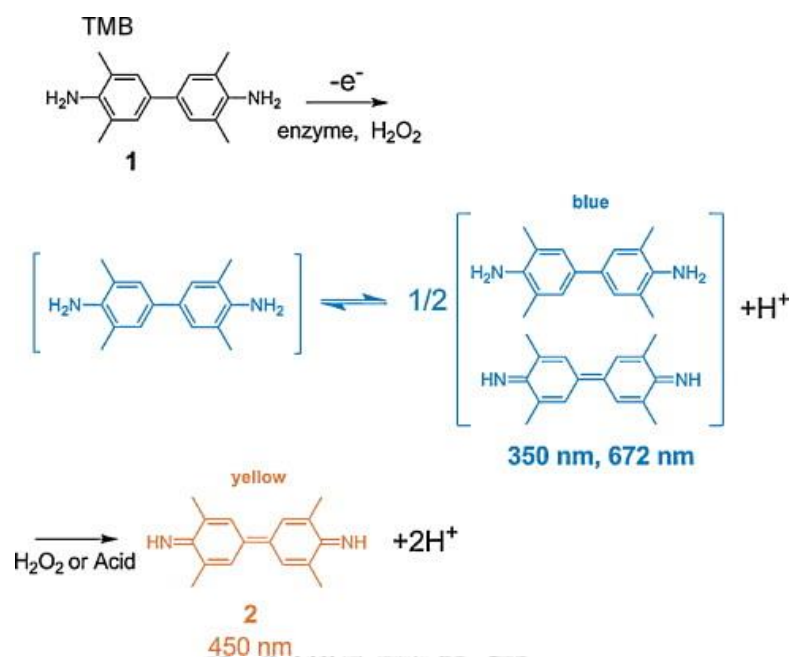
Figure 1.25 The structure of TMB and its peroxidase reaction products
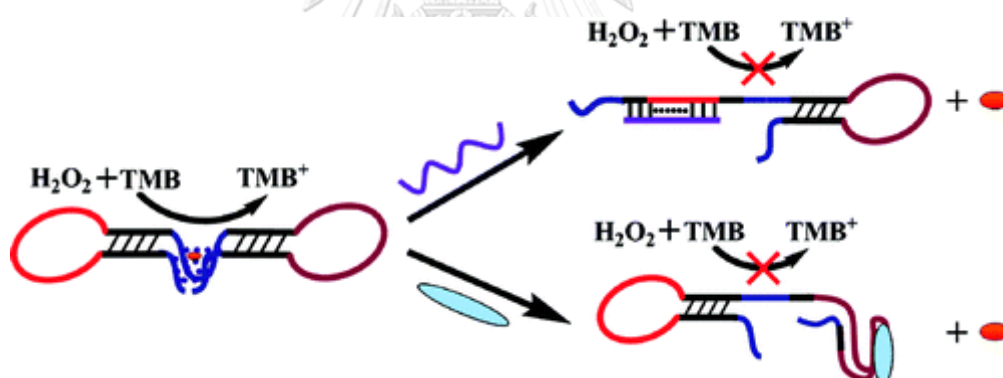
Figure 1.26 A schematic representation of the bifunctional oligonucleotide probe for colorimetric analysis of DNA or thrombin[93]

In 2011, Zhang and co-workers developed a label free bifunctional colorimetric DNA probe for biomolecules (DNA and thrombin) detection.[93] **Figure 1.26** showed the catalytic molecular beacon containing a double hairpin structure, one for thrombin detection and another one for DNA detection. The two hairpin structures were designed to carry half of the G-quadruplex forming sequence in the linker and the other G-quadruplex forming half were split between the two ends of the joined beacon probe. In the absence of the target, the G-quadruplex could form

and catalyze the TMB oxidation to give a blue solution. The catalytic activity decreased after the addition of either of the target because the structure of G-quadruplex was destroyed. Again, this is a signal-off detection process.

Based upon the previous literature on the use of G-quadruplex-hemin DNAzyme for peroxidase activities, the key to the probe design was based on the switching of the quadruplex structure which can associate or dissociate after the binding between the probe and its target. Importantly, the catalytic nature of the DNAzyme reaction potentially improve the sensitivity of the assay since many signals can be generated from one DNAzyme molecule which is in contrast to most fluorescence-based assay that one hybridization event will generate only one signal. Thus, the procedure for target detection did not require high concentrations of the probe and could be conducted by naked-eye colorimetric detection. However, the probe must be carefully designed in order to prevent the side reactions between the binding region and the quadruplex region. Furthermore, many of the DNAzyme-based probe designs work in signal-off format, which is not ideal and there are still rooms for further improvements.

1.7 Objectives of this study

From the previous studies summarized above, there are still needs for new DNA sensing platforms that are more specific, sensitive and simple to use. The use of PNA probes instead of conventional DNA probes offers a promising strategy to improve the performance of the existing DNA sensing platforms further. Also, the double labeling of the probes should be avoided so that the probes can be more easily synthesized. To this end, a new platform based on to the use of readily accessible guanine bases as the quencher in combination with fluorescently labeled acpcPNA probes was proposed. Although the use of G-rich or G-quadruplex forming sequences as a quencher of DNA probes for nucleic acid detection are well known, most of them require covalent linking or base pairing. To the best of our knowledge, no examples of using G-rich sequences as an external quencher had been reported in the literature. In addition, similar strategies have not been previously reported in the context of PNA probes. Thus, this study aims to develop a simple and sensitive

method for DNA detection by using a fluorescently labeled acpcPNA as a probe and oligodeoxyguanosine as a quencher. In this proposed research, we will study the factors that affect the quenching ability of the fluorescent acpcPNA probe by oligodeoxyguanosine, the fluorescence restoration by DNA target, selectivity, sensitivity and application in DNA sensing. Moreover, we are interested in adapting this platform to detect the non-DNA targets such as metal ions. In addition, we aim to develop another G-quadruplex-hemin DNAzyme-based DNA colorimetric detection system that operates in a signal-on mode and with improved sensitivity and specificity by the combination of the advantages of PNA probe and the DNAzyme-based assay.

CHAPTER 2

EXPERIMENTAL SECTION

2.1 Chemicals

All chemicals used in this study were purchased from various standard chemical suppliers and they were used without further purification. Oligonucleotides were purchased from Pacific Science (Thailand) and Ward Medic (Thailand). 2.0 mg/mL of graphene oxide nanocolloids in H_2O (GO) and 3,3',5,5'-tetramethylbenzidine (TMB) were from Sigma Aldrich. Hemin was obtained from TCI Co., Ltd. Hydrogen peroxide (30%) was from MERCK. Nitrogen gas (99.9% purity) was from Labgaz Co., Ltd (Thailand). HPLC grade solvents for HPLC experiments were obtained from Merck and Burdick & Jackson (USA) and were filtered using a 47 mm, 0.45 μm Nylon membrane filter from Vertical Chromatography Co., Ltd (Thailand). The commercial and analytical grade solvents were used without further purification for the column chromatography and the reaction, respectively. The water used throughout the experiments was obtained from an ultrapure water system fitted with a Millipak® 40 filter unit 0.22 μm, Millipore (USA). The separation by column chromatography was performed on silica gel (70-230 mesh).

For solid phase peptide synthesis, anhydrous *N,N*-dimethylformamide (DMF) (H_2O ≤ 0.01%) which was used as the solvent in the synthesis was purchased from RCI Labscan (Thailand). 1,8-Diazabicyclo[5.4.0]undec-7-ene (DBU), *N,N*-diisopropylethylamine (DIEA), piperidine, trifluoroacetic acid (TFA), *O*-(7-azabenzotriazol-1-yl)-*N,N,N',N'*-tetramethyluronium hexafluorophosphate (HATU), and TentaGel S RAM Fmoc resin (0.24 mmol/g) as a solid support was obtained from Fluka. 1-Hydroxy-7-azabenzotriazole (HOAt) was purchased from GLBiochem (Shanghai). 5(6)-Carboxyfluorescein *N*-hydroxysuccinimide ester (Flu-NHS) and 5(6)-carboxy tetramethylrhodamine *N*-hydroxysuccinimide ester (TMR-NHS) were purchased from Thermo Scientific Co., Ltd (USA) and Sigma Aldrich (USA), respectively. The reaction progress was monitored by thin layer chromatography (TLC) and spots were observed on TLC using visualization under UV light (254 nm).

2.2 Equipment

Reverse phase HPLC experiments were performed on a Water Delta 600 HPLC system equipped with gradient pump and Water 996 photodiode array detector. A 4.6×150 or 4.6×50 mm ACE C18-AR HPLC column was used for both preparative and analytical purposes. MALDI-TOF mass spectra were recorded on a Microflex MALDI-TOF mass spectrometer (Bruker Daltonics, USA). Melting temperature (T_m) measurements and UV-visible spectra were performed on a CARY 100 Bio UV-visible spectrophotometer (Varian, Inc., USA) equipped with a temperature controller. Fluorescence experiments were performed on a Varian Cary Eclipse Fluorescence Spectrophotometer. CD spectra were recorded on JASCO J-815 spectropolarimeter (JASCO, Japan).

2.3 Synthesis of pyrrolidinyl peptide nucleic acid (acpcPNA)

2.3.1 Synthesis of acpcPNA monomers
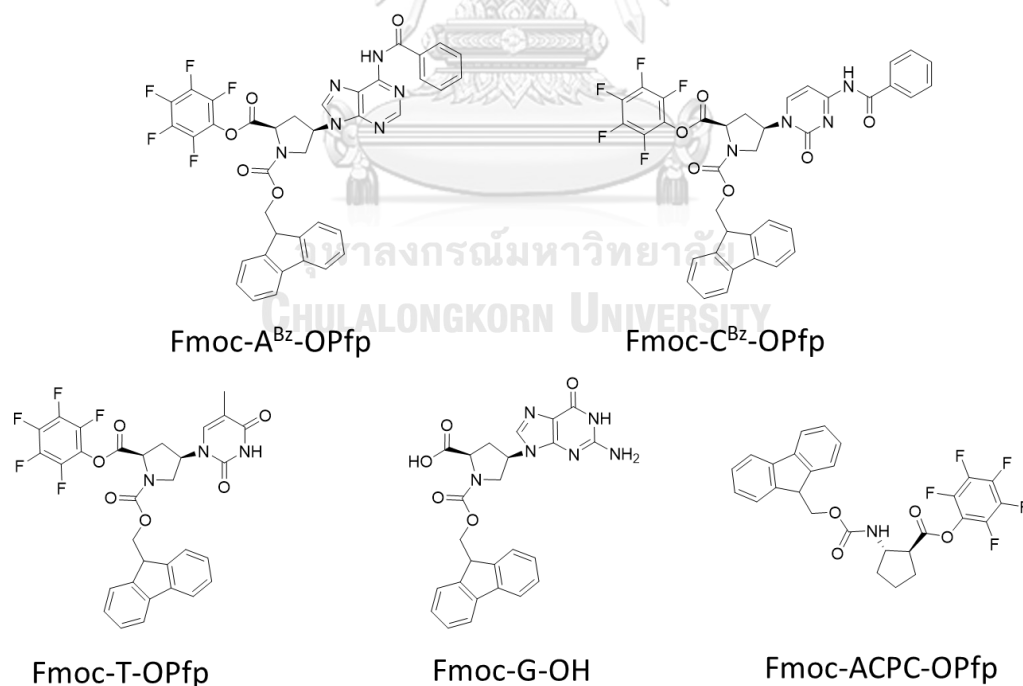
Figure 2.1 Structure of Fmoc-protected acpcPNA monomers and β-amino acid spacer for solid phase peptide synthesis

The Fmoc-protected acpcPNA monomers A[Bz], C[Bz] and T (Fmoc-A[Bz]-OPfp, Fmoc-C[Bz]-OPfp, Fmoc-T-OPfp) and ß-amino acid spacer (Fmoc-(1*S*,2*S*)-2-amino-1-cyclopentaneanecarboxylic acid) were synthesized by members of Prof. Vilaivan's lab following the protocol from previous publications.[41, 94, 95] The G monomer of acpcPNA (Fmoc-G-OH (G)) was synthesized as described below.

2.3.1.1 Synthesis of N-Boc-trans-4-tosyloxy-D-proline diphenylmethyl ester[96]
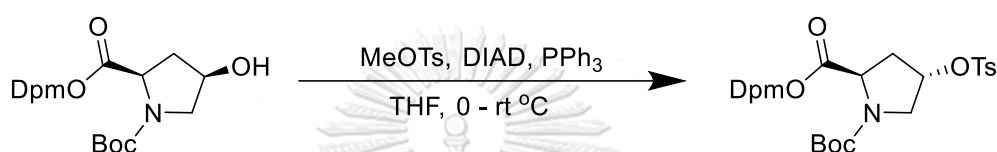
A solution of N-Boc-*cis*-4-hydroxy-D-proline diphenylmethyl ester (5.02 g, 12.4 mmol) and triphenylphosphine (PPh$_3$) (3.91 g, 14.8 mmol) in anhydrous THF (30 mL) in a round bottomed flask was cooled at 0 °C under N$_2$ atmosphere. Methyl p-toluenesulfonate (MeOTs) (2.82 g, 14.8 mmol) was added into the mixture and then followed by the drop wise of diisopropyl azodicarboxylate (DIAD) (3.0 mL, 14.8 mmol,After the reaction was stirred for overnight and monitored by TLC with Hexane:EtOAc (1:1), the solution was dried under vacuum and the residue was crystallized from ethanol to give *N-Boc-trans-4*-tosyloxy-D-proline diphenylmethyl ester as a white fluffy solid (3.1 g, 44% yield). ^{1}H NMR (400 MHz, CDCl$_3$) δ 7.75 (d, J = 8.1 Hz, 2H), 7.32 (m, 12H, CH), 6.89,6.84 (2s, 1H, CH), 4.97 (m, 1H, CH), 4.50 (m, 1H), 3.61 (m, 2H), 2.58 (m, 1H, CH$_2$), 2.45 (s, 3H CH$_3$), 2.04 – 1.94 (m, 1H, CH$_2$), 1.41, 1.21 (2s, 9H, CH$_3$x2).

2.3.1.2 Synthesis of N-Boc-cis-4-G^{Cl}-D-proline diphenylmethyl ester
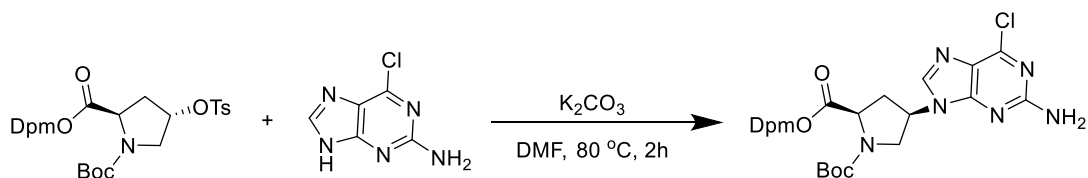
A mixture of *N*-Boc-*trans*-4-tosyloxy-D-proline diphenylmethyl ester (1.1215 g, 2 mmol), 2-amino-6-chloropurine (0.33 mg, 2 mmol) and dry potassium carbonate (0.34 mg, 2.4 mmol in DMF (5 mL) was stirred at 80 °C for 2 hrs. The organic phase was diluted with CH_2Cl_2 (50 mL), washed with water (50 mL × 6) and dried under vacuum. The residue was purified by column chromatography by using silica gel as a stationary phase and the gradient of hexane:EtOAc (9:1 to 1:1) as a mobile phase to give *N*-Boc-*cis*-4-G^{Cl}-D-proline diphenylmethyl ester as a yellow foam (0.350 g, 33% yield, R_f = 0.2 by 1:1 Hexane:EtOAc). ^{1}H NMR (400 MHz, CDCl$_3$) **δ** 7.76, 1.71 (2s, 1H CH), 7.27 (m, 10H, CH), 6.88 (s, 1H, CH), 4.92 (m, 1H, CH), 4.63, 4.52 (2m, 1H), 4.52 (s, 1H), 4.03 – 3.84 (2m, 2H), 2.86 (m, 1H), 2.50 (m, 1H), 1.47, 1.28 (2s, 9H, CH$_3$x2).

2.3.1.3 Synthesis of N-Fmoc-cis-4-guanine-D-proline (G monomer)
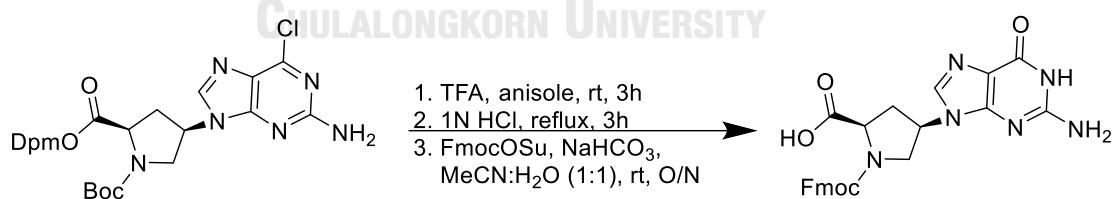
N-Boc-*cis*-4-G^{Cl}-D-proline diphenylmethyl ester (690 mg, 1.24 mmol) was treated with 10% anisole in TFA (3 mL) for 3 hrs. After the TFA was removed by a stream of nitrogen gas, the residue was washed with diethyl ether to give a white precipitate. This was dissolved in 1 N HCl (10 mL) and refluxed for 3 hrs. Next, the acid was evaporated and the residue was dissolved with 1:1 H$_2$O:MeCN (5 mL) and

treated with NaHCO$_3$ (200 mg, 2.48 mmol). *N*-(9-fluorenylmethoxycarbonyloxy)succinimide (FmocOSu) (300 mg, 1.11 mmol) was added and the reaction mixture was stirred for 8 hrs. After that, the reaction mixture was evaporated, and the residue was diluted with water (10 mL) and extracted with diethyl ether (20 mL, 3 times). The aqueous layer was purged with nitrogen gas to remove the partially dissolved ether followed by acidification to pH 2. The precipitate was collected by filtration, washed with water diethyl ether and dried under vacuum to give the *N*-Fmoc-*cis*-4-guanine-D-proline as a white solid (450 mg, 70% yield). ^{1}H NMR (400 MHz, DMSO) **δ** 10.77 (s, 1H), 7.86, 7.77, 7.66, 7.37 (m, 8H, CHx8) 6.54 (br, 2H, NH$_2$), 4.82 (m, 1H), 4.44, (m, 1H) 4.28 (m, 1H, CH), 4.10 – 3.67 (m, 2H), 2.94 – 2.70 (2m, 2H).

2.3.1.4 Synthesis of 6-Azidomethylnicotinic acid (Pyr-N$_3$)[97]
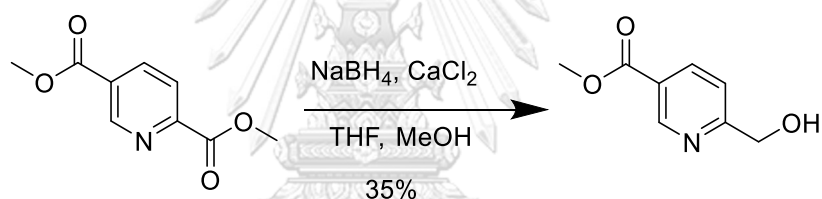
2,5-Pyridinedicarboxylic acid dimethyl ester (500 mg, 2.8 mmol), CaCl$_2$ (1.1 g, 11 mmol) were dissolved by 10 mL of mixture of anhydrous THF and MeOH (1:2) and cooled down in an ice bath. Next, NaBH$_4$ (250 mg, 6.5 mmol) was added and the reaction was stirred at 0 °C. After 3 hours, the reaction was quenched by water and extracted with DCM (20 mL x 3).Then, the organic layer was dried with MgSO$_4$ and removed under vacuum to provide 6-hydroxymethyl-nicotinic acid methyl ester as white solid (150 mg; 35% yield) ^{1}H NMR (400 MHz, CDCl$_3$) **δ** 9.16 (s, 1H, CH), 8.29 (d, *J* = 8.2 Hz, 1H, CH), 7.36 (d, *J* = 8.0 Hz, 1H, CH), 4.83 (s, 2H, CH$_2$), 3.95 (s, 3H, CH$_3$).
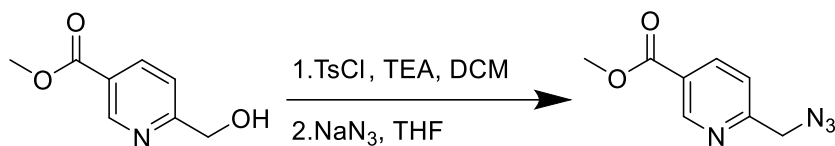
6-Hydroxymethyl-nicotinic acid methyl ester (150 mg, 0.9 mmol) was dissolved in dichloromethane (DCM, 20 mL), and then *p*-toluenesulfonyl chloride (TsCl, 260 mg, 1.35 mmol) and triethylamine (TEA, 620 μL, 4.5 mmol) were added, respectively. After the reaction was stirred for 2 hours, solvent was removed under vacuum. The crude product was dissolved in 10 mL of THF, followed by the addition of sodium azide (60 mg, 1 mmol). The reaction was stirred at room temperature for 1 day. Next, water was added to the reaction and the aqueous layer was extracted with ethyl acetate three times. The organic layer was washed with brine, dried over $MgSO_4$, and concentrated under the vacuum. The crude product was purified by column chromatography on silica gel (4:1 hexanes: ethyl acetate) to give methyl 5-(azidomethyl)nicotinate as a yellow oil (146 mg, 85% yield). ^{1}H NMR (400 MHz, $CDCl_3$) δ 9.18 (s, 1H, CH), 8.33 (d, *J* = 7.7 Hz, 1H, CH), 7.45 (d, *J* = 8.1 Hz, 1H, CH), 4.57 (s, 2H, CH_2), 3.96 (s, 3H, CH_3).
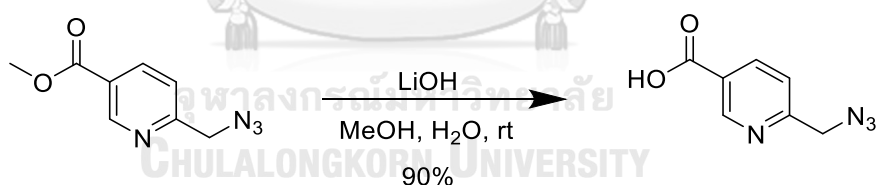
Methyl 5-(azidomethyl)nicotinate (100 mg, 0.5 mmol) was dissolved in methanol (2.5 mL). Then, 1.0 M solution of LiOH in water (1.50 mL, 1.50 mmol) was added and stirred for 30 minutes. Then, the crude product was dried under vacuum and purified with a gradient from ethyl acetate + 1% acetic acid to 4% acetonitrile in ethyl acetate + 1% acetic acid to get 80 mg (86%) of 6-azidomethylnicotinic acid (Pyr-N_3) as a yellow oil. ^{1}H NMR (400 MHz, DMSO) δ 9.02 (s, 1H, CH), 8.21 (d, *J* = 8.0 Hz, 1H, CH), 7.40 (d, *J* = 7.8 Hz, 1H, CH), 4.53 (s, 2H, CH_3).

2.3.2 Solid phase peptide synthesis

All acpcPNA probes with the sequences shown in **Table 2.1** were manually synthesized by Fmoc solid phase peptide synthesis (SPPS) on the Tentagel S RAM resin at 1.5 μmol scale. The reactions were performed in a home-made glass column (150 x 7 mm) with a short fritted glass plug (2-3 mm) using the four Fmoc-protected acpcPNA monomer (A^{Bz}, C^{Bz}, T, G) the **β**-amino acid spacer (Fmoc-(1S,2S)-2-aminocycolpentanecarboxylic acid). To improve the solubility in aqueous media, one or more lysine units were included in all acpcPNA sequences either at the C- or N-termini. In the SPPS, there were three steps in each cycle including:

1) Deprotection: The Fmoc protecting group at the N-terminal position of the peptide chain on the resin was removed by treatment of the resin with 100 μL of the deprotecting solution consisting of 20% piperidine and 2% DBU in DMF for 5 min at room temperature with occasional agitation to give the active free amino group.

2) Coupling: In the case of the Pfp-activated monomers including Fmoc-Lys(Boc)-OPfp, acpcPNA monomer (T, A^{Bz}, C^{Bz}) or ACPC spacer, 4 equiv. of the monomer were prepared in 30 μL of coupling solution containing 4 equiv. of HOAt and 7% of DIEA in DMF. In the case of the acpcPNA G monomer and Fmoc-Tyr(alk)-OH (from Dr. Duangrat Nimanussornkul), which was used as the free carboxylic acid due to the instability of the Pfp ester, 4 equivalents of the free acid were activated with 3.9 equiv. of HATU in the presence of 7% of DIEA in DMF (30 μL) for a few minutes prior to the coupling reaction. The deprotected resin was treated with the coupling solution for at least 30 min at room temperature with occasional agitation.

3) Capping: The unreacted free amino groups were capped to prevent further sequence extension in the next cycles by acetylation with 10% acetic anhydride and 7% DIEA in DMF (30 μL) for 5 min at room temperature with occasional agitation.

After finishing each step, the resin was exhaustively washed with DMF to ensure the complete removal of excess reagents. The cycle was repeated until the desired sequence was obtained. Then, the Fmoc protection on the final N-terminal amino group was removed and the liberated free amino group was capped with an acetyl group or a fluorescent dye (**Section 2.2.3**).[50]

Table 2.1 Sequences of PNA and their purposes

Sequence (N → C)	Purpose (section)
Ac-GTAGATCACT-KKKKK	HG (**3.4**)
Ac-AGTGATCTAC-KKKKK	GO (**3.2.2**)
Flu-GTAGATCACT-K	GO (**3.2**), GX, MD (**3.3**), HG (**3.4**)
Flu-GTAGATCACT-KKKKK	GO (**3.2**), GX (**3.3**)
Flu-GCTTTTTTACA-KKKKK	GX (**3.3.3.1**)
Flu-AGTCTGATAAGC-KKKKK	GX (**3.3.3.1**)
Flu-TTAATACCTTTGCTC-KKK	GX (**3.3.3.1**)
TMR-CTAAATTCAGA-KKKK	GX (**3.3.3.2**)
Flu-KKKKK-GTAGA-Tyr(AlK)	RXN (**3.3.3.4**)
Flu-TT-Tyr(AlK)	RXN (**3.3.3.4**)
Ac-TT-Tyr(AlK)	RXN (**3.3.3.4**)
N_3-TT-KKKKK	RXN (**3.3.3.4**)
N_3-TCACT-KKKKK	RXN (**3.3.3.4**)
Nr-GTAGATCACT-K	GO (**3.2.1**)
STR-GTAGATCACT-K	GO (**3.2.1**)

*__GO__ = PNA-Graphene platform, **GX** = PNA-oligodeoxyguanosine (PG) platform, **MD** = Metal detection by PG, **RXN** = reaction detection by PG, **HG** = Hemin-G-quarduplex DNAzyme

2.3.3 Attachment of the fluorescent dye and azide molecule on acpcPNA

2.3.3.1 Attachment of fluorescent dye via amide coupling

The N-terminal Fmoc group of the PNA (0.5 µmol) was deprotected whilst still on the solid support using the conditions similar to the deprotection step in the SPPS cycle (**Section 2.3.2**). Next, the free amino group was treated with 5(6)-carboxyfluorescein *N*-hydroxysuccinimide ester (2 mg, 8 equiv.) or 5(6)-carboxytetramethylrhodamine *N*-hydroxysuccinimide (2.1 mg, 8 equiv) in 20 µL DMF solution containing 10% DIEA at room temperature in the absence of light. The progress of the reaction was monitored by MALDI-TOF MS. Due to the sluggishness of the reaction, prolonged reaction periods were employed to ensure complete reaction (3 and 5 days for Flu and TMR, respectively).

2.3.3.2 Attachment of fluorescent dye via click reaction

The N-terminal Fmoc group of the PNA (0.5 µmol) on the solid support was deprotected using the conditions similar to the deprotection step in the SPPS cycle and the free amino group was modified with the azide group by reductive alkylation reaction with 4-azidobutanal (15 µmol), in the presence of $NaBH_3CN$ (30 µmol) and acetic acid (30 µmol) in MeOH (200 µL) at room temperature for overnight.[98]

2.3.3.3 Attachment of 6-Azidomethylnicotinic acid (Pyr-N$_3$)

The N-terminal Fmoc group of the PNA (0.5 µmol) on the solid support was deprotected using the conditions similar to the deprotection step in the SPPS cycle and the free amino group was modified with the $Pyr-N_3$ (4 equiv.) by using 3.9 equiv. of HATU in the presence of 7% of DIEA in DMF (30 µL) for at least 1 hour at room temperature with occasional agitation.

2.3.4 PNA purification, and characterization

After the PNA synthesis and N-terminal modification was completed, the nucleobase side chain was deprotected by treatment of the PNA on the resin with aqueous NH_3/dioxane (1:1) (2 mL) in a screw-capped test tube at 65 °C for 8 hrs. Then, the sidechain deprotected PNA was cleaved from the solid support by treatment with trifluoroacetic acid (TFA) containing 1% water (500 µL × 30 min x 3). The TFA in the cleavage solution was evaporated under a stream of nitrogen gas and the crude PNA in the residue was reprecipitated by diethyl ether. The precipitate was centrifugally washed with diethyl ether (3 times) and air-dried. The crude PNA was then dissolved in 120 µL of water, and purified by reverse-phase HPLC using 0.1% TFA in water:methanol (W:M) gradient as a mobile phase with the flow rate of 0.5 mL/min. The gradient elution was proceeded with W:M 9:1 for 5 minutes, then the ratio of W:M was changed to 1:9 over 60 minutes. The HPLC peaks were monitored in real time by the Waters 996 photodiode array detector via the Waters Empower software. Fractions were collected manually and those containing the desired PNA

according to MALDI-TOF MS analysis were combined and freeze-dried to obtain the purified acpcPNA. The combined fractions were characterized by MALDI-TOF MS using α-cyano-4-hydroxycinnamic acid (CCA) as the matrix. The purity of the PNA was confirmed by reverse phase HPLC analysis by using the similar gradient elution W:M 9:1 for 5 minutes, then the ratio was changed to 1:9 over 30 minutes.

2.3.5 PNA concentration determination

The concentration of the PNA stock solution was determined using UV-vis spectrophotometry as follows. An appropriate volume of the PNA stock solution (typically 2 μL) was diluted with 10 mM sodium phosphate buffer pH 7.0 to the final volume of 1 mL in a 10 mm path length quartz cuvette. The absorbance at 260 nm was measured and the OD_{260} was calculated using the **equation 2.1** below.

$$OD_{260} = \frac{A_{260} \times \text{total volume}}{\text{sample volume}} \quad \textbf{(2.1)}$$

Next, the concentration of the PNA was calculated using the **equation 2.2** below using the extinction coefficients value (ε) that is unique for the sequence of the PNA strand. This value was obtained by summing the contribution to the absorption at 260 nm from various nucleobases as well as the dye label. The ε_{260} value was conveniently retrieved from an in-house web-based software (http://www.chemistry.sc.chula.ac.th/pna/pna.asp) written by Vilaivan's group.

$$\text{PNA concentration } (\mu M) = \frac{OD_{260}}{\varepsilon} \times 1000 \quad \textbf{(2.2)}$$

2.4 General Characterization

2.4.1 UV-visible and thermal denaturation experiments

UV-visible experiments were performed at 20 °C in a 10 mm path length quartz cuvette with a Teflon stopper. The samples were prepared at the specified concentration in a suitable buffer with a total volume of 1 mL. For melting temperature (T_m) measurements, the temperature was increased from 20 C to 95 C

at a rate of 1.0 C/min. The absorption at 260 nm at each temperature was recorded. The result was processed using Kaleidagraph 4.0 (Synergy software) and Microsoft Excel. Then, the T_m was calculated from the maximum value of the first derivative plot.

2.4.2 Circular dichroism (CD) experiments

The samples were prepared at the specified concentration in a suitable buffer with a total volume of 1 mL in a 10 mm path length quartz cuvette with a Teflon stopper. The CD spectra were measured at 25 °C, with 4 repetitions, scanning over the range of 200 to 400 nm and at the scanning rate of 100 nm/min. The data were then subtracted from the spectrum of the blank (buffer only) under identical conditions.

2.4.3 Gel electrophoresis

The acrylamide gel (17%) was prepared by mixing acrylamide/bisacrylamide solution (29:1), 40% (w/v) (5 mL), ammonium persulfate (10 mg), 10×Tris borate-EDTA buffer (TBE) (1 mL), and milli-Q water (3 mL) in a 15 mL polypropylene tube. Next, 10 µL of *N,N,N',N'*-tetramethylenediamine (TEMED) was immediately added. The solution was mixed rapidly and transferred to the gel electrophoresis apparatus. After leaving for the polymerization to proceed for 1 h at room temperature, the 10 µL of samples consisting PNA (0.5 nmol) and/or DNA (0.6 nmol), and 1× loading dye (1 µM) were loaded onto the gel. The electrophoresis apparatus was connected to a power supply, and the experiment was performed at a voltage of 150 V for 1.5 hrs. The gel was visualized under a UV transilluminator (365 nm) and by UV shadowing (256 nm) over a silica gel GF254-coated TLC plate. The photographs were taken under UV transilluminator model VILBER LOURMAT TCP-20.LM either at 365 or 256 nm using a Canon EOS M digital camera through a yellow filter.

2.5 Fluorescence experiment

The samples (1 mL) were prepared in a suitable buffer at the specified PNA and DNA concentrations in a 10 mm quartz cell with a Teflon stopper. The excitation

and emission slits width were set at 5 nm. **Table 2.2** shows the excitation and emission wavelength for each dye.

Table 2.2 Excitation and emission wavelength of each dye

Fluorescent dye	Excitation (nm)	Emission (nm)
Fluorescein	460*, 490**	470*, 500**
TAMRA	520	530
Styryl dye	550	560
Nile red	580	590

* For section 3.2 ** for section 3.3

In the case of fluorescence quenching and restoration experiments, the data were reported in term of brightness percentage at the specific emission wavelength as shown in the **equation 2.3** below.

$$\text{Brightness percentage} = \frac{F_{sample}}{F_{ssPNA}} \times 100 \quad \textbf{(2.3)}$$

2.5.1. PNA-Graphene oxide platform

2.5.1.1 Graphene oxide quenching experiments

The working solution consisting of the dye labeled acpcPNA (0.1 μM) in 10 mM Tris-HCl buffer pH 7.4 (1 mL) was added graphene oxide (GO) at the specify concentration. After the incubation at room temperature for 30 min, the fluorescence spectrum of the mixture was measured, and the brightness percentage calculated.

2.5.1.2 Fluorescence restoration experiments

The DNA targets were added into the GO-quenched PNA probe solution at the specified concentration. The solution was incubated at room temperature for 30 min before recording the fluorescence spectrum. The brightness percentage was then calculated according to **equation 2.3**.

2.5.1.3 Sensitivity

The complementary DNA target was added into the GO-quenched fluorescein-labeled PNA probe solution at various concentrations (three independent experiments were performed for each concentration). The solution was incubated at room temperature for 30 min before recording the fluorescence spectrum. The fluorescence at 525 nm were plotted against the DNA target concentration to give a linear calibration graph. The limit of detection was calculated from the **equation 2.4** below:

$$\text{Limit of Detection } (LOD) = \frac{3SD}{slope} \quad \textbf{(2.4)}$$

2.5.1.4 Invasion experiments

The sample consisting of 1 μM of fluorescein-labeled acpcPNA probe (FluK5) was mixed with 1.2 μM of the 30mer dsDNA targets and incubated at 25 °C for 30 min. Next, the pseudo complementary acpcPNA strand (antiPNAK5) was added and the mixture was incubated for 8 hours. Next, the PNA-dsDNA-antiPNA mixture was treated with GO at 5 μg/mL and the fluorescence quenching was examined by fluorescence spectroscopy. The brightness percentage was then calculated according to **equation 2.3**.

2.5.1.5 Naked-eye detection

The working solution consisted of the dye labeled acpcPNA (10 μM) and GO (50 μg/mL) in 10 mM Tris-HCl buffer pH 7.4 with a total volume of 20 μL was incubated at room temperature for 10 min. Next, the target DNA (12 μM) was added and the solution was incubated at room temperature for 30 min. After that, the photographs were taken under a UV transilluminator at 365 nm using a digital camera through a yellow filter.

2.5.2. PNA-Oligodeoxyguanosine platform

2.5.2.1 Oligodeoxyguanosine quenching experiments

   The working solution consisting of the dye labeled acpcPNA (1 µM or 0.1 µM) in 10 mM phosphate buffer pH 7 (1 mL) was added the oligodeoxyguanosine or other guanine-rich DNA sequence at the specified concentration. After incubation at room temperature for 30 min, the fluorescence spectrum of the mixture was measured, and the brightness percentage was calculated by **equation 2.3**. Moreover, the absorption and CD spectra were also measured for certain samples.

2.5.2.2 Fluorescence restoration experiments

   The DNA targets were added into the GO-quenched PNA probe solution at the specified concentration. The solution was incubated at room temperature for 30 min before recording the fluorescence spectrum. The brightness percentage was then calculated according to **equation 2.3**.

2.5.2.3 Sensitivity

   The complementary DNA target was added into the oligodeoxyguanosine-quenched PNA probe solution at various concentrations (three experiments were conducted for each concentration). The solution was incubated at room temperature for 30 min before recording the fluorescence spectrum. The limit of detection was calculated from the **equation 2.4** as explained in **Section 2.5.1.3**.

2.5.2.4 Naked-eye detection

   The working solution consisted of the dye labeled acpcPNA (10 µM) and oligodeoxyguanosine (12 µM) in 10 mM phosphate buffer pH 7 with a total volume of 20 µL was incubated at room temperature for 10 min. Next, the target DNA was added to give the final concentrations of PNA, oligodeoxyguanosine and DNA = 10, 12 and 12 µM, and the solution was incubated at room temperature for 30 min. After that, the photographs were taken under a UV transilluminator at 365 nm using a digital camera through a yellow filter.

2.5.2.5 Metal ions detection

The PNA-DNA solution was first prepared by mixing the fluorescent dye labeled acpcPNA (0.1 μM) and DNA target at the specified concentration in 10 mM MOPS buffer (1 mL) and incubated for 10 min at room temperature. Then, the metal ion (Ag^+ or Hg^{2+}) at the specific concentration was added and incubated at room temperature for 15 minutes. Next, the oligodeoxyguanosine (0.1 μM) was added to the solution. After incubated at room temperature for 30 min, the fluorescence spectrum was recorded. The brightness percentage was then calculated according to **equation 2.3**.

2.5.2.6 Click chemistry detection

A solution containing 500 μM of azide-PNA and 100 μM of alkyne-PNA was prepared in 1:1 H_2O:^tBuOH (20 μL). Then, 100 μM of [$CuSO_4$·$5H_2O$], 100 μM of tris-hydroxypropyltriazolylmethylamine (THPTA),[99] and 400 μM of sodium ascorbate were added, respectively, and the mixture was incubated at room temperature for 2 hours. Next, 10 μL of the reaction was sampled and diluted with 10 μL of 10 mM phosphate buffer pH 7. Then, dG10 was added to the solution with a final volume 20 μL to give the final concentration of 12 μM. After incubated at room temperature for 15 min, the photographs were taken under a UV transilluminator at 365 nm using a digital camera through a yellow filter.

2.6 Hemin-G-quadruplex colorimetric assay

2.6.1 Naked-eye detection for Hemin/dG DNAzyme

The working solution consisting of the TMB dye (100 μM), hemin (0.125 μM) and quadruplex DNA (1 μM) in 20 μM HEPES buffer pH 7.4 containing 200 mM of NH_4OAc with a total volume of 20 μL was prepared in a PCR tube. Then 1 μL of H_2O_2 (10 mM) was added and the photographs were taken under visible light using a digital camera. The photographs were recorded every five minutes until no further color change was observed.

2.6.2. Naked- eye detection for DNA displacement

A solution containing 3 µM of PNA and 3 µM DNA with guanosine overhang was prepared in 20 µM of HEPES buffer pH 7.4 containing 200 mM of NH$_4$OAc with a total volume of 20 mL was prepared in a PCR tube. Then, 3 µM of the DNA target was added and the reaction was incubated for 30 minutes. After that, TMB dye (100 µM) and hemin (0.08 µM) were added, respectively. Finally, 1 µL of 30% H$_2$O$_2$ (10 mM) was added and the photographs were taken under visible light using a digital camera. The photographs were recorded every five minutes until no further color change was observed.

2.6.3. UV-visible spectrophotometry

The working solution consisting of the TMB dye (100 µM), hemin (0.08 µM) and quadruplex-forming DNA (0.4 µM) in 20 µM of HEPES buffer pH 7.4 containing 200 mM of NH$_4$OAc with a total volume of 1 mL was prepared in a quartz cuvette with 10 mm pathlength. Then, 30% H$_2$O$_2$ was added to the final concentration of 1 mM, and the absorption was immediately recorded from 200 – 700 nm every 5 min interval for 30 minutes.
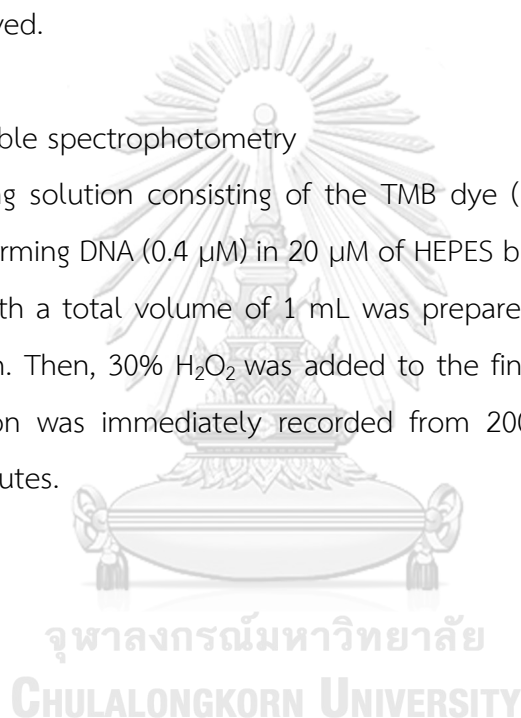
CHAPTER 3

RESULTS AND DISCUSSION

This chapter presents the development of a new DNA sensing platform that can change its fluorescence signal in respond to the correct DNA target. The sensor consisted of a fluorescently labeled acpcPNA probe and an external quencher including graphene oxide and oligodeoxyguanosine. The chapter is divided into four parts. The first part demonstrates the synthesis, modification, and characterization of the acpcPNA probe. The second part highlights the development of the sensor of fluorescently labeled acpcPNA probe (F-PNA) with graphene oxide. The third part focuses on the quenching phenomena between the F-PNA and the oligodeoxyguanosine (dG) and the applications of the F-PNA and dG platform. The final part presented the preliminary studies of another DNA sensing platform based on PNA probe and Hemin/G-quadruplex DNAzyme.

3.1 Synthesis of peptide nucleic acid probes

3.1.1 Synthesis of acpcPNA

All acpcPNA probes were manually synthesized using Fmoc-solid phase peptide synthesis (SPPS) on the Tentagel S RAM resin at 1.5 μmol scale using Fmoc-protected acpcPNA monomer (A^{Bz}, C^{Bz}, T, G) and β-amino acids spacers (Fmoc-(1S,2S)-2-aminocycolpentanecarboxylic acid). In order to improve the solubility and prevent the self-aggregation in aqueous solution, all acpcPNA sequences were incorporated with at least one lysine unit at either C- or N-terminus.[100] The PNAs were synthesized through the synthetic cycle which consisted of three steps: 1) the deprotection of Fmoc group with DBU/piperidine solution, 2) the coupling reaction to incorporate the amino acid, acpcPNA monomer and spacer, and 3) the capping of uncoupled amino groups by acetic anhydride to prevent further reactions. To remove the excess reagents after completing each step, the resin was exhaustively washed with DMF for at least three times. The synthesis cycle of the PNA was repeated until the desired

sequences were obtained. Then, the final N-terminal group was deprotected and capped by the acetyl group or a fluorescent dye (Section 3.1.2).

3.1.2 Attachment of the fluorescent dye

The labelling of the fluorescent dyes on the acpcPNA, two methods were employed. Before the dye was attached to the N-terminal amino group, the N-terminal Fmoc group of the PNA on the solid support was removed using the piperidine solution resulting in the formation of free amino group ready for the modification. This was followed by treatment with aqueous NH_3/dioxane (1:1) at 65 °C for 8 hours to remove the nucleobase protecting groups to avoid subsequent treatment of the dye-labeled PNA to this rather harsh conditions. In case of fluorescent dyes containing the activated carboxylic group such as 5(6)-carboxyfluorescein *N*-hydroxysuccinimide ester and 5(6)-carboxytetramethyl-rhodamine *N*-hydroxysuccinimide ester, the dyes were attached to the PNA directly in the presence of a base (10% of DIEA in DMF solution). The reaction was sluggish and required 3 to 5 days to complete according to MALDI-TOF MS analysis. In case of the fluorescent dye containing the alkyne group, the free amine group at the N-terminus of the last PNA monomer was modified with an azide group through the reductive alkylation reaction with 4-azidobutanal. In such case, the final ACPC spacer was omitted to avoid complication due to double alkylation of the free NH_2 group. Then, the propargylated dye labels including Nile red (synthesized in another project)[46] and styryl dye[52] was attached to the PNA via Click chemistry in the presence of $Cu(I)PF_6$-TBTA-Na ascorbate.[98]

3.1.3 Purification and characterization of acpcPNA

The crude acpcPNA (typically 0.5 µmol) was purified by C_{18} reverse phase HPLC, eluting with a gradient system of 0.1% TFA in methanol/water or acetonitrile/water. Fractions collection was assisted by monitoring the UV absorption at 310 nm. The fractions containing the pure PNA as determined by MALDI-TOF MS were combined, freeze-dried and re-dissolved in 120 µL of water. The concentration of the PNA was determined by UV-Vis spectrophotometry at the absorption 260 nm

and calculated by equation 2.2. The identity of the PNA probes was verified by MALDI-TOF MS and the purity was confirmed to be >90% by analytical reverse phase HPLC. Most fluorescein-labeled probes (Flu-sequence-Lys$_n$) appeared as two peaks in the HPLC chromatogram due to the presence of two isomers (5 and 6-carboxy), but no attempts were made to isolate the pure isomers because of the peaks overlaps and the irrelevance of the pure isomer to the purpose of this work. As a result, they were used as a mixture. For some short PNA sequences (less than five bases) such as Ac-TT-Tyr(Alk), N$_3$-(nX)-TT-KKKKK, Flu-K-GTAGA-Tyr(Alk), N$_3$-(nX)-TCACT-KKKKK, etc. no purification was performed if the MALDI-TOF analysis suggested good purity.

Table 3.1 Characteristics of all acpcPNA probes used in this dissertation

Sequence (N → C)	*m/z* cald (M•H$^+$)	*m/z* found	t$_R$ (min)	%yield
Ac-GTAGATCACT-KKKKK	4,071.5	4068.9	N.D.	19
Flu-GTAGATCACT-K	3,875.1	3879.5	33.1	25
Flu-GTAGATCACT-KKKKK	4,387.8	4385.7	29.4	30
Flu-GCTTTTTTACA-KKKKK	4,86.1	4685.4	30.3	21
Flu-AGTCTGATAAGC-KKKKK	5,086.5	5085.5	30.3	17
Flu-TTAATACCTTTGCTC-KKK	5,738.2	5737.4	30.4	23
TMR-CTAAATTCAGA-KKKK	4,640.1	4637.7	32.7	18
Flu-KKKKK-GTAGA-Tyr(Alk)	2,875.2	2875.0	N.D.	N.D.
Flu-TT-Tyr(Alk)	1,169.2	1,171.3	N.D.	N.D.
Ac-TT-Tyr(AlK)	853.0	850.2	N.D.	N.D.
N$_3$-TT-KKKKK	1,312.5	1309.5	N.D.	N.D.
N$_3$-TCACT-KKKKK	2,288.5	2,288.0	N.D.	N.D.
Nr-GTAGATCACT-K	3878.6	3880.7	N.D.	13

*N.D. = Not determined

3.2 PNA-based DNA sensing with graphene oxide as a quencher

At the early stage of this dissertation, the DNA detection experiments were started by using (acpcPNA) as a probe in combination with graphene oxide (GO) as a quencher. This material contains various oxygenated functional groups (epoxide, hydroxyl, and carboxyl group) decorated on the monolayer of graphene making it negatively charged and can be well-dispersed in water.[101] GO was known to preferentially adsorb single-stranded DNA over double-stranded DNA. It was reported that the unpaired nucleobases almost laid flat on the surface of GO via π-π stacking interaction.[102] If the DNA carries a fluorescence label, the close contact between the GO and the labeled DNA would result in quenching of the fluorescence signal.[55] Hybridization with another complementary DNA strand restores the fluorescence because the duplex DNA would interact less strongly with the GO due to the participation of the nucleobases in the Watson-Crick type base pairing. This principle has been extensively developed into several DNA sensing platforms. Over the past decades, several DNA sensing platforms employing the combination of GO and fluorescent DNA probes have been proposed.[103] These include the simple GO-DNA combination[17] and the more sophisticated designs such as the GO-based MB probes[104, 105] and the GO-based DNA biosensor with enzymatic based amplification.[106] Most of these platforms typically employed DNA as the probe. Only recently that PNA was introduced as an alternative probe. In 2013, an aegPNA-GO platform was proposed as a novel, sensitive and selective DNA sensor.[18] The result showed that the use of PNA as a probe could increase the quenching ability and selectivity of the detection. Since then, the aegPNA-GO sensing platform has been adopted in various biosensing applications.[61, 107-109] .

In this work, we were interested in applying the same concept to acpcPNA probes (**Figure 3.1**), which are known to form hybrids with DNA with higher affinity and specificity than DNA and aegPNA probes with the expectation that it would offer a good DNA sensing performance.
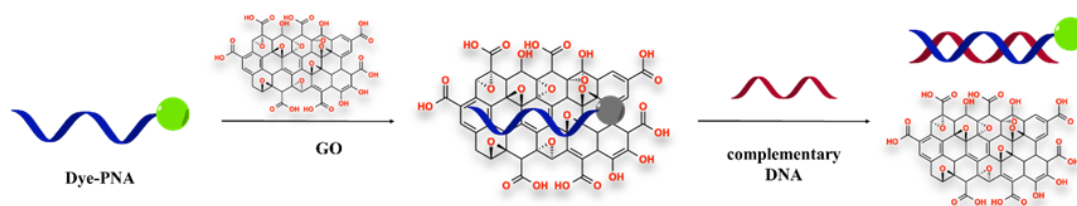
Figure 3.1 The principle of PNA-GO platform for DNA sensing

3.2.1 Types of fluorescent dye on acpcPNA

The study employed acpcPNA labeled with a fluorescent dye including fluorescein, Nile red and a styryl dye (from Dr. Boonsong Ditmangklo)[52] as a reporter probe (**Figure 3.2)** for sequence specific detection of DNA through its interaction with GO. To achieve this goal, a 10mer florescent dye-labeled acpcPNA probe (Dye-PNA) was incubated with GO for 30 min followed by addition of the DNA target. The fluorescence spectra were measured by fluorescence spectrophotometry at an appropriate excitation wavelength of the dye (460 nm, 590 nm, and 550 nm for fluorescein, Nile red, and styryl dye, respectively).

DyeK1 : Dye-GTAGATCACT-Lys	**DNAnon**:	3'-GATTTACGTCT-5'.
DNAcom: 3'-<u>CATCTAGTGA</u>-5'	**DNAcomL**:	3'-GGTCCCGTAC<u>CATCTAGTGA</u>CATGCGGCGC-5'
DNAMisC: 3'-<u>CATCT</u>C<u>GTGA</u>-5'	**DNAssmmL**:	3'-GGTCCCGTAC<u>CATCT</u>T<u>GTGA</u>CATGCGGCGC-5'
DNAMisG: 3'-<u>CATCT</u>G<u>GTGA</u>-5'	**DNAdbmmL**:	3'-GGTCCCGTAC<u>CATC</u>GC<u>GTGA</u>CATGCGGCGC-5'
DNAMisT: 3'-<u>CATCT</u>T<u>GTGA</u>-5'	**DNAnonL**:	3'-GCGCCGCATGTCACTAGATGGTACGGGACC-5'
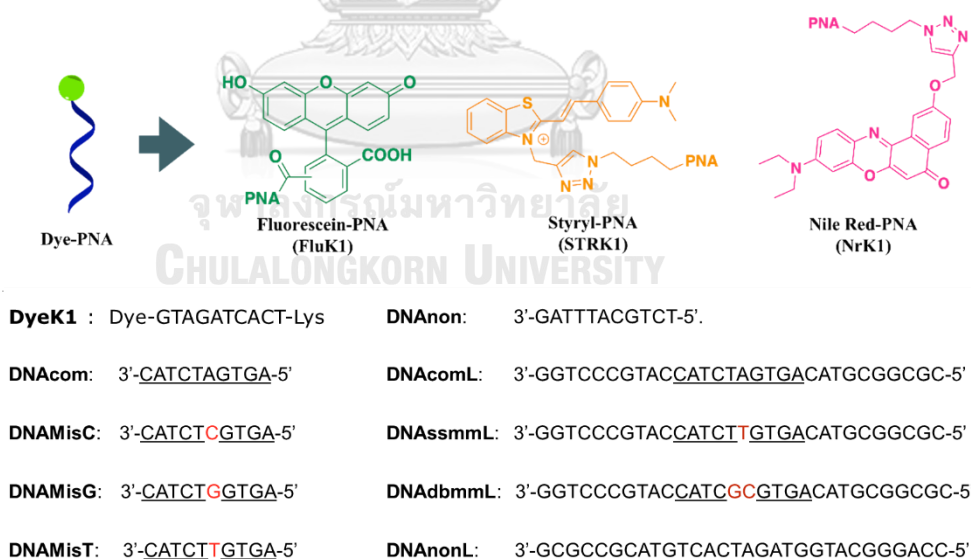
Figure 3.2 The acpcPNA labeled with fluorescent dyes and all sequences in type of fluorescent dye study

3.2.1.1 Fluorescein labeled acpcPNA

The interaction of a 10mer fluorescein-labeled acpcPNA probe (FluK1) and GO was studied by fluorescence spectrophotometry. In all studies, the concentration of FluK1 was fixed at 0.1 µM and then the quenching of the fluorescence by GO was investigated. The results showed that the fluorescence signal of single-stranded FluK1 was dramatically quenched after titration of the GO (0 to 1.5 µg/mL) into the FluK1 solution (**Figure 3.3**). At the concentration of GO above 2 µg/mL, the fluorescence remained stable suggesting that the maximum quenching had been achieved. From the results, it could be concluded that the fluorescein labeled acpcPNA probe (FluK1) could interact with the surface of GO leading to the fluorescence quenching phenomenon like DNA or the commercial aegPNA.[18, 101, 110, 111]

Figure 3.3 Quenching ability of FluK1-GO platform Conditions: [PNA] = 0.1 µM, [GO] = 0 - 1.5 µg/mL in 10 mM Tris-HCl pH 7.4, excitation wavelength at 460 nm

Next, the fluorescence of a 0.1 µM solution of FluK1 was quenched to 10% of the original fluorescence value by the selected GO concentration at 1.5 µg/mL. After that, various DNA targets with a similar length (the sequences are shown in **Figure 3.2**) were added into the GO-quenched PNA probe. Pleasingly, the signal was rapidly restored to 95% of the original value when 1.2 equiv. the

complementary DNA (DNAcom) were added at room temperature. On the other hand, the single mismatched DNAs (DNAmisC, DNAmisG, DNAmisT) and non-complementary DNA (DNAnon) could not restore the fluorescence signal under the same conditions (**Figure 3.4**). This GO-quenched FluK1 probe was next applied for the detection of longer DNA targets including complementary DNA (DNAcomL), single mismatched DNA (DNAsmisL), double mismatched DNA (DNAdmisL), and non-complementary DNA (DNAnonL). The results as shown in **Figure 3.5** revealed that this platform could discriminate between the complementary DNA (DNAcomL) and other DNA targets (DNAsmisL, DNAdmisL, DNAnonL). However, the discrimination between complementary and mismatched targets was less effective than the shorter DNA targets. This is largely due to the incomplete fluorescence signal restoration of the long complementary DNA targets, which might be affected by quenching of the DNA-bound probe by the extra DNA bases presented in these long DNA targets. Nevertheless, this platform could detect the longer DNA sequences and still significantly discriminate between the complementary DNA target and other DNA targets.

Figure 3.4 Brightness percentage at 525 nm of FluK1-GO DNA sensing system with similar length of DNA target Conditions: [PNA] = 0.1 μM, [GO] = 1.5 μg/mL, and [DNA] = 0.12 μM in 10 mM Tris-HCl pH 7.4, excitation wavelength at 460 nm

When compared to other reported fluorescein labeled DNA-GO and PNA-GO sensors under comparable conditions,[18] this acpcPNA-GO platform gave a more rapid and better signal restoration, and did not require heating as in the case of aegPNA, which was reported to require the temperature of 45 °C to affect the displacement reaction.[18] Because of the neutral backbone of acpcPNA and a higher stability of the acpcPNA-DNA duplex when compared to other probes, the duplex of acpcPNA could, therefore, detach from the GO's surface more easily.

Figure 3.5 Brightness percentage at 525 nm of FluK1-GO DNA sensing system with longer DNA target Conditions: [PNA] = 0.1 µM, [GO] = 1.5 µg/mL, and [DNA] = 0.12 µM in 10 mM Tris-HCl pH 7.4, excitation wavelength at 460 nm

A calibration curve was constructed by plotting the restored fluorescence and the concentration of DNA (**Figure 3.6**). From the calibration graph, the acpcPNA-GPO detection platform consisting of 0.1 µM of FluK1 and 1.5 µg/mL of GO could detect the DNA target down to 0.7 ± 0.02 nM (calculated by **equation 2.4**) with a linearity range from 5 to 50 nM. Thus, it can be concluded that the combination of fluorescein-labeled acpcPNA and GO can be used for a specific detection of DNA. The sub-nanomolar levels sensitivity was comparable to other PNA-GO systems (0.8 nM).[18] In the next experiments, acpcPNA probes labeled with

other fluorescent dyes were evaluated to compare the fluorescent properties with the fluorescein-labeled PNA probe.
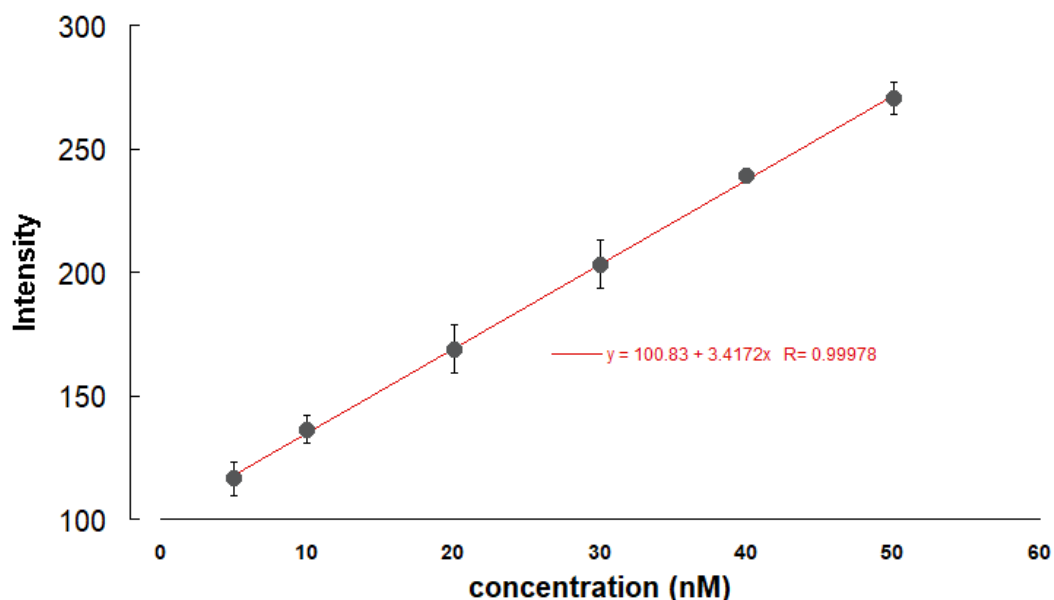
Figure 3.6 Detection limit of FluK1-GO DNA sensing system Conditions: [PNA] = 0.1 μM, [GO] = 1.5 μg/mL, and [DNA] = 5 - 50 nM in 10 mM Tris-HCl pH 7.4, excitation wavelength at 460 nm

3.2.1.2 Styryl dye labeled acpcPNA

Styryl dye is a class of extended π-conjugated system fluorescent dyes that consists of an electron-rich aromatic ring and an electron-deficient *N*-alkylated heterocyclic ring linked to each other via a double bond.[112] In this study, the styryl dye labeled acpcPNA probe was obtained from Dr. Boonsong Ditmangklo.[52] At 0.1 μM concentration of the acpcPNA probe STRK1, its fluorescence was decreased dramatically after the addition of 0.1 to 0.3 μg/mL of GO **(Figure 3.7)**. No further quenching was observed at a GO concentration beyond 0.4 μg/mL. Hence, 0.4 μg/mL of GO was selected for the fluorescence restoration and selectivity studies.
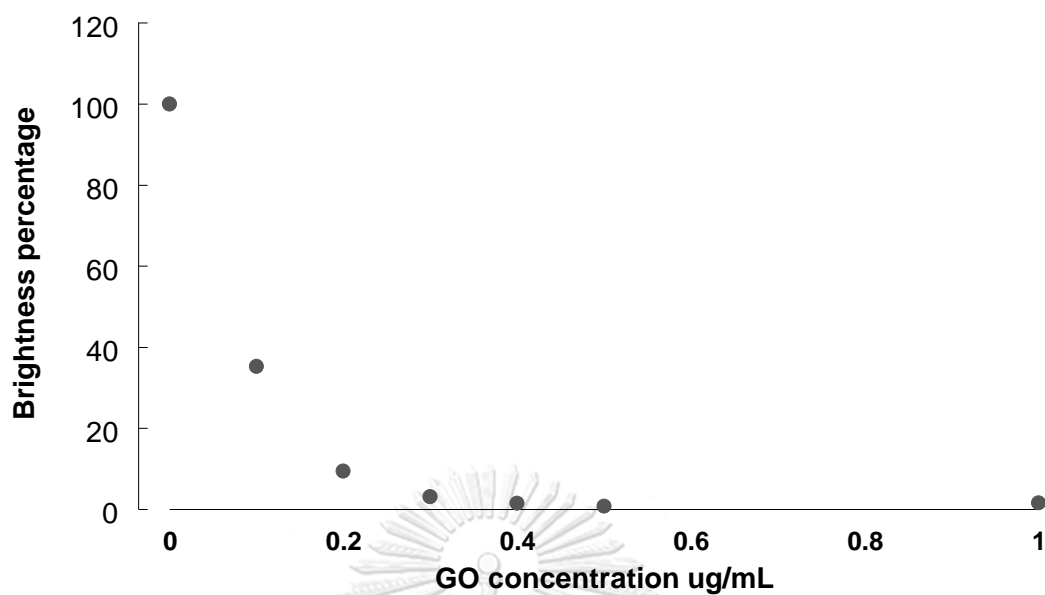
Figure 3.7 Quenching ability of STRK1-GO DNA sensing system Conditions: [PNA] = 0.1 μM and [GO] = 0 - 1 μg/mL in 10 mM Tris-HCl pH 7.4, excitation wavelength at 550 nm
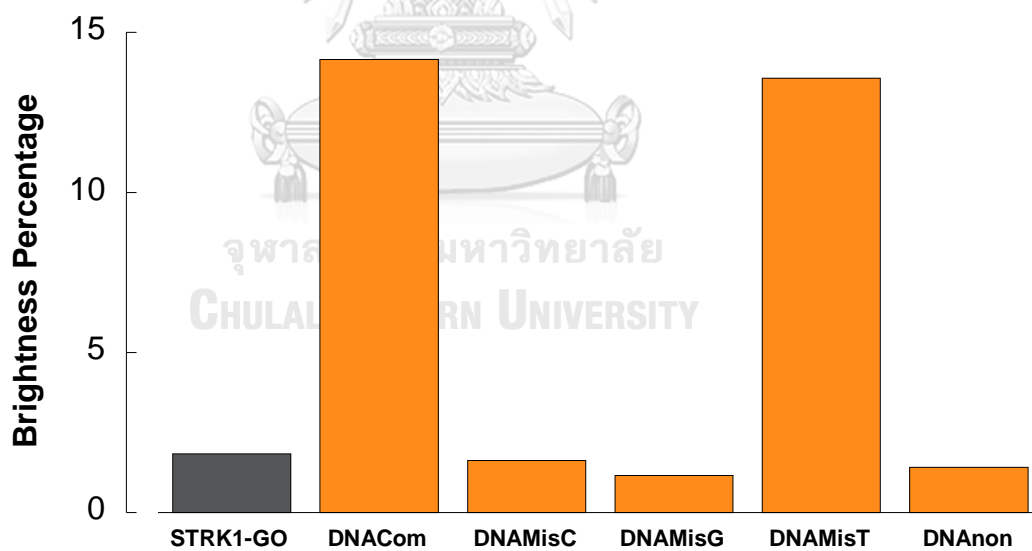
Figure 3.8 Brightness percentage at 540 nm of STRK1-GO DNA sensing system with similar length of DNA target Conditions: [PNA] = 0.1 μM, [GO] = 0.4 μg/mL, [DNA] = 0.12 μM in 10 mM Tris-HCl pH 7.4, excitation wavelength at 550 nm

In the selectivity study of the STRK1-GO platform, the 0.1 μM STRK1 probe solution was first quenched by mixing with GO at 0.4 μg/mL. The brightness percentage after the incubation dramatically decreased to 2.5% of the original value of the STRK1 probe. The quenching efficiency of this STRK1 appeared to be better than the FluK1 probe since lower amounts of GO was required to achieve a higher quenching effect. This can be explained by the fact that styryl dye is positively charged and may contribute to the adsorption and quenching by the negatively charged GO surface. After the addition of the DNA targets as shown in **Figure 3.8**, the fluorescence of the STRK1 probe was only partially restored, up to around 14% of the original value, by the complementary target (DNAcom). The low fluorescence restoration might be attributed to the cationic nature of the dye that makes it interact more strongly with the GO and thus providing additional stabilizing force that may require higher DNA concentrations to completely displace the probe from the GO surface. There seems to be some selectivity since no signal restoration was observed in the cases of DNAMisC and DNAMisG as well as the DNAnon. Unfortunately, the DNAmisT showed a fluorescence restoration similar to the DNAcom. The selectivity is even worse with long DNA targets. As shown in and **Figure 3.9**, the DNAmisL showed almost the same fluorescence restoration as the DNAcomL, although the DNAnonL did not. It should be noted that for these long DNA targets, the fluorescence restoration was much higher than the short DNA targets. In fact, the fluorescence was even higher than the original STRK1 probe. This can be explained by the interaction of the styryl dye label to the nucleobase overhang in the DNA strand. The non-selective fluorescence signal restoration might result from the environment sensitivity of the styryl dye that could enhance the fluorescence when binding with DNA and thus complicating the analysis and interpretation.[113] Thus, although the quenching was good and signal restoration with some selectivity was observed, this system was not studied further.
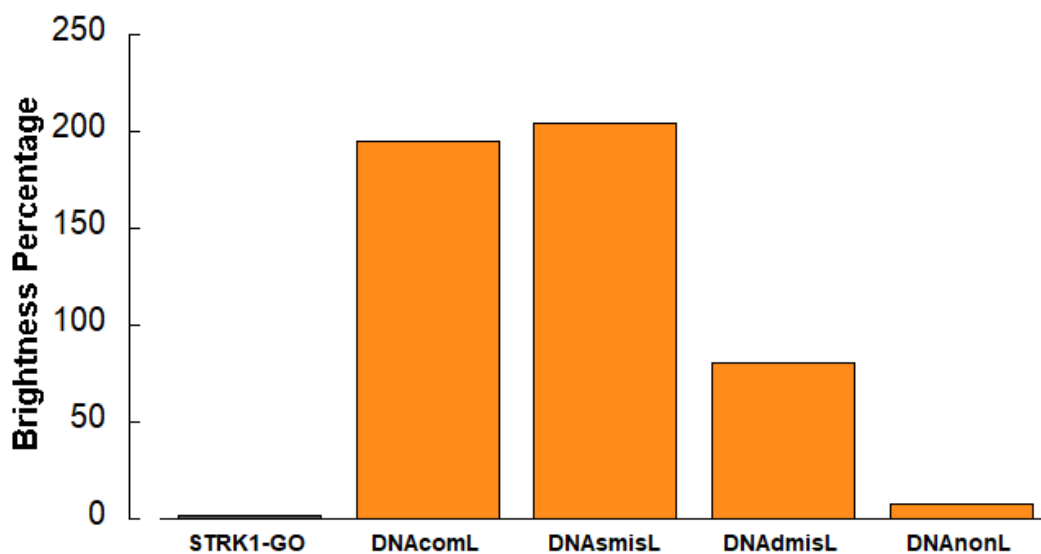
Figure 3.9 Brightness percentage at 540 nm of STRK1-GO DNA sensing system with longer DNA target Conditions: [PNA] = 0.1 µM, [GO] = 0.4 µg/mL, [DNA] = 0.12 µM in 10 mM Tris-HCl pH 7.4, excitation wavelength at 550 nm

3.2.1.3 Nile red labeled acpcPNA
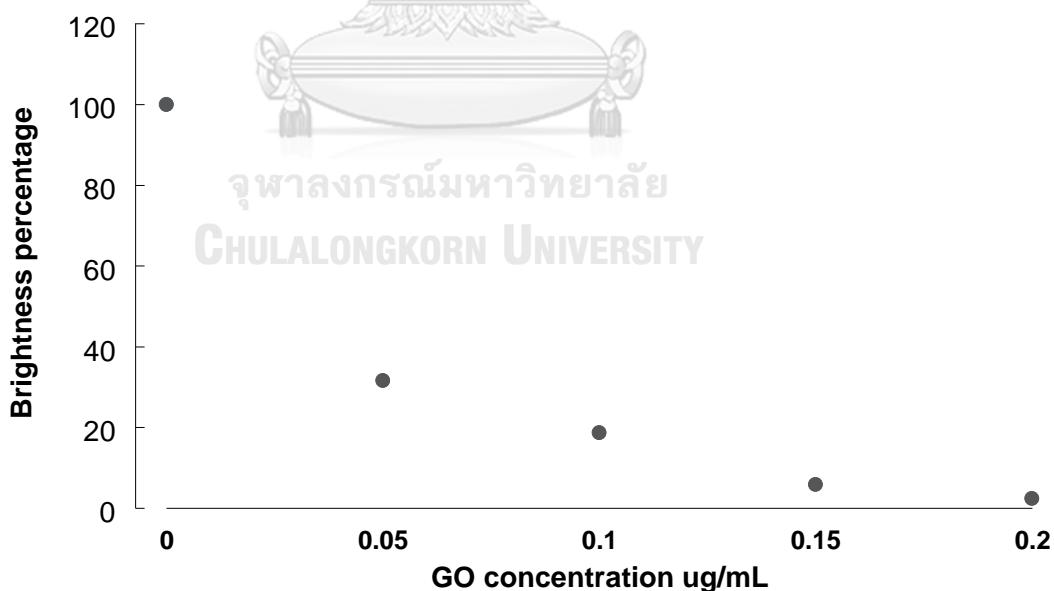
Figure 3.10 Quenching ability of NrK1-GO DNA sensing system Conditions: [PNA] = 0.1 µM, and [GO] = 0 – 0.2 µg/mL in 10 mM Tris-HCl pH 7.4, excitation wavelength at 580 nm

Nile red is an uncharged hydrophobic benzophenoxazine dye which was included in this study as a representative electrostatically neutral dye. This dye was labeled onto the acpcPNA probe at the N-terminus via click chemistry. In the optimization stage, the 0.1 µM solution of the NrK1 probe was mixed with various concentrations of GO. The results showed that the brightness percentage of NrK1 decreased to 30% from the single-stranded NrK1 when 0.05 µg/mL of GO was present. The signal was further decreased to 3% at the GO concentration of 0.2 µg/mL (**Figure 3.10**). Thus, the NrK1 PNA probe carrying the electrostatically neutral Nile red label can also be quenched as effectively as the STRK1 PNA probe carrying the cationic styryl dye. Importantly, the quenching of these two dyes by GO was much more effective than the FluK1 PNA probe bearing a negatively charged fluorescein label. This is consistent with the negative charge nature of the GO surface.
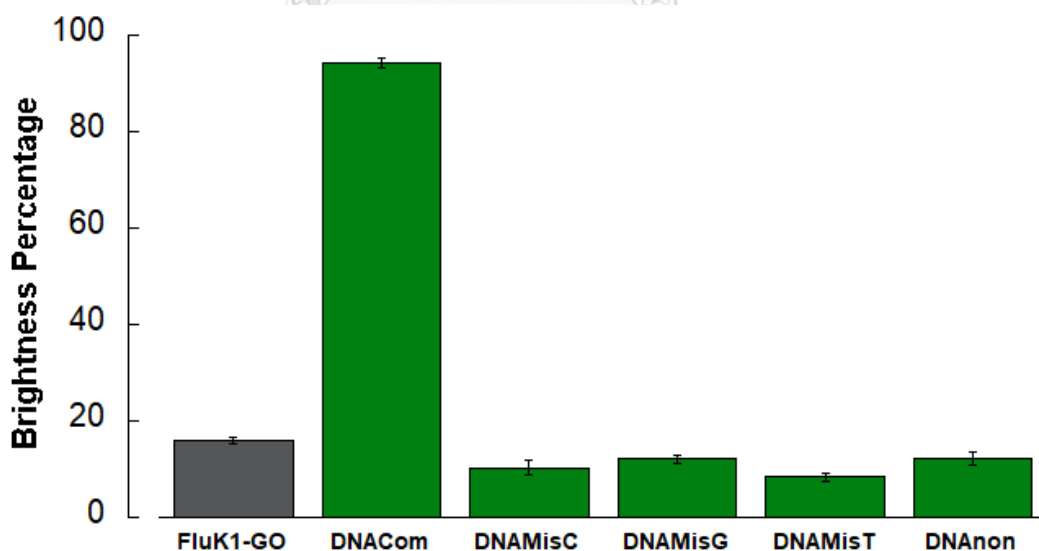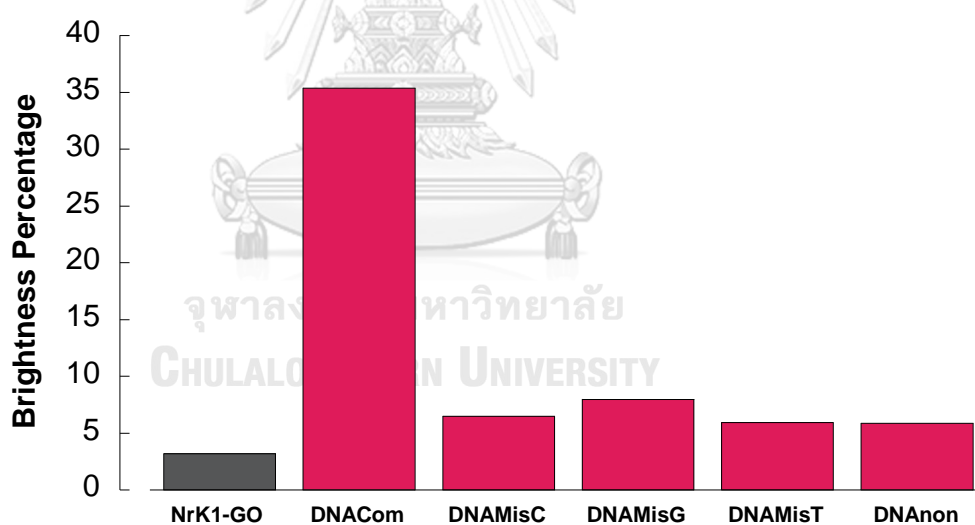

Figure 3.11 Brightness percentage at 580 nm of NrK1-GO DNA sensing system with similar length of DNA target Conditions: [PNA] = 0.1 µM, [GO] = 0.2 µg/mL, [DNA] = 0.12 µM in 10 mM Tris-HCl pH 7.4, excitation wavelength at 580 nm

The selectivity of this NrK1-GO DNA sensor is shown in **Figure 3.11** and **Figure 3.12.** The 0.1 µM solution of NrK1 was first quenched by addition of 0.2 µg/mL of GO, which resulted in a reduction of the fluorescence signal to 3%

comparing with the single-stranded DNA. This platform could clearly discriminate the complementary and mismatched targets with the same length as the probe, which was better than the styryl dye-labeled PNA probe, but the fluorescence restoration was lower than the case of fluorescein-labeled PNA probe. Unfortunately, the discrimination of longer DNA targets was not good even for double mismatched targets.

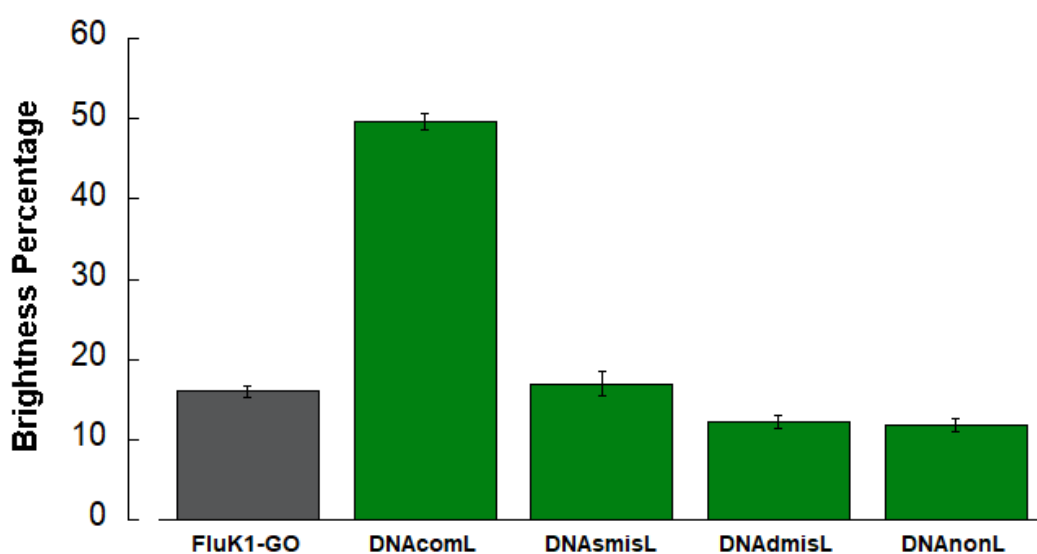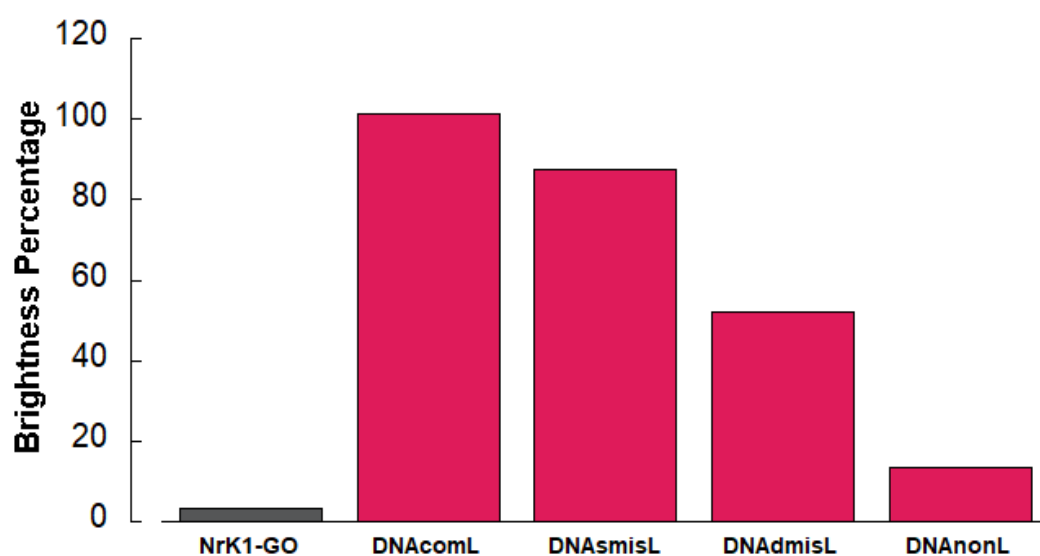**Figure 3.12** Brightness percentage at 580 nm of NrK1-GO DNA sensing system with longer DNA target. Conditions: [PNA] = 0.1 µM, [GO] = 0.2 µg/mL, [DNA] = 0.12 µM in 10 mM Tris-HCl pH 7.4, excitation wavelength at 580 nm

3.2.1.4 Comparison of the three probes

Table 3.2 summarizes the performance of the DNA sensing systems employing three different fluorescent dye-labeled acpcPNA probes and GO as a quencher. Thus, the maximum quenching of the FluK1 probe (at 0.1 µM) by GO was around 15% of the single-stranded PNA probe. This quenching effect was more pronounced in the STRK1 and NrK1 probes at the same probe concentrations, which were quenched down to 1% and 3%, respectively. Although it should be noted that different probes required different concentration GO to achieve the maximum quenching, the above conclusion is still true. At the same concentration of the probe (0.1 µM), the quenching of Nile red and styryl dye was better and required less

concentration of GO (0.2 and 0.4 µg/mL, respectively) than fluorescein (1.5 µg/mL) to achieve the same level of quenching. It can be explained the surface of graphene oxide containing the high density of negatively charge so the interaction of the positively charge or neutral dyes was favorable or neutral. In case of fluorescein, the probe could interact with the surface of graphene oxide via hydrophobic or π-π stacking interaction. However, since the fluorescein dye is negatively charged at neutral pH, there was also contributions from the electrostatic repulsion between the dye and the GO surface. Liu and co-workers had previously reported that fluorescence quenching of positively charged dye was more effective than neutral and negatively charged dyes in the context of DNA probes, which was also explained by the different electrostatic interaction between the dye and GO.[114] In the fluorescence restoration experiment, only the FluK1 showed good fluorescence restoration and the expected selectivity towards complementary DNA targets for both short and long DNA targets. This suggests that the favorable electrostatic interaction that contributed to good quenching on one hand also interfered with the DNA hybridization and the probe displacement from the GO surface on the other hand. Accordingly, only the FluK1 probe showed a good response to its complementary DNA target in the fluorescence restoration process. Hence, fluorescein labeled acpcPNA was selected as the probe for the next studies.

Table 3.2 The brightness percentage of the three PNA-GO DNA sensing systems

Condition/DNA	Brightness Percentage*						GO (µg/mL)
	PNA-GO	Com	ComL	ssmmL	dbmmL	nonL	
FluK1	15	94	50	16	11	11	1.5
STRK1	1	14	194	204	80	7	0.4
NrK1	3	35	101	87	51	13	0.2

Conditions: [PNA] = 0.1 µM, [GO] = 0.2 – 1.5 µg/mL, [DNA] = 0.12 µM in 10 mM Tris-HCl pH 7.4 *Brightness percentage = $F_{dyeK1-dX}/F_{dyeK1}$*100. **PNA and DNA sequences are shown in **Figure 3.2.**

3.2.2 The detection of PNA invasion by using graphene oxide
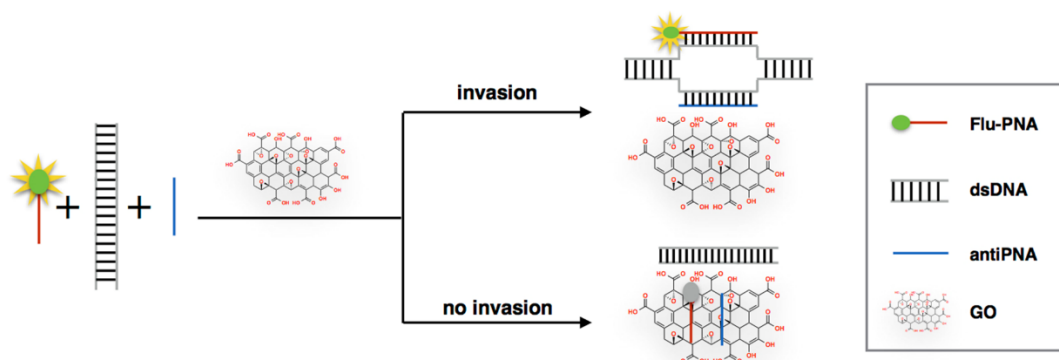
Figure 3.13 The concept of the detection of DNA duplex invasion by labeled acpcPNA probe and GO

PNA has a unique ability to strand-invade into duplex DNA in a sequence-specific fashion, and the effect can be used for gene-specific inhibition of transcription.[115] PNA can form stronger base pairs to complementary DNA (comDNA) than conventional oligonucleotides, hence the process is thermodynamically favorable since the DNA-DNA hydrogen bonding and base stacking was replaced by the PNA-DNA counterparts. While DNA duplex invasion by single-stranded PNA is possible,[116] in practice two strands of PNA are often used on combination to achieve the so-called double duplex invasion. Such double duplex invasion complex is even more thermodynamically favorable since one set of hydrogen binding and base stacking in DNA-DNA duplex was replaced by two sets of hydrogen binding and base stacking in the newly formed PNA-DNA duplexes. However, since the two strands of PNA are designed to target the same region of a DNA duplex, they are inevitably complementary and hence naturally bind more strongly to each other than to the respective DNA targets. To overcome this problem, the A and T bases of the PNA were modified by 2,4-diaminopurine (D) and 2-thiouracil (U^s) to destabilize the self-hybrids between two PNA strands due to the steric effect in the D-U^s pairing.[117, 118] Advantageously, such base modification is not required for acpcPNA probes, whereby self-hybrid formation has not been observed due to the bulkiness of the acpcPNA

backbones. The invasion between of DNA duplex by PNA is typically studied by gel electrophoresis which was rather tedious and time-consuming.

FluK5	Flu-GTAGATCACT-KKKKKNH₂	DNAsmis	3'-GGTCCCGTACCATCTTGTGACATGCGGCGC-5'
DNAcom	3'-GGTCCCGTACCATCTAGTGACATGCGGCGC-5'	DNAdmis	3'-GGTCCCGTACCATCGCGTGACATGCGGCGC-5'
DNAnon	3'-GCGCCGCATGTCACTAGATGGTACGGGACC-5'	DNAtmis	3'-GGTCCCGTACCATATACTGACATGCGGCGC-5'
Anti-FluK5	Ac-AGTGATCTAC-KKKKKNH₂	DNAfFlu	3'-CATCTAGTGACATGCGGCGC-5'
		DNAnFlu	3'-GGTCCCGTACCATCTAGTGA-5'

Figure 3.14 Sample preparation for fluorescent detection and the sequences of acpcPNA probes and DNA in the detection of PNA invasion by using graphene oxide

In this study, we were interested in applying the GO-based DNA sensing system for monitoring the invasion of acpcPNA probes into dsDNA. The strategy is illustrated in **Figure 3.13**. This is based on the fluorescence quenching of single-stranded fluorescently labeled acpcPNA probes and the fluorescence restoration when the probe binds with its complementary DNA that was developed earlier (**section 3.2.1**). To achieve this goal, 1 μM of the 10mer fluorescein-labeled acpcPNA probe (FluK5) was mixed with 1.2 μM of 30mer of dsDNA for 1 h and then 1.2 μM of unlabeled 10mer antiparallel PNA (Anti-FluK5) was added. It should be noted that the PNA probe was modified multiple lysine residues (5 in this case) to facilitate the invasion process by the favorable electrostatic attraction between the PNA probe and the DNA target. After the incubation for overnight at room temperature, the fluorescence of the PNA-dsDNA-antiPNA was measured before and after the addition of GO (**Figure 3.14**).
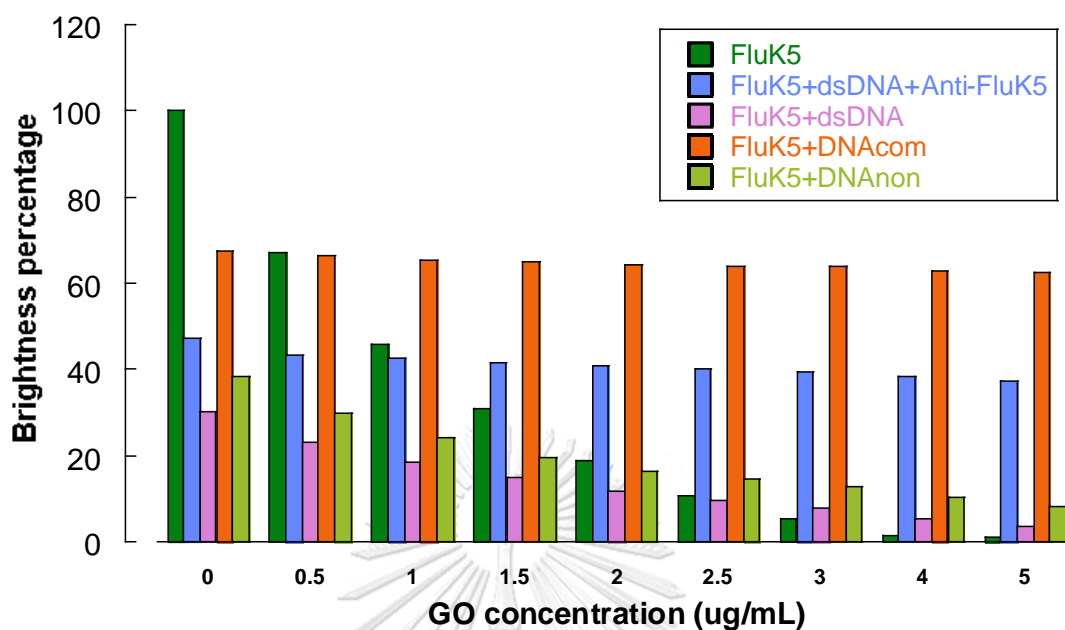
Figure 3.15 Brightness percentage at 525 nm (F/FPNA*100) after the variation of graphene oxide with various environments Conditions: [PNA] = 1-1.2 μM, [DNA] = 1.2 μM, [GO] = 0 - 5 μg/mL in 10 mM phosphate buffer pH 7.0, excitation wavelength at 490 nm

Figure 3.15 revealed the optimization of the reaction condition to allow monitoring the invasion process. In this study, the concentration of GO was varied from 0 to 5.0 μg/mL. These were added to the samples which included the free PNA probe (FluK5), the complete invasion system (FluK5+dsDNA+Anti-FluK5), the single-stranded PNA probe with dsDNA (FluK5+dsDNA), the PNA probe with its complementary DNA (FluK5+DNAcom) and the PNA probe with its non-complementary DNA (FluK5+DNAnon). It was observed that 5 μg/mL of GO showed the best discrimination between the free and hybridized PNA probes. Hence, the following discussion will focus on this concentration of GO. The results showed that the GO could not significantly quench the fluorescence of FluK5+DNAcom and FluK5+dsDNA+Anti-FluK5, which represented the positive control PNA-ssDNA duplex and the PNA-dsDNA-PNA invasion complex, at all concentrations tested. While significant fluorescence signal was observed in the single-base mismatched case

(FluK5+DNAsmis), the signal of other mismatched systems (FluK5+DNAdmis and FluK5+DNAtmis) were quenched by the GO as expected. The fact that the fluorescence of FluK5+DNAcom and FluK5+dsDNA+Anti-FluK5 could not be quenched by the GO indicated hybridization and invasion of the PNA probe to the DNA target.

Next, the selectivity experiments were performed with various DNA targets and the data are summarized in **Table 3.3**, which compared the ability of GO to discriminate the successful invasion from other states of PNA-DNA binding. This table presents the results of FluK5 binding with its complementary DNA (DNAcom), non-complementary DNA (DNAnon), single base mismatched (DNAsmis), double-base mismatched (DNAdmis), triple-base mismatched (DNAtmis), and dsDNA (DNAcom+DNAnon). The results showed that the GO quenching of PNA probe in the presence of double mismatched and non-complementary, as well as dsDNA targets in the absence of the second PNA probe was larger than the PNA and its complementary DNA, indicated the absence of binding between the probe and the target, which is in accordance with the expectation.

Interestingly, the fluorescence signal of the reporter probe in the presence of its complementary target decreased in varying degrees after the hybridization even before adding the GO quencher. This suggests the possibility of fluorescence quenching that is mediated by the close contact between the overhanging bases from the long complementary DNA targets and the fluorescein label on the acpcPNA probe. To verify this proposal, two 20mer complementary DNA targets - one carrying the overhang at the 3'-end (DNAnFlu) and the other at the 5'-end (DNAfFlu) - were hybridized with the PNA probe and their fluorescence spectra measured. The results are shown in the last two rows of **Table 3.3**, which demonstrated that the fluorescence signal of the hybrid FluK5-DNAfFlu carrying the 5'-overhangs which was far from the position of the fluorescein dye attached to the N-terminus of the PNA strand was higher. In contrast, the signal of the hybrid between the probe and the DNA target with the overhang at the 3'-end of the DNA strand (PNA-DNAnflu) which was closer to the fluorescein label on the PNA strand was similar to the complementary hybrid (FluK5-DNAcom). Thus, it was confirmed

that the decrease of fluorescence signal was caused by the close contact between the fluorescent dye and the nucleobase overhangs in the vicinity of the fluorescent label. Therefore, this factor should be taken for consideration in the design of the probe as well.

Table 3.3 Brightness percentage ($F/F_{PNA}*100$) of PNA and various type of long sequences DNA target before and after adding 5 µg/mL of graphene oxide into various conditions

PNA+DNA	Brightness Percentage		Ratio of Brightness Percentage after/before adding GO
	Before adding GO	After adding GO	
FluK5	100.0	1.0	0.01
FluK5+dsDNA+Anti-FluK5	47.3	37.1	**0.72**
FluK5+dsDNA	30.3	3.5	0.11
FluK5+DNAcom	67.6	62.5	**0.92**
FluK5+DNAnon	38.4	8.3	0.21
FluK5+DNAsmis	79.9	51.6	**0.65**
FluK5+DNAdmis	64.2	8.2	0.12
FluK5+DNAtmis	28.0	1.7	0.06
FluK5+DNAfFlu	152.5	151.4	**0.99**
FluK5+DNAnFlu	74.7	50.6	**0.66**

Conditions: [PNA] = 1-1.2 µM, [DNA] = 1.2 µM, [GO] = 0 - 5 µg/mL in 10 mM phosphate buffer pH 7.0, excitation wavelength at 490 nm. Sequences of PNA and DNA are in **Figure 3.14**

3.2.3 acpcPNA-GO for dual color, multiplex detection of DNA targets

Figure 3.16 Dual color naked-eyed detection; **tube1**:FluK5, **tube2**:FluK5 + GO, **tube3**:FluK5 + GO + dcomFlu, **tube4**:TMR-O-K4, **tube5**:TMR-O-K4 + GO, **tube6**:TMR-O-K4 + GO + dcomTMR, **tube7**:mixedPNA, **tube8**:mixedPNA + GO, **tube9**:mixedPNA + GO + dcomFlu, **tube10**:mixedPNA + GO + dcomTMR, **tube11**:mixedPNA + GO + dcomFlu + dcomTMR Conditions: [PNA] = 10 μM, [DNA] = 12 μM, [GO] = 50 μg/mL in 10 mM Tris-HCl pH 7.4; **FluK5:**Flu-GTAGATCACT-KKKKKNH$_2$, **TMR-O-K4:**TMR-O-CTAAATTCAGA-KKKKNH$_2$, **dcomFlu**:5'-AGTGATCTAC-3', **dcomTMR**:5'-TCTGAATTTAG-3'

To investigate the capability of the PNA-GO for DNA sensing in multiplex format, two PNA probes carrying two different dyes were selected for the experiment. The first one was the FluK5 PNA probe (Flu-GTAGATCACT-KKKKKNH$_2$) and another one was a TAMRA-labeled PNA probe (TMR-O-K4: TMR-O-CTAAATTCAGA-KKKKNH$_2$) obtained from Dr. Chalothorn Boonlua. In view of practical usage in the point-of-care application, only the naked-eyed detection experiments were performed. First, 20 μM of PNA in 10 mM Tris-HCl pH 7.4 was quenched with 50 μg/mL of GO. Since the PNA concentration was high, it was necessary to use a larger concentration of GO than previous experiments to affect the same quenching effect. After the incubation for 15 min, the DNA targets were added and the mixture was incubated for 30 min to achieve the fluorescence restoration. **Figure 3.16** showed that the GO could effectively quench the fluorescence of FluK5 (**tube2**), TMR-O-K4

(**tube5**), and mixture of the two PNA probes (**tube8**). In the restoration experiments, the observed color depended on the DNA target added to the experiments. Green (**tube9**), orange (**tube10**), and yellow (**tube11**) colors were observed for the addition of DNA targets dcomFlu (5'-AGTGATCTAC-3'), dcomTMR (5'-TCTGAATTTAG-3'), and their mixture (dcomFlu + dcomTMR), respectively. The results are completely consistent with the expectation and indicated that the acpcPNA-GO platform can be used to simultaneously detect two DNA targets in a multiplex, multicolor detection format.

3.3 PNA-based DNA sensing with oligodeoxyguanosine as a quencher

Table 3.4 The PNA and DNA sequences used in the oligodeoxyguanosine experiments

Type	Name	Sequence
PNA	FluK1	Flu-<u>GTAGATCACT</u>-K
	FluK5	Flu-<u>GTAGATCACT</u>-KKKKK
DNA	FluD	5'-Flu-<u>GTAGATCACT</u>-3'
	dHA	5'-<u>AGTGATCTAC</u>AAAAA-3'
	dHC	5'-<u>AGTGATCTAC</u>CCCCC-3'
	dHG	5'-<u>AGTGATCTAC</u>GGGGG-3'
	dHT	5'-<u>AGTGATCTAC</u>TTTTT-3'
	dGQ1	5'-TGAGGGTGGGTAGGGTGGTAA-3'
	dGQ2	5'-AGGGTTAGGGTTAGGGTTAGGG-3'
	dG1	dGMP
	dG5	5'-GGGGG-3'
	dG9	5'-GGGGGGGGG-3'
	dG10	5'-GGGGGGGGGG-3'
	dC10	5'-CCCCCCCCCC-3'
	dA10	5'-AAAAAAAAAA-3'
	dT10	5'-TTTTTTTTTT-3'

3.3.1 Quenching study

Initial studies were performed to determine the quenching mechanism, development of the sensing system and its performance evaluation as follows.

3.3.1.1 Quenching of fluorescein by overhang nucleobases


```
PNA:      Flu-GTAGATCACT-KKKKK
dHA: 3'-AAAAACATCTAGTGA-5'
dHC: 3'-CCCCCCATCTAGTGA-5'
dHG: 3'-GGGGGCATCTAGTGA-5'
dHA: 3'-TTTTTCATCTAGTGA-5'
```

Figure 3.17 The concept and sequences of the PNA probe and the DNA targets carrying various 3'-overhanging nucleobases (dHX)

Since the overhang bases that adjacent nucleobase locating near the fluorophore were previously shown to decrease the fluorescence intensity of the free PNA probe (**section 3.2.2**), the hybridization between the five-lysine labeled probe (FluK5) and its complementary DNA target carrying various 3'-overhanging nucleobases (dHX) was conducted to study the effect of different nucleobase locating near the fluorophore (**Figure 3.17**). According to the melting temperature studies of its duplex with complementary DNA, the FluK5 probe showed a T_m of 71.3 °C which was higher than the probe FluK1 with only one lysine modification (47.6 °C). This can be explained by the favorable electrostatic interaction between the positively charged PNA probe and the negatively charged DNA target.
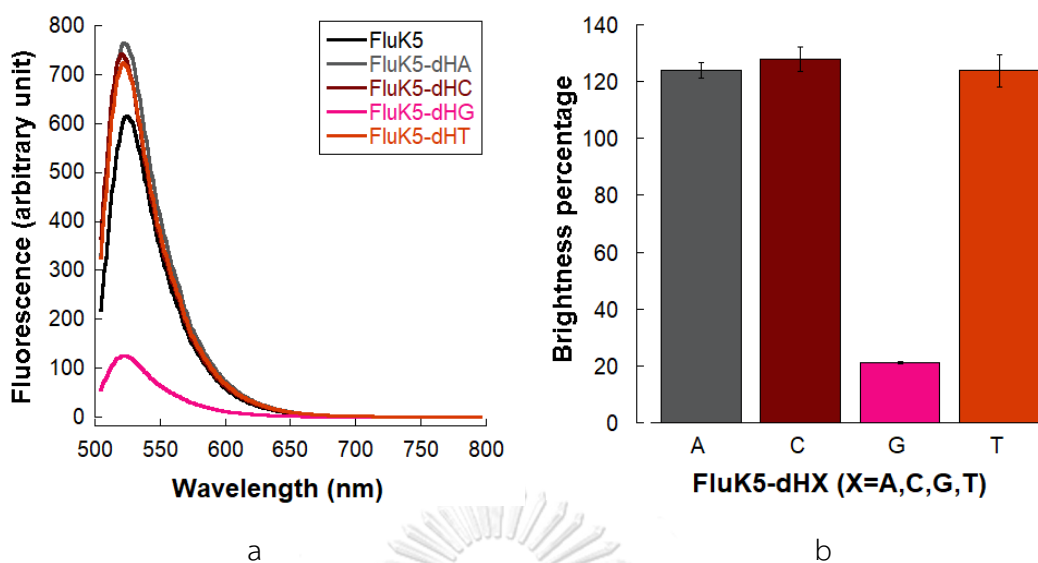
Figure 3.18 (a) Fluorescence spectra, and (b) brightness percentage at 525 nm of the FluK5 PNA probe in the absence and presence of complementary DNA targets carrying various 3'-overhangs. Conditions: [FluK5] = 1.0 μM, [dHX] = 1.2 μM in phosphate buffer pH 7.0, excitation wavelength at 490 nm

In **Figure 3.18**, the hybrids formed by mixing 1 μM of fluorescent PNA probe (FluK5) and 1.2 μM of DNA target carrying 3'-overhangs with the same nucleobase repeating five times (dHG) showed a significantly decreased fluorescence signals down to 20% of the free FluK5 probe. No decrease in the fluorescence signal was observed with DNA targets carrying other nucleobase overhangs (dHA, dHC, dHT). In fact, the signal in each case was increased by around 20% compared to the free probe. The results might be explained by the self-quenching between the nucleobases and the hydrophobic fluorophores which was facilitated by the compact folded structure of PNA in aqueous solution as already reported in the literature.[49] Since the PNA sequence contain a few deoxyguanosine (dG) residues which is known to be a good quencher for fluorescein,[64] it could be envisioned that such self-quenching is possible in the free state. The process is facilitated by the folding of the PNA into a compact structure, making a close contact between the dye and the nucleobase. The time-dependent fluorescence spectra of the free PNA probe in **Figure 3.19** showed that the fluorescence of the probe slightly decreased by 15-20% in the buffer solution over a period of 30 min. This can be explained by

the conformational reorganization of the single-stranded PNA probe upon changing the media from the highly acidic conditions in the stock PNA solution to the neutral pH in the buffer. Subsequent hybridization with the DNA target would unfold the structure, resulting in the decrease in the intra-strand interaction between the fluorescein label and the nucleobases due to the rigidification of the structure and the participation of the nucleobases in the Watson-Crick base pairing. This eventually resulted in the observed increase in fluorescence relative to the single-stranded PNA probe in the case of DNA targets with overhanging bases other than dG.
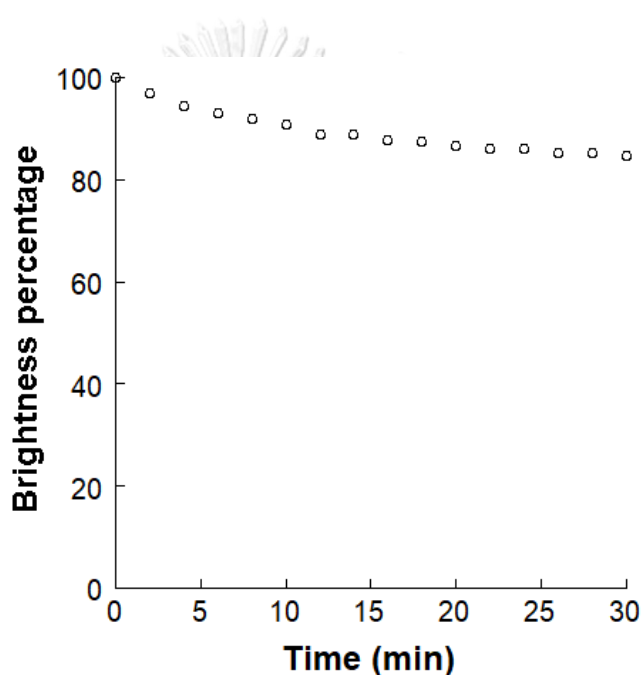
Figure 3.19 Brightness percentage of free FluK5 probe at 525 nm. Conditions: [FluK5] = 1.0 μM in phosphate buffer pH 7.0, excitation wavelength at 490 nm

From the above experiments, the overhanging nucleobases on the complementary DNA targets exert a remarkable effect on the brightness of the fluorescein-labeled PNA probe, with dG being the most effective quencher. In the DNA case, dG was found to be the most effective quencher of many fluorophores including fluorescein because its oxidation potential was the lowest when comparing with other bases.[66] The photoinduced electron transfer (PET) mechanism, in which the electron of dG was donated to a fluorescent dye in its excited singlet state causing a non-radiative relaxation of the dye to the ground state, have been

demonstrated to be responsible for the quenching in DNA.[73, 119] This experiment demonstrates that the dG was also an effective quencher for fluorescein label in the context of acpcPNA probe, most likely by the same PET mechanism.

This guanine-quenching system could in principle be developed into a kind of strand displacement probe by employing fluorescently labeled acpcPNA as a reporter probe and DNA target carrying 3'-oligo dG overhangs as a quencher probe. The working principle is the same as a previously reported acpcPNA-derived strand displacement probe, but with an oligo dG as a quencher instead of organic dyes.[50] Hybridization with the complementary target would result in a displacement of the quencher strand, leading to the separation of the dG from the fluorescein label and thus the restoration of the fluorescence. However, according to the literature this strategy proved not to be very efficient in the context of DNA probes due to the small quenching effect (less than 40%).[120] In addition, the design of quenching probe was challenging because the strand displacement probe complex must have a sufficiently high stability to achieve an effective quenching. On the other hand, the stability should not be too high so that the hybridization with the DNA target and subsequent strand displacement reaction are inhibited. This means that multiple reporter/quencher probes combinations may need to be synthesized to find the optimal one. Moreover, when the sequences of probe were changed, the sequences of the quenching probe must also change accordingly.

In the previous studies, most DNA sensing previously developed by using DNA as a probe and dG as a quencher involves some forms of covalent linking of the quencher and the labeled probe, or at least the probe strand and the quencher strand must form a hybrid by Watson-Crick base pairing. [69, 71, 119] We herein propose a new strategy for developing a new DNA sensing system based on PNA probes and guanine quencher without forming a covalent bond or a hydrogen bonding complex. Since PNA probes can be easily modified to carry either positive or negative charges by incorporation of appropriate amino acids, it was hypothesized that the electrostatic interaction between the positive charges on PNA probe and the negative charges on a G-rich DNA quencher should provide sufficient quenching effects without the need for the hybridization or covalent bonding.
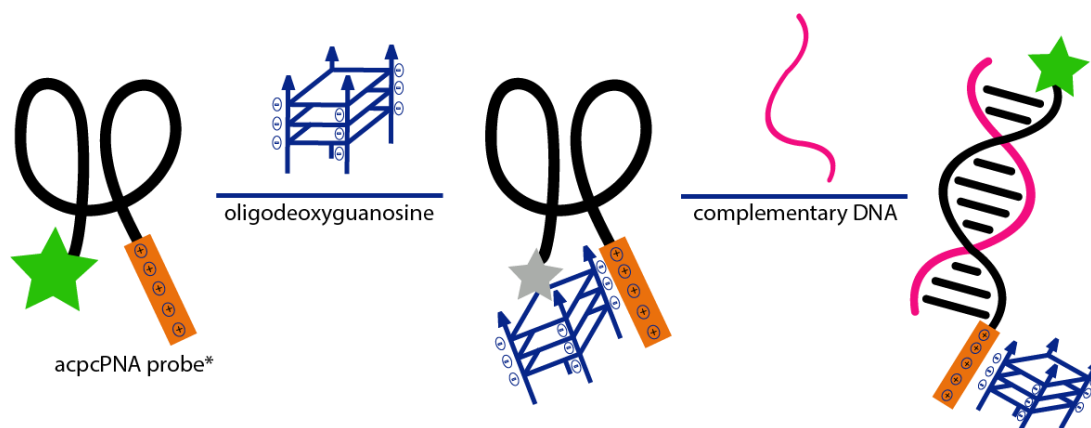
Figure 3.20 The principle of the DNA sensing platform employing positively charged lysine-modified fluorescein-labeled acpcPNA probe and oligodeoxyguanosine (dG_n) quencher

The principle of the new DNA detection system is summarized in **Figure 3.20**. First, the positively charged lysine-modified fluorescein-labeled acpcPNA probe electrostatically interacts with the negatively charged oligodeoxyguanosine (dG_n) or other G-rich DNA sequences, resulting in the quenching of the fluorescein dye. After adding the DNA target, the formation of the rigid complementary PNA-DNA duplex structure would result in separation of the fluorescein label from the dG_n quencher and led to the restoration of the fluorescence.

To investigate this viability of the DNA sensing approach according to this hypothesis, the quenching study was conducted using the same FluK5 acpcPNA probe and the four homo-oligodeoxynucleotides (dX10), namely oligodeoxyadenosine (dA10), oligodeoxycytosine (dC10), oligodeoxyguanosine (dG10), and oligothymidine (dT10). The length of these nucleotides was arbitrarily chosen based on the assumption that the length of the quencher and the probe should be the same. The results in **Figure 3.21** revealed that the fluorescence intensities of the PNA probe mixture with dA10 (grey), dT10 (orange), dC10 (red) and dG10 (pink) decreased relative to the free PNA probe by 10%, 20%, 40%, and 90%, respectively. This trend was in good agreement with the redox potential of the nucleobases. A comparison of the $E_{red}°$ (fluorescent dye) and $E_{ox}°$ (nucleobase) in **Figure 1.14** revealed that the quenching of the fluorescent dye and the nucleobase via the PET

mechanism could occur only when the $E_{red}°$ the fluorescent dye was higher than $E_{ox}°$ of nucleobase.[121] Thus, only guanine could quench the fluorescence of the fluorescein label. Since dG10 displayed the strongest quenching ability compared to other oligodeoxynucleotides, it was chosen as the external quencher for the next experiments.
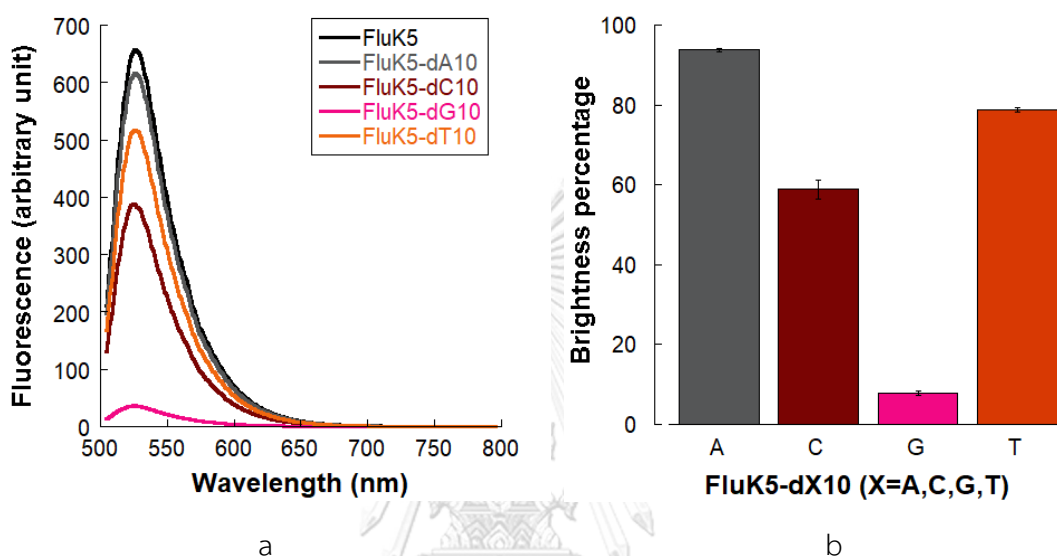
Figure 3.21 (a) Fluorescence spectra and (b) brightness percentage at 525 nm* of FluK5 PNA probe with homo-oligodeoxynucleotides. Conditions: [FluK5] = 1.0 μM, [dX10] = 1.2 μM in phosphate buffer pH 7.0, excitation wavelength at 490 nm

3.3.1.2 Effect of charges on the PNA probe

In the previous experiments, the interaction between the lysine-modified PNA probe (positively charged) and phosphate backbone of dG10 (negatively charged) was proposed to be electrostatic in nature. To evaluate the importance of the charge on the PNA probe, the quenching of other probes bearing the same sequence but different charge by dG10 were next performed. The chosen probe was FluK1 which was a modified acpcPNA with only one lysine. Thus, FluK1 probe carried smaller number of positive charges than the FluK5 probe. Furthermore, a fluorescein-labeled DNA probe having the same sequence (FluD) which represented the fully negatively charged probe and the free fluorescein dye (Flu) which represented negatively charged dye were also included for comparison.

a

b
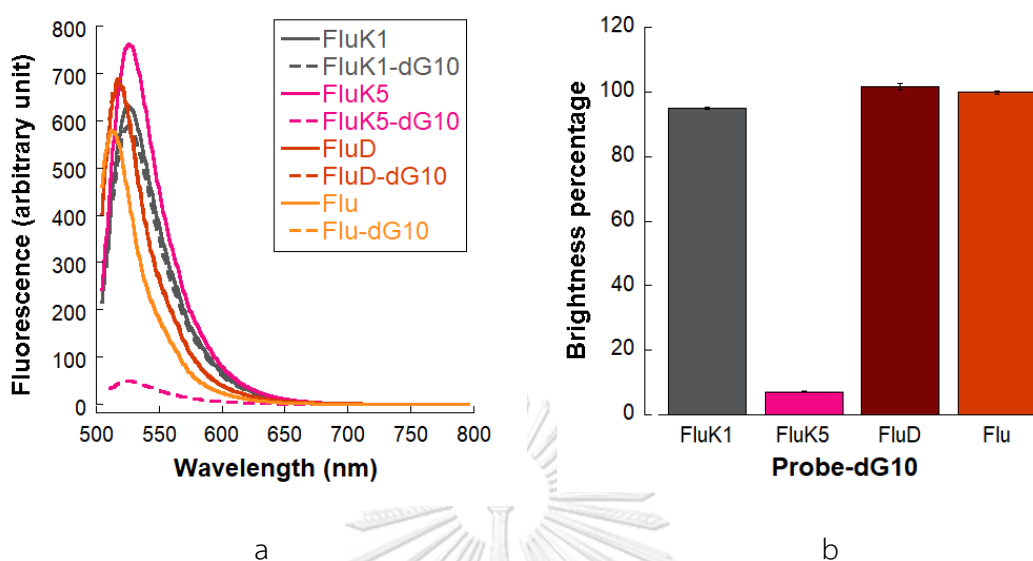
Figure 3.22 (a) Fluorescence spectra, and (b) Brightness percentage at 525 nm* of FluK1 and FluK5 probes in comparison with free fluorescein and fluorescein-labeled DNA probe without and with dG10. Conditions: [Probe] = 1.0 µM, [G10] = 1.2 µM in phosphate buffer pH 7.0, excitation wavelength at 490 nm

The results in **Figure 3.22** showed that only the multiple lysine-modified fluorescein-labeled PNA probe (FluK5) was effectively quenched by dG10, resulting in 90% decrease of the fluorescence signal relative to the free probe. In contrast, the FluK1 probe showed very small quenching effect, and no significant quenching was observed for both the fluorescein-labeled DNA probe and the free fluorescein dye after the addition of the same amount of dG10. These experiments clearly indicated that the presence of multiple positive charges on the PNA probe was important for the quenching of the PNA probe by the dG10, thus confirming the electrostatic nature of the interactions between the probe and the dG10 quencher.
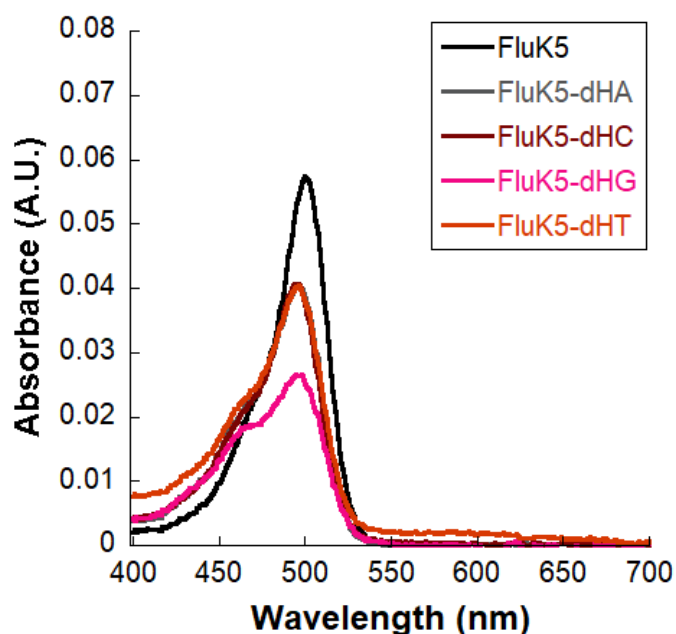
Figure 3.23 UV-visible spectra of FluK5 with its complementary DNA containing various 3' overhangs. Conditions: [FluK5] = 1.0 μM, [DNA] = 1.2 μM in phosphate buffer pH 7.0

The UV-absorption spectra of the fluorescein absorption region of the duplexes of the FluK5 PNA probe and DNA targets in **Figure 3.23** provides a further insight into the nature of the interaction between them. The absorption spectra of the FluK5 probe (black line) changed significantly after the hybridization with the DNA targets carrying base overhangs regardless of the identity of the nucleobases. In all cases hypsochromic shifts together with a decrease in molar absorption coefficients were observed. The effect was most pronounced with dG-overhang (pink line), but some spectral changes were also observed for other overhangs which indicated that the label may also interact with other nucleobases but did not lead to the same quenching effect as observed with dG. The results support the previous proposal that all nucleobases could interact with fluorescein due to the close proximity effect, but only the dG base could quench the fluorescence of the fluorescein label via the photoinduced electron transfer process due to its favorable oxidation potential.

The absorption spectra of the mixtures of FluK5 and the four homo-oligonucleotides are also shown in **Figure 3.24**. In the case of FluK5 with dG10, the spectrum was very similar to that of FluK5 with the DNA dHG with a five dG-overhang (**Figure 3.23**). This information suggested that the quenching mechanism of FluK5 by dG10 was similar to the dG-overhang despite the different nature of the interactions between the PNA probe and the DNA quencher (electrostatic for dG10 vs hydrogen bonding and π-π stacking for dHG). No significant change in the absorption spectra was observed in the cases of FluK5 probe with dA10, dT10 and dC10, whereby the absorption spectra were almost the same as the free probe. In addition, the absorption spectra of dG10 with the FluK1 and FluD probes (**Figure 3.25**) indicated the absence of interaction between the probes and the dG10, which is fully consistent with the results from the aforementioned fluorescence studies.
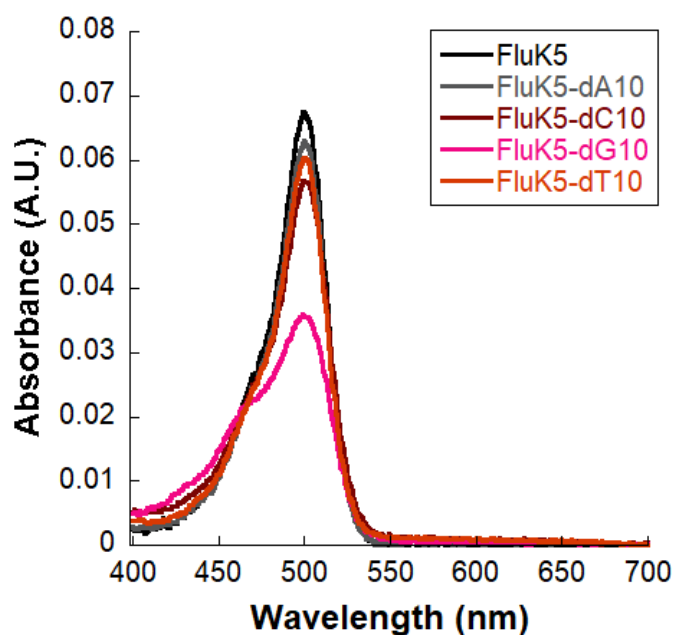
Figure 3.24 UV-visible spectra of FluK5 with homo-oligodeoxynucleotides. Conditions: [FluK5] = 1.0 µM, [DNA] = 1.2 µM in phosphate buffer pH 7.0
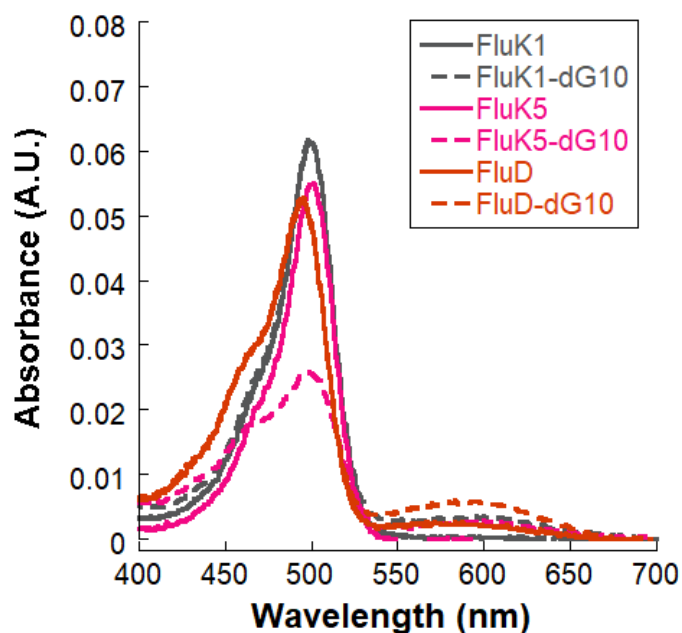
Figure 3.25 UV-visible spectra of FluK1 and FluK5 probes in comparison with free fluorescein and fluorescein-labeled DNA probe without and with dG_{10}. Conditions: [Probe] = 1.0 µM, [DNA] = 1.2 µM in phosphate buffer pH 7.0

3.3.1.3 Effect of oligodeoxyguanosine chain length

In the previous studies, dG10 was employed as a quencher based on the length of the quencher, which was similar to the PNA probe. Since the oligodeoxyguanosine is the key component to this DNA sensing platform, the effect of the guanine-containing quencher was next investigated. **Figure 3.26** showed the quenching ability of FluK5 by various oligodeoxyguanosine carrying different dG residues. This study was divided into two experiments. The first experiments compared the fluorescence quenching by keeping the total number of guanine base constant. The other experiment investigated the fluorescence quenching at the same strand concentration of the oligodeoxyguanosine.

The results showed that dG5, dG9, and dG10 exhibited similar level of quenching ability at the same total concentration of dG. Interestingly, no quenching occurred in the case of deoxyguanosine monophosphate (dG1) even at the same total concentration of dG as in other dGX sequences. When compared at the same strand concentration of dGX (1.2 µM), dG10 which carries a larger number of dG

exhibited higher quenching ability than dG5. These results together with the poor quenching of FluK1 by dG10 suggest that the multiple electrostatic interaction between the phosphodiester groups on the oligodeoxyguanosine and the poly-lysine modification on the PNA tail is the important contributor to the quenching efficiency, probably by increasing the stability of the PNA-dGX complex. It is interesting to note that effective quenching of the fluorescein label was observed even though the positive charge was located on the PNA strand at the opposite end of the fluorescein label (C- vs N-terminus). This could be explained in terms of the compact folding of the PNA strand which made the fluorescein label and the guanine quencher within the distance that allows effective quenching as shown in **Figure 3.19**.
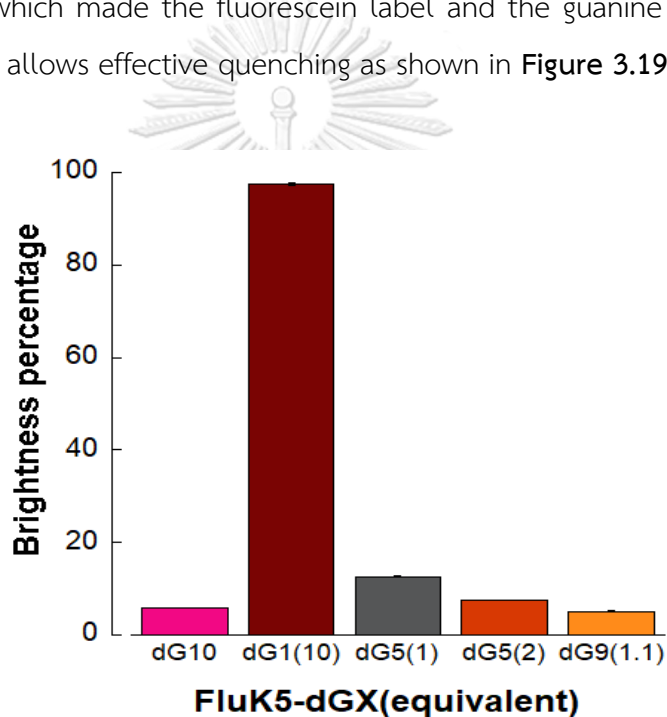
Figure 3.26 Brightness percentage of FluK5 PNA probe with different dGX quenchers. Conditions: [FluK5] = 1.0 μM, [dG10] = 1.2 μM, [dGX] = $\frac{10}{X}$ equiv of dG10, in phosphate buffer pH 7.0, excitation wavelength at 490 nm
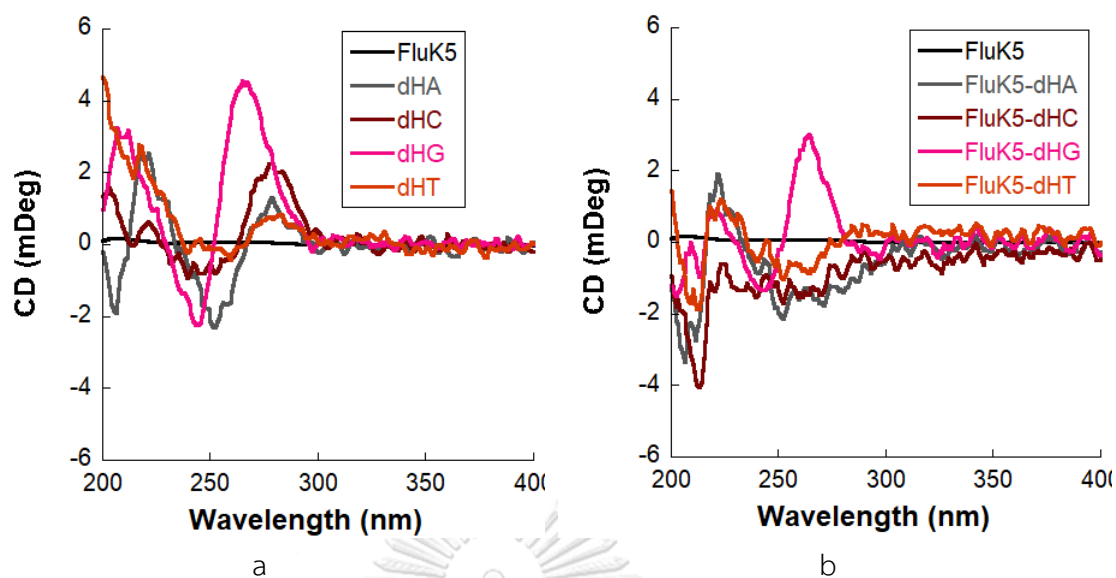
Figure 3.27 CD spectra of (a) free FluK5 and free complementary DNA containing various 3' overhangs (b) FluK5 with its complementary DNA containing various 3' overhangs homo-oligodeoxynucleotides. Conditions: [FluK5] = 1.0 μM, [DNA] = 1.2 μM, in phosphate buffer pH 7.0.

Figure 3.27 showed the CD spectra of the free overhang DNA and its duplex with the PNA probe FluK5. Only the CD spectra of dHG and its complex displayed the negative band near 240 nm and a positive band around 260 nm. These patterns were characteristics for the parallel-stranded G-quadruplex structure, which is consistent with the literature.[122] CD spectra of dG10 and its complex with FluK5 (**Figure 3.28**) revealed the same trend whereby the free dG10 also showed the strong negative and positive band as the same region as the overhang DNA. These results indicate that the oligodeoxyguanosine and the DNA with oligo(dG) overhang exist as parallel G-quadruplex structures both in the presence and absence of FluK5. This indicates that the quadruplex structure is still stable after the interaction with FluK5.
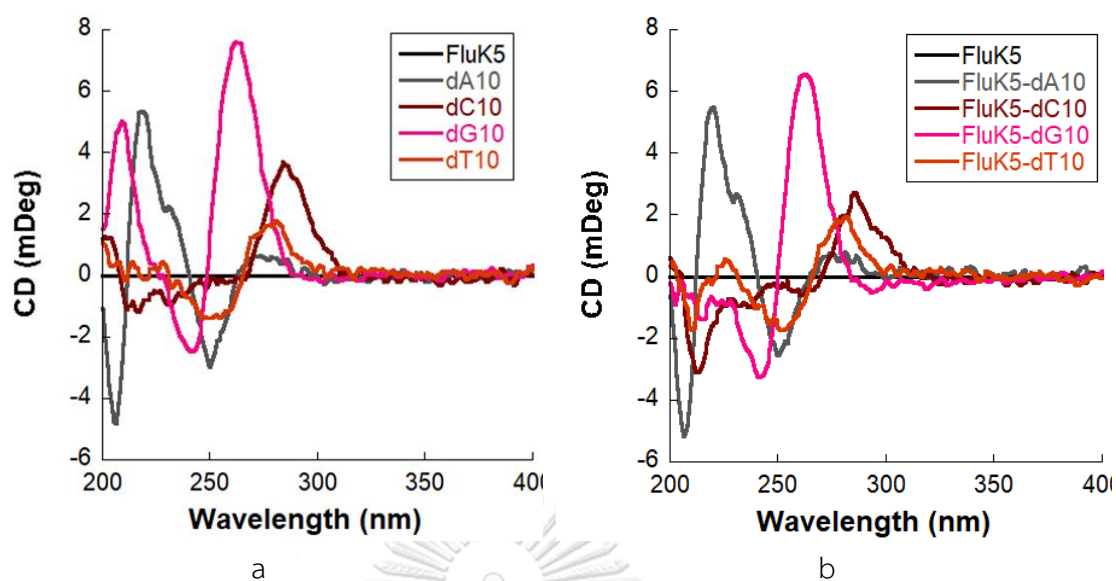
Figure 3.28 CD spectra of (a) free FluK5 and free oligodeoxynucleotides (b) FluK5 with oligodeoxynucleotides. Conditions: [FluK5] = 1.0 µM, [DNA] = 1.2 µM, in phosphate buffer pH 7.0
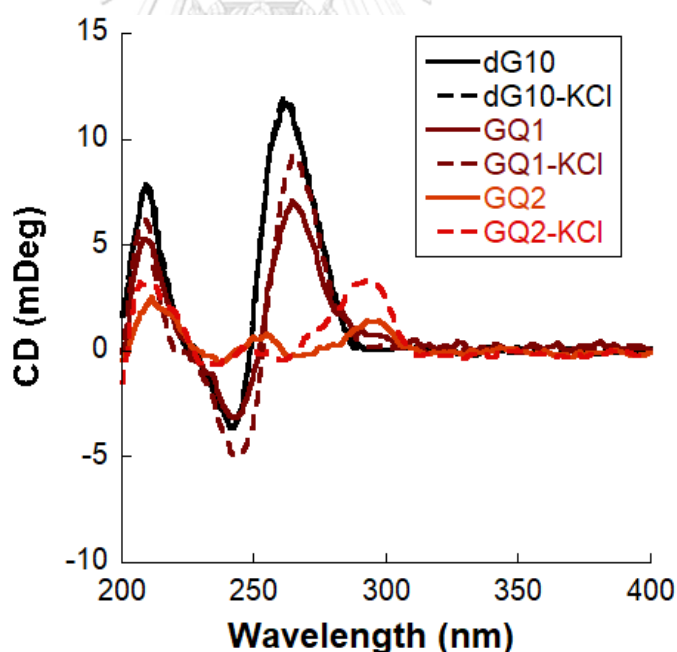
Figure 3.29 CD spectra of FluK5 with various types of G-quadruplexes. Conditions: [FluK5] = 1.0 µM, [DNA] = 1.2 µM, [KCl] = 0 or 10 mM, in phosphate buffer pH 7.0,

Since dG-rich DNA can form quadruplex structures (**Figure 1.20**), it is interesting to investigate how the different types of G-quadruplexes influence the

quenching. Two types of G-quadruplex were selected according to the literature. The oligodeoxyguanosine (dG10) and the c-Myc sequence (GQ1) formed the parallel structure both in the presence and absence of potassium ion, while the 22AG sequence (GQ2) formed an antiparallel structure in the absence of potassium ion and transformed to the hybrid structure in the presence of potassium ion (**Figure 3.29**).[123]
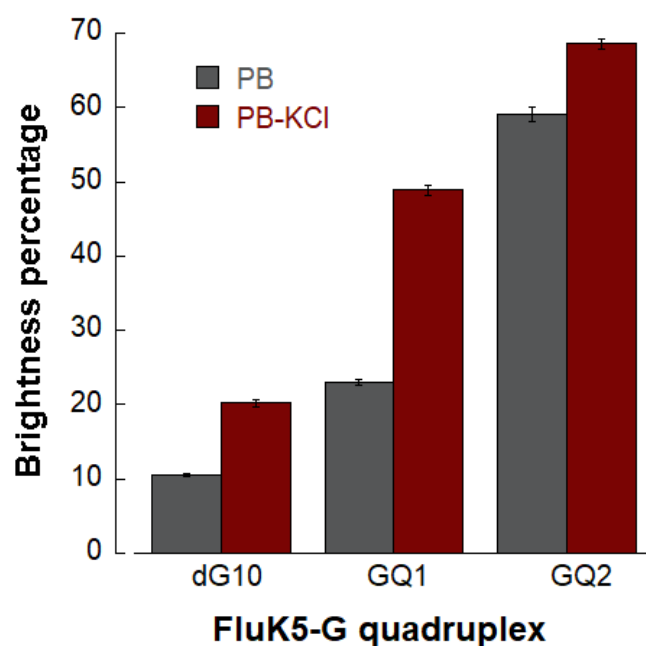
Figure 3.30 Brightness percentage of FluK5 PNA probe with different types of G-quadruplex structures. Conditions: [FluK5] = 1.0 µM, [GQX] = [dG10] = 1.2 µM, [KCl] = 0 or 10 mM in phosphate buffer pH 7.0, excitation wavelength at 490 nm

Figure 3.30 showed the brightness percentage of the FluK5 after the addition of various types of G-quadruplex, both in the absence and presence of potassium ion which could stabilize the G-quadruplex structures. From all G-quadruplex-forming sequences tested, dG10 could still function as the most effective quencher compared to other G-quadruplex-forming sequences. The addition of K^+ seems to have a negative impact on the quenching efficiency despite the expected stabilization of the quadruplex structures. This might be due to the attenuation of the electrostatic interaction at high salt concentrations. Thus, it was concluded that dG10 provided the highest quenching ability than other types of G-quadruplex. From

the experiments, while it could not clearly confirm whether the quadruplex formation was essential for the quenching process, but at least the number of dG units seems to be the key to the effective quenching rather than the ability to form G-quadruplex structures.

3.3.1.4 The effect of salt
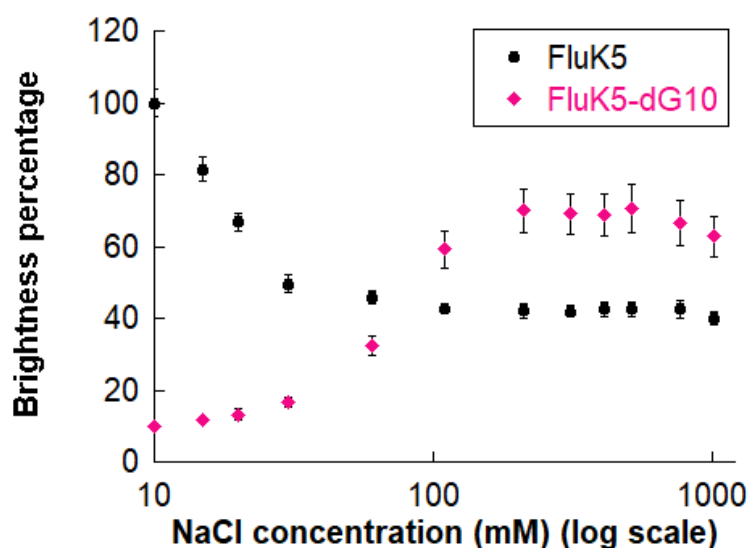
Figure 3.31 Brightness percentage at 525 nm of FluK5 and dG10 at various salt concentrations. Conditions: [FluK5] = 1.0 μM, [dG10] = 1.2 μM in phosphate buffer pH 7.0, excitation wavelength at 490 nm

Since the interaction between the PNA probe and the dG10 quencher is electrostatic in nature, it is expected that the quenching efficiency should be sensitive to the ionic strength. The effect of salt on the fluorescence quenching of FluK5 by dG10 was next investigate as shown in **Figure 3.31**. At low concentrations of NaCl (0-30 mM), the quenching efficiency was still high as shown by the brightness percentage of only around 10% of the free FluK5 probe. Then, the quenching efficiency decreased rapidly after increasing the concentration of NaCl from 50 to 300 mM. After the that, the fluorescence was almost constant at around 70–80% of the original value of the free probe. The results indicated inefficient quenching at high salt concentrations. It should be noted that the fluorescence of the free probe was

also sensitive to the presence of salt to some extent. It might be assumed that the high concentration of salt would promote the formation of the folded PNA structure, leading to a lower fluorescence. The addition of salt would interrupt the interaction between the positive charge on PNA and the negative charge on oligodeoxyguanosine and brought about the fluorescence restoration. The experiments thus confirmed that the electrostatic interaction was an important factor that promoted the quenching.

3.3.2 Fluorescence restoration studies

Table 3.5 The PNA and DNA sequences used in the fluorescence restoration studies (**section 3.3.2**) and applications (**section 3.3.3.1** and **3.3.3.2**)

Type	Name	Sequence
PNA	FluK5	Flu-GTAGATCACT-KKKKK
	PNA1	Flu-GCTTTTTTACA-KKKKK
	PNA2	Flu-AGTCTGATAAGC-KKKKK
	PNA3	Flu-TTAATACCTTTGCTC-KKK
	TMRK4	TMR-CTAAATTCAGA-KKKK
DNA	dCs/dFK5	5'-AGTGATCTAC-3'
	dMs	5'-AGTGCTCTAC-3'
	dNs/dTK4	5'-TCTGAATTTAA-3'
	dNs11	5'-TCTGAATTTAA-3'
	dNs10	5'-GTAGATCACT-3'
	dCl	5'-CGCGGCGTACAGTGATCTACCATGCCCTGG-3'
	dMl	5'-CGCGGCGTACAGTGCTCTACCATGCCCTGG-3'
	dNl	5'-CCAGGGCATGGTAGATCACTGTACGCCGCG-3'
	DNA1	5'-TGTAAAAAAGC-3'
	DNA2	5'-TAGCTTATCAGACTGATGTTGA-3'
	DNA3	5'-GAGCAAAGGTATTAA-3'

After showing that the FluK5 PNA probe could be effectively quenched by dGX as a result of electrostatic interaction and PET between the guanine and fluorescein, the fluorescence restoration experiments were next performed employing the PNA probes and DNA targets shown in **Table 3.5** in order to develop a new DNA sensing system that operates in a fluorescence turn-on mode.

3.3.2.1 Optimized condition for DNA sensing platform

To develop the novel DNA sensing system by using the combination of FluK5 and dG10, the optimization of the ratio between the probe and the quencher was first studied. Ideally, the sensing system should give the highest signal in the presence of DNA target while maintaining the low background signal of the probe-quencher complex. Following the addition of various concentrations of dG10 (0.05, 0.1, 0.15 and 0.2 μM) with the concentration of the FluK5 probe being fixed at 0.1 μM, the fluorescence signal drastically dropped to 20–25% of the original fluorescence of the free probe. The signal further decreased to 15–20% after being left for 10 min (**Figure 3.32a**). The results indicated that only sub-stoichiometric amounts of the dG10 were already sufficient to quench the FluK5 probe. In all cases, after the addition of a slight excess (0.12 μM) of the complementary DNA strand, the brightness percentage of each ratio increased to over 80% of the original probe within 15 min (**Figure 3.33b**). The results showed that the best condition for signal restoration was observed around 0.05–0.1 μM of quencher. Higher concentrations of the dG10 quencher would give lower signal to background ratio due to the incomplete signal restoration. The kinetic of the quenching and restoration process showed the almost constant signals were observed at 10 and 15 min for the quenching and restoration processes, respectively. Therefore, the incubation periods of 10 and 15 min for the quenching and restoration steps were chosen for the next experiments.
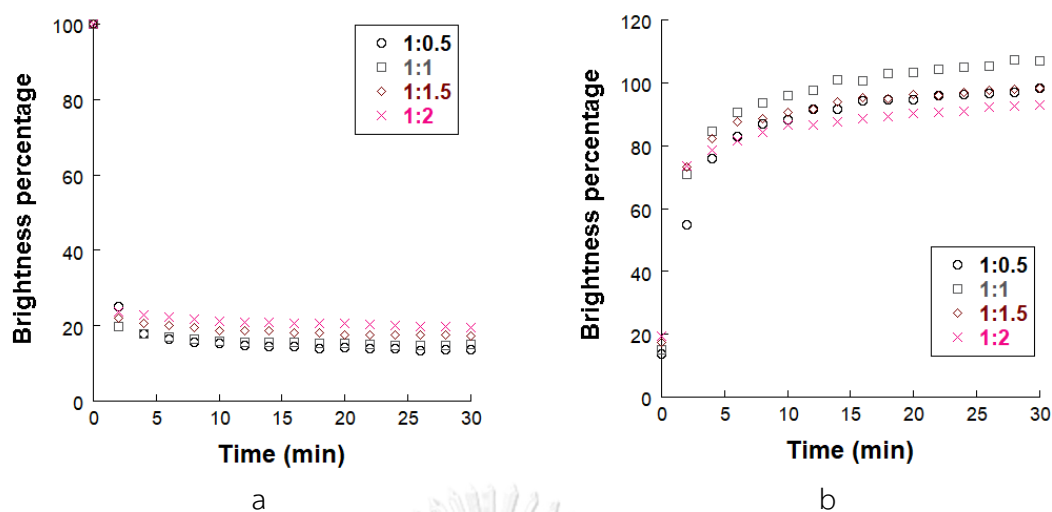
Figure 3.32 Brightness percentages of the ratio between FluK5 and dG10 for the (a) quenching and (b) restoration process. Conditions: [FluK5] = 0.1 µM, [dG10] = 0.5-2.0 µM [DNA] = 0.12 µM, in phosphate buffer pH 7.0, excitation wavelength at 490 nm

3.3.2.2 Selectivity

Since the fluorescence quenching of this FluK5-dG10 DNA sensing system could be restored by the addition of the complementary DNA target. However, it was not clear whether the fluorescence restoration was specific to the complementary DNA target binding. The addition of other DNAs might as well replace displace the dG10 quencher from the probe in a non-specific fashion that could also lead to the observed fluorescence restoration. To confirm the specificity of this platform, the experiments were performed by monitoring the percentage brightness of the FluK5-dG10 (PG) system in the absence and presence of different DNA targets relative to the free FluK5 probe. Two groups of DNA were tested. These include 1) short DNA targets having the same number of nucleotide as the probe, which consist of complementary target (dCs), one-base mismatched target (dMs), and non-complementary target (dNs) and 2) long DNA targets with overhanging-nucleotides, which consist of complementary target (dCL), one-based mismatched target (dML), and non-complementary target (dNL) (**Table 3.5**). The results are summarized in **Figure 3.33**.
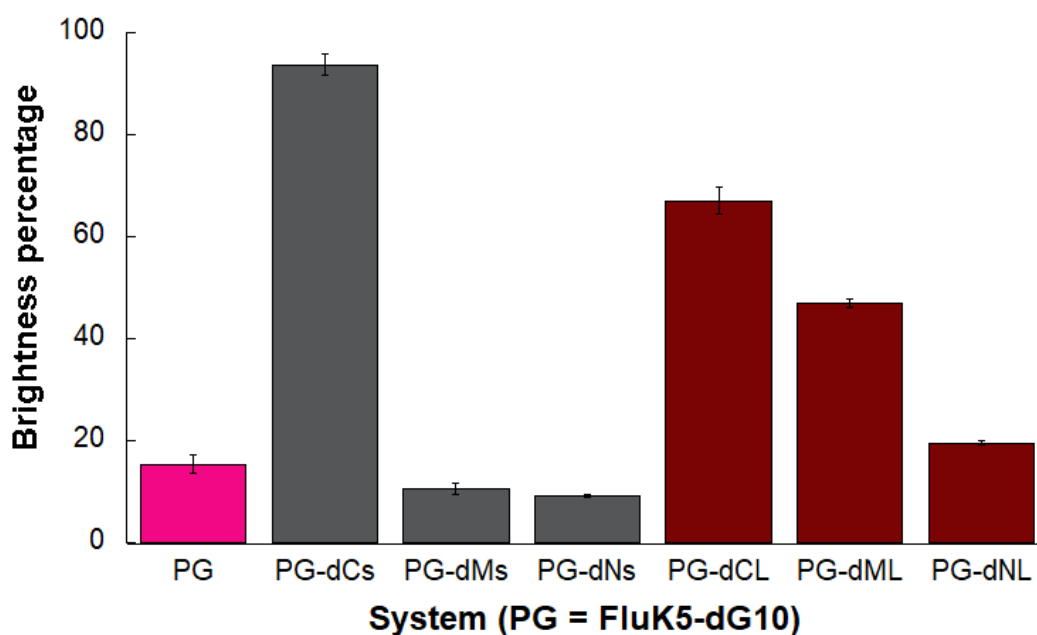
Figure 3.33 The brightness percentage at 525 nm of the fluorescence restoration experiments of FluK5-dG10 by various target DNAs at 20 °C. Conditions: [FluK5], [dG10] = 0.1 μM, [DNA] = 0.12 μM in phosphate buffer pH 7.0, excitation wavelength at 490 nm

In accordance with the previous experiments, mixing of the solution of the FluK5 probe and dG10 quencher (0.1 μM each) resulted in a dramatic reduction of the fluorescence signal of the FluK5 probe down to 15% of the original signal of the free probe. In cases of targets with the same length as the probe, the FluK5-dG10 system could discriminate the complementary target from other DNAs as shown by the grey bars in **Figure 3.33**. The fluorescence restoration by the complementary DNA target (dCs) was largest than the one-base mismatched (dMs) and non-complementary (dNs) DNA targets. The results clearly showed that this DNA detection platform is sequence-specific, at least for the short DNA targets. The selectivity for complementary over mismatched DNA targets confirms the proposed working principle of the DNA sensing system as shown in **Figure 3.20**. To further confirm the specificity of the DNA sensing system, the interaction of the FluK5-dG10 and excess of non-complementary targets were also examined. The results in **Figure**

3.34 showed that the fluorescence restoration did not occur even when 10 equiv. of non-complementary DNA targets were added. This suggests that the interaction between the probe and the dG10 quencher was sufficiently strong to withstand the non-specific displacement by non-target DNA, which is in sharp contrast to the GO-based DNA sensing platforms whereby non-specific displacement is a significant problem.[124, 125]
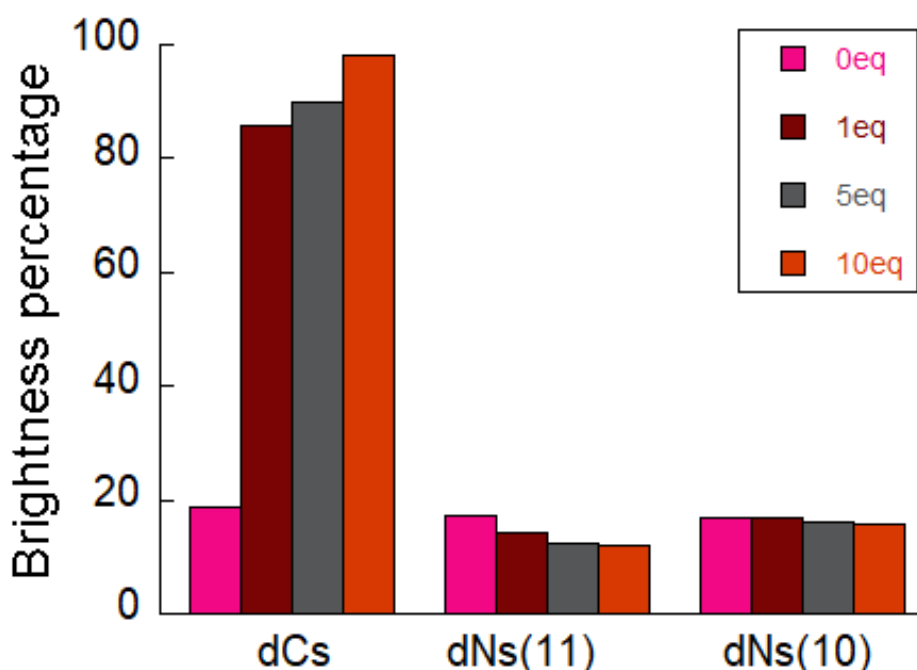
Figure 3.34 Brightness percentage of PG platform at 525 nm with the non-complementary targets. Conditions: [FluK5] = [dG10] = 0.1 μM, [DNA target] = 0.1 – 1.0 μM in phosphate buffer pH 7.0, excitation wavelength at 490 nm

While the acpcPNA-GO system was effective in distinguishing complementary from mismatched DNA in the context of short DNA target sequences, the discrimination of the longer DNA targets as shown in **Figure 3.33** (scarlet bar) was less clear-cut. The addition of both complementary and mismatched target resulted in almost comparable fluorescence restoration. In the case of long DNA targets, the binding between the probe and the targets would be stabilized by the overhanging nucleotides and thereby increasing the duplex stability. Indeed, the melting temperature of the duplexes of the FluK5 PNA probe with the mismatched DNA

target (dML) was relatively high (52.9 °C) suggesting that the mismatched duplex was quite stable at ambient temperature (**Table 3.6**). This explains the difficulty in discriminating between these two targets. However, since the melting temperature of the complementary and mismatch target was different by 20 °C (**Table 3.6**), it should be possible to discriminate among these long DNA targets by performing the experiment at a temperature that is high enough to destroy the mismatch duplex but not the complementary duplex.

Table 3.6 Melting temperature of duplexes of FluK5 and DNA targets

PNA	DNA	Sequence (N to C)	T_m (°C)
FluK5		Flu-GTAGATCACT-KKKKK	
	dCs/dFK5	3'-<u>CATCTAGTGA</u>-5'	71.3
	dCL	3'-GGTCCCGTAC<u>CATCTAGTGA</u>CATGCGGCGC-5'	82.5
	dML	3'-GGTCCCGTAC<u>CATCTCGTGA</u>CATGCGGCGC-5'	59.2

Melting temperature measured by UV-visble spectroscopy at 260 nm Conditions: [PNA] = 1 µM, [DNA] = 1.2 µM in phosphate buffer pH 7.0

　　　　Figure 3.35 revealed an improvement in the discrimination between complementary and single-base mismatched DNA targets upon increasing the temperature. The maximum discrimination was observed at 60 °C. It could be explained that the complementary duplex remained stable, but the mismatched duplex dissociated from the probe, which would return to the single-stranded state and was quenched by the oligodeoxyguanosine. Beyond this temperature, the discrimination became poor again because the complementary hybrid would also start to dissociate. At 95 °C, there was no significant difference between the two targets because of the complete dissociation of probe-target hybrids at such a high temperature. When cooled down to room temperature, the signal returned to the same level as the starting point, indicating that the fluorescence change due to the hybridization with the DNA target was reversible. Hence, increasing the temperature could help discriminating complementary from mismatched targets in the case of long DNA target sequences. This experiment also indicated that the

oligodeoxyguanosine remained attached to the PNA probe even at high temperature. This is consistent with the electrostatic nature of the interaction which should not be very sensitive to the temperature change. This can considered as another advantage of the new system compared to the DNA-GO, which is known to dissociate at high temperature, leading to false positive signals.[60]
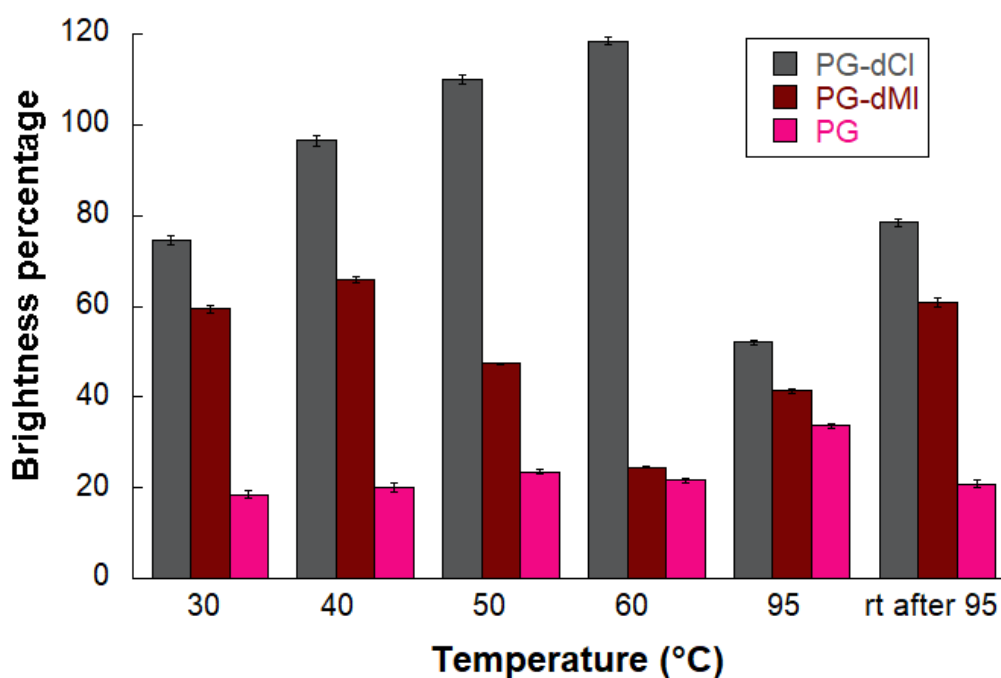
Figure 3.35 Brightness percentages at 525 nm of thermal discrimination of long chain target DNA. Conditions: [FluK5] and [dG10] = 0.1 µM, [DNA] = 0.12 µM in phosphate buffer pH 7.0, excitation wavelength at 490 nm

Gel electrophoresis experiments were performed to confirm the fate of the oligodeoxyguanosine quencher before and after the hybridization with the DNA target. The results as shown in **Figure 3.36** revealed that the oligodeoxyguanosine should remain complex with the PNA probe even after the hybridization with the DNA target. This is supported by the significant smearing of the band of the FluK5-dG10-DNA mixture (**lane4**) compared to the relatively sharp band of the PNA-DNA hybrid alone (**lane7**). It should be noted that the oligodeoxyguanosine band usually appears as a smearing band presumably due to the presence of various binding forms.[126]
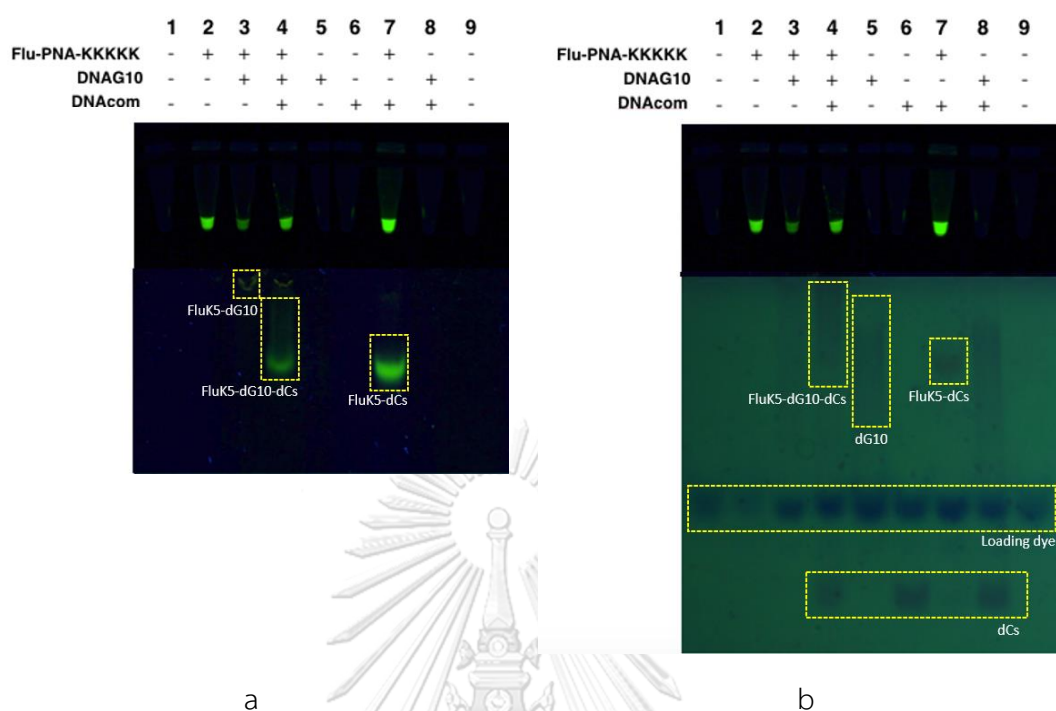
Figure 3.36 Gel electrophoresis experiments (a) visualized under transilluminator (365 nm) (b) visualized by UV shadowing (256 nm) over a silica gel GF254-coated TLC plate. The amounts of PNA and DNA (dCs/dG10) in each lane are 0.5 and 0.6 nmol, respectively. (**lane1**: blank, **lane2**: FluK5, **lane3**: FluK5-dG10, **lane4**: FluK5-dG10-dCs, **lane5**: dG10, **lane6**: dCs, **lane7**: FluK5-dCs, **lane8**: dG10-dCs, and **lane9**: blank).

3.3.2.3. Sensitivity

To investigate the sensitivity of this PNA-dGX DNA sensing system, various concentrations of the complementary DNA target (dCs) were added to the quenched mixture of the FluK5 probe (0.1 µM) and the dG10 quencher (0.1 µM). A linear relationship between the fluorescence intensity and concentrations of dCs was observed over the concentration range from 5 to 25 nM (y = 8.0613x + 90.9, R^2 = 0.99817) as shown in **Figure 3.37**. The detection limit of this detection was 2.4 nM as calculated from **equation 2.4**. To compare the performance of this platform with other fluorescence-based DNA detection systems, this platform showed a detection limit that is comparable to or better than several platforms without signal

amplification such as the PNA-DNA strand displacement (10 nM),[127] DNA beacon FRET probe (24 nM),[128] graphene oxide-based nanostructured DNA sensor (120 nM),[129] and polydopamine nanosphere sensing platform (5 nM).[130]
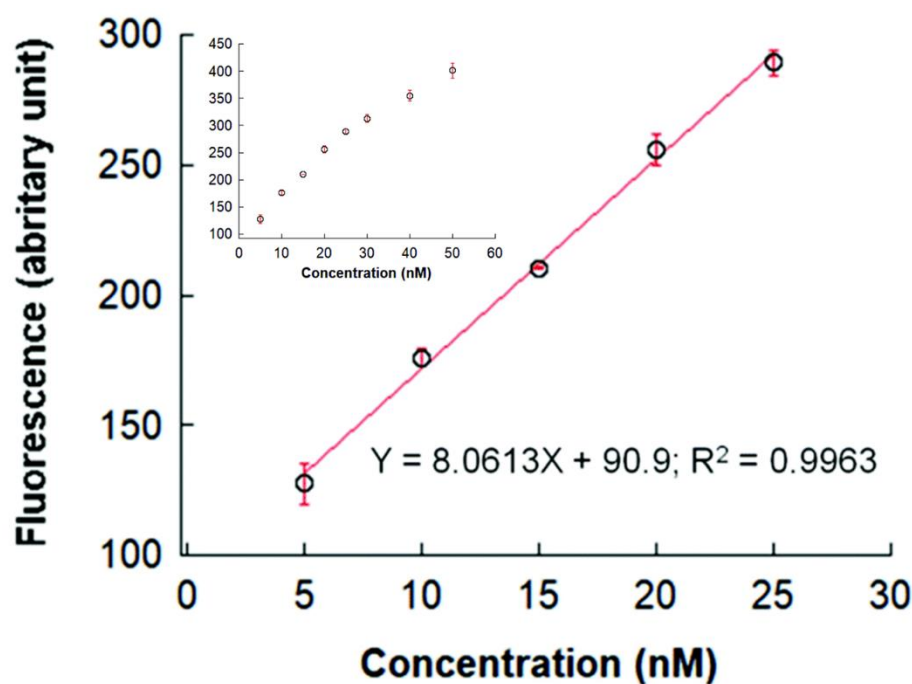
Figure 3.37 The calibration graph and detection limit of this platform Conditions: [FluK5] and [dG10] = 0.1 μM, [DNA] = 5 – 25 nM. in phosphate buffer pH 7.0, excitation wavelength at 490 nm.

3.3.3 Applications

Previous experiments have clearly demonstrated that the combination of multiple-lysine-modified dye-labeled acpcPNA as a probe and oligodeoxyguanosine resulted in quenching by virtue of the electrostatic interaction between the positive charges on the PNA strand and the negative charges on the oligodeoxyguanosine. Importantly, the fluorescence signal was almost completely restored after the addition of stoichiometric quantities of the complementary DNA target with a good specificity for complementary over mismatched DNA targets with acceptable sensitivity in the low nanomolar level. However, all experiments had been performed with a single PNA probe sequence. To demonstrate the general

applicability of this new DNA detection system, the experiments below were further performed to showcase the application of this PNA-dGX DNA detection system to other sequences.

3.3.3.1 Applicability with other PNA probe sequences
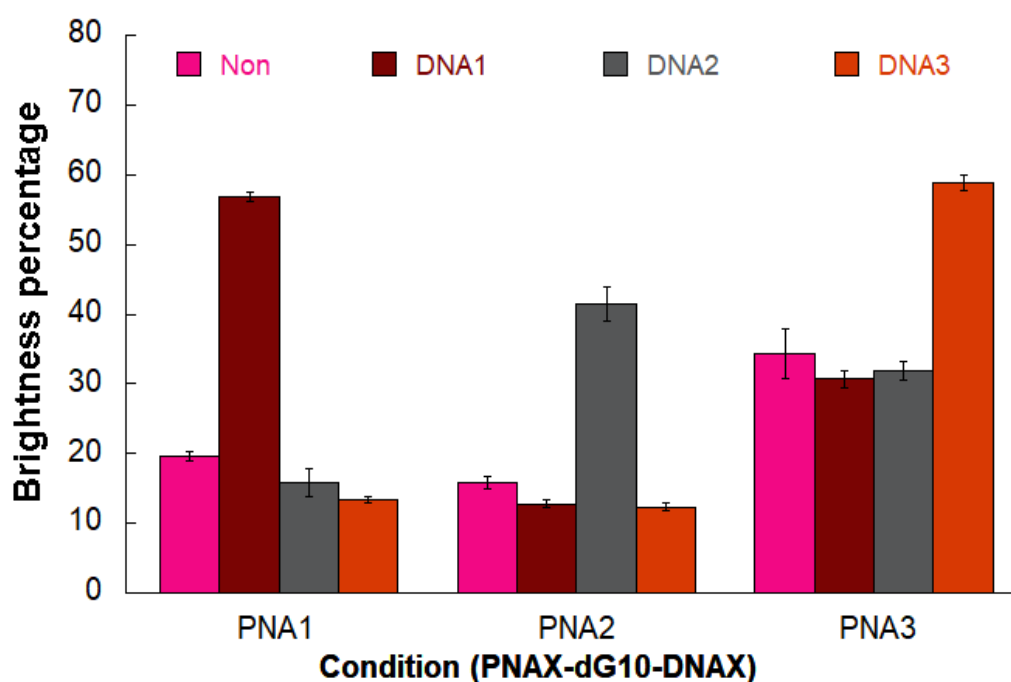
Figure 3.38 Brightness percentage of three PNA probes and DNA targets, which were separately measured using [PNA] and [dG10] = 0.1 µM and [DNA] 0.12 µM in phosphate buffer pH 7.0, excitation wavelength at 490 nm

Figure 3.38 demonstrates the general applicability of the sensor design. In the experiments, three additional fluorescein-labeled PNA probes (PNA1, PNA2, and PNA3) were designed to target three different DNA sequences (sequences of PNAs are shown in **Table 3.5**). The PNA1 and PNA2 were modified with five lysine residues while PNA3 was modified with three lysine residues. The DNA targets used to demonstrate the selectivity of the three probes include DNA1 and DNA3 which were short DNA sequences, and DNA2 which carried 3'-overhanging bases. Each PNA probe was separately quenched with dG10 and hybridized with each of the three DNA targets. The probe PNA1 and PNA2 were effectively quenched as shown by the

percentage brightness of 15-20% of the original value. Lower quenching efficiency was observed with the probe PNA3. This was not totally unexpected considering that this probe carried only three lysine residues instead of five. Nevertheless, the experiment indeed demonstrate that the quenching was still more effective than in the case of one lysine residue. The hybridization experiments revealed that the dG10-quenced acpcPNA probes PNA1, PNA2 and PNA3 responded selectively to their respective DNA targets, namely DNA1, DNA2, and DNA3, respectively. In all cases, the complementary targets show significantly larger signal than the background (no DNA target) and other non-complementary targets. Even the poorest discriminating probe-target pair (PNA3-DNA3), the signal of the correct DNA target (DNA3) was still almost twice as large as that of non-complementary targets (DNA1 and DNA2) and background (no DNA) indicating the general applicability of the developed DNA sensing platform.
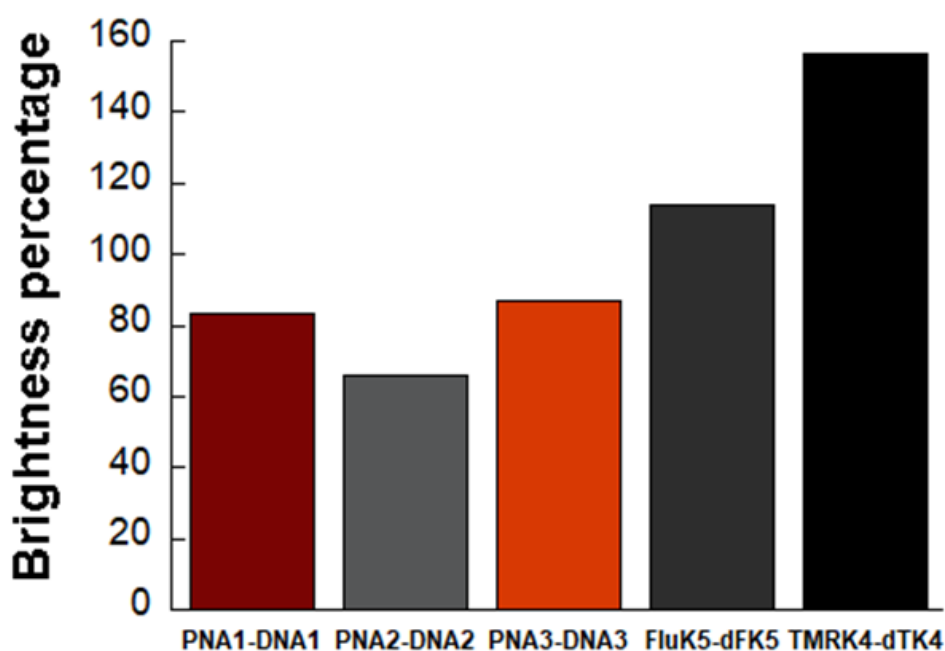
Figure 3.39 Brightness percentage of PNA-DNA duplex at 525 nm of four Flu-PNA probes (PNA1, PNA2, PNA3, and FluK5) and at 555 nm of TMR-PNA probe Conditions: [PNA] 0.1 µM and [DNA] 0.12 µM in phosphate buffer pH 7.0, excitation wavelength at 490 and 525 nm

The fluorescence restoration of various DNA targets appears to be variable, depending on the sequence (sequences of PNAs and DNAs are shown in **table 3.5**). An experiment was performed to determine whether this is really the maximum fluorescence restoration by measuring the fluorescence of the duplexes formed from the probes with their respective DNA targets in the absence of dG10 (**Figure 3.39**). The fluorescence data clearly indicate that the restoration depends on the sequence of the probe/target which may contribute to different level of quenching of the fluorophore and the neighboring nucleobase by the PET process. In general, the quenching efficiency of bases is G > C ≥ A ≥ T and the capability of electron transmission of base-pairs in double-stranded DNA is GC > TA. Thus, PNA1 containing two CG base pairs or PNA2 containing the overhang bases might reveal the lower restoration than FluK5 that containing one CG base pair.

3.3.3.2 Multicolor probes for multiplex DNA detection

To extend the capability of the DNA sensing platform further, a multicolor platform for the simultaneous detection of two or more DNA targets (multiplex detection) was demonstrated. The FluK5 probe was used in combination with another acpcPNA probe TMRK4, which was modified with four lysine residues and labeled with the 5(6)-carboxytetramethylrhodamine dye. The mixture of the two probe and quenched with excess of dG10 and separately hybridized with the DNA targets specific for each probe (dFK5 and dTK4, respectively). **Figure 3.40** demonstrates the multicolor detection employing two fluorescent PNA probes. At the excitation of 490 nm (λ_{ex} of Flu, solid lines), the fluorescence intensity of the FluK5 probe at 525 nm was quenched from 300 (black solid line) to 40 unit (pink solid line) after the addition of dG10. The quenching by dG10 was also observed in the region of TMRK4 at 580 nm was quenched from 150 (black solid line) to 10 unit (pink solid line). Then, the signal at 525 nm was restored to above the original value of the free FluK5 probe after the addition of the dFK5 target (brown solid line). There was no fluorescence restoration of the TMRK4 probe at 580 nm. The reverse is true when the dTK4 DNA which was complementary to the TMRK4 probe was added

(compare pink and red solid lines). When both DNA targets were present, the fluorescence restoration was observed at both 525 and 580 nm (Flu and TMR emissions) (yellow solid lines). When the excitation was performed at 520 nm (λ_{ex} of TMR, dash lines), only the region of TMR could be observed, and the fluorescence of the TMRK4 PNA was also dramatically dropped from 250 to 10 arbitrary units after the addition of dG10. Then, the fluorescence restoration occurred only in the presence of dTK4 target (red and yellow dotted lines).
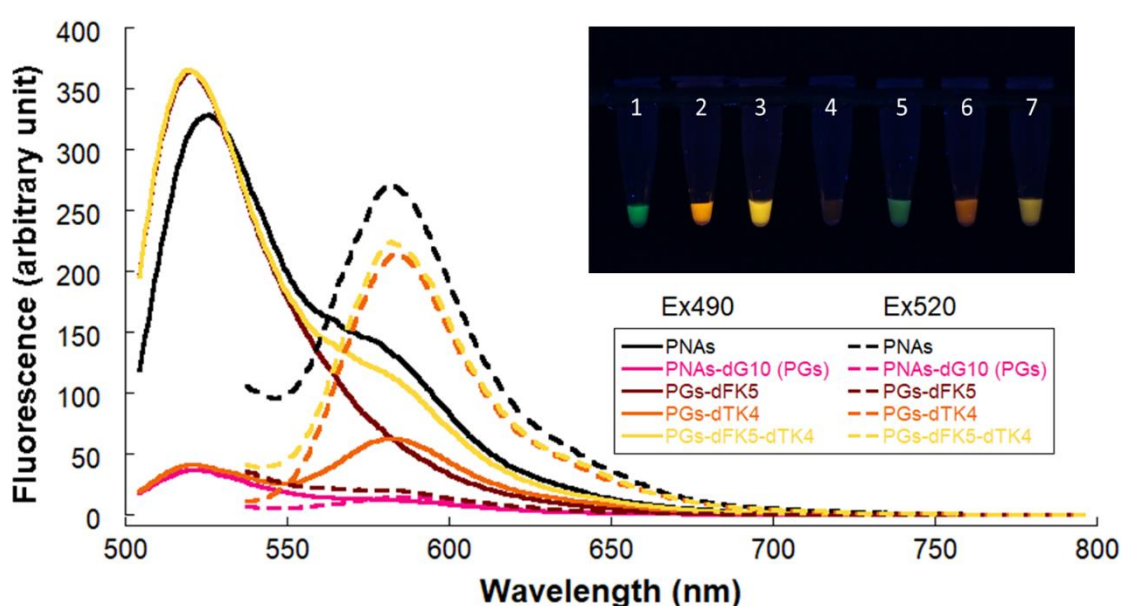
Figure 3.40 The fluorescence spectra of the mixing of two colors of PNA with their target at excitation wavelength 490 and 520 nm and Naked-eye detection visualized under transilluminator (365 nm) fluorescent Conditions: [PNA] = [dG10] = 0.1 µM, [DNA] = 0.12 µM and naked-eyed conditions: [PNA] = [dG10] = 10 µM, [DNA] = 12 µM in 10 mM phosphate buffer pH 7.0, (**Tube1**: FluK5, **Tube2**: TMRK4, **Tube3**: FluK5+TMRK4 (PNAs), **Tube4**: PNAs+dG10 (PGs), **Tube5**: PGs+dFK5, **Tube6**: PGs+dTK4, **Tube7**: PGs+dFK5+dTK4).

Thus, it could be confirmed that 1) the dG10 can effectively quench both fluorescein and TAMRA labels 2) the fluorescence signals of both the Flu and TAMRA-labeled PNA probes increase in the presence of DNA targets 3) the fluorescence restoration is sequence specific and 4) the assay can be performed in

multiplex detection format to simultaneously detect two DNA sequences. Furthermore, at a high concentration of these probes (10 µM), the fluorescence quenching and restoration in the presence of either or both targets could be observed by naked eyed under UV light as shown in the inset of **Figure 3.40.**

3.3.3.3 Metal detection

The detection of metal ions using nucleic acid probes was already introduced in Chapter 1. The binding between mercury(II) ion (Hg^{2+}) and two thymine DNAs was selective due to the ability of the Hg^{2+} to stabilize the T-T mismatched duplex by the formation of a very stable $T-Hg^{2+}-T$ complex.[81] Likewise, silver(I) ion (Ag^+) can stabilize the C-C mismatches in DNA duplexes by the formation of a stable $C-Ag^+-C$ complex.[82] To the best of our knowledge, the phenomena had not yet been evaluated in the context of PNA probes. Herein we explore the use of acpcPNA probe for the metal ion detection purpose.

Table 3.7 PNA and DNA sequences for metal detection

Type	Name	Sequence
PNA	PNAK5	Ac-GTAGATCACT-KKKKKNH$_2$
	FluK5	Flu- GTAGATCACT-KKKKKNH$_2$
DNA	misC	5'-AGTCATCTAC-3'
	misT	5'-AGTGTTCTAC-3'

The sequence of the PNA and DNA used for the metal detection study is shown in **Table 3.7**. Following the literature procedure,[80] 10 mM of MOPS buffer which did not precipitate nor form complexes with the metal ion has been widely used for the metal detection was selected for all experiments under this topic. To test the hypothesis whether the T-T and C-C mismatches in the PNA-DNA duplexes could be stabilized by Hg^{2+} and Ag^+ as observed in the case of DNA-DNA duplexes, the melting temperature experiments below were performed.

The T_m results in **Figure 3.41** revealed the change of the melting profiles of the PNA-DNA duplexes before (pink line) and after (red line) the metal ion addition. The results showed that the melting temperature of the C-C mismatched PNA-DNA duplex formed from PNAK5 and DNA C mismatch increased from 38 to 57 °C after Ag$^+$ was added. The stabilization is specific for the Ag$^+$ ion since the addition of Hg^{2+} ion did not increase the T_m of the same duplex. Likewise, the T-T mismatched PNA-DNA duplexes deriving from PNAK5 and DNA T mismatch was selectively stabilized by only Hg^{2+} but not Ag$^+$. From these experiments, it can be concluded that similar to the case of DNA-DNA duplexes, the T-T and C-C mispairings in the acpcPNA-DNA duplex were selectively stabilized by Ag$^+$ and Hg^{2+}, respectively.
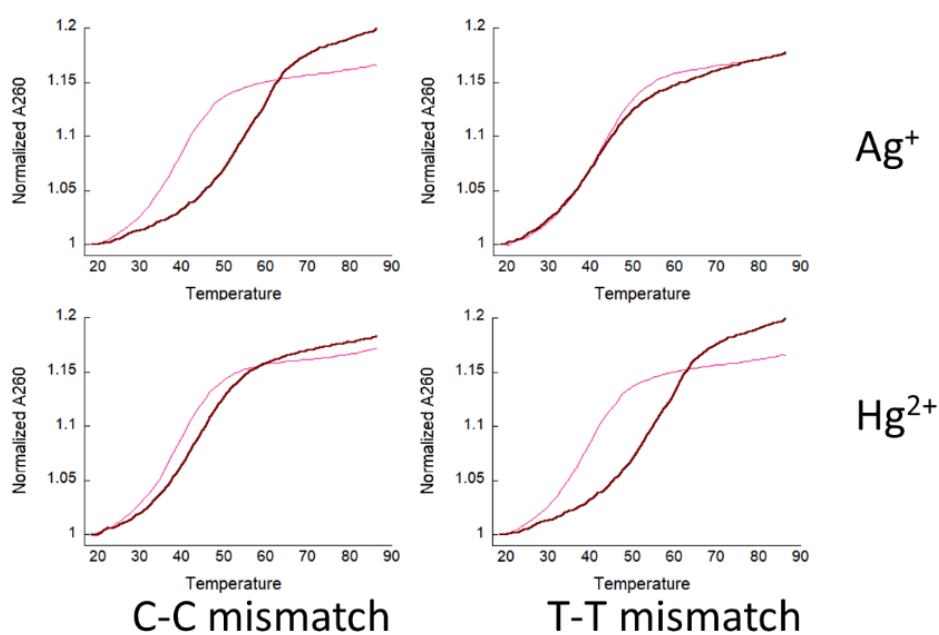
Figure 3.41 Melting temperature of mismatch PNA-DNA duplex before (pink solid) and after (red solid) the addition of metal ion. Conditions: [PNA] = 1 μM, [DNA] = 1.2 μM, [Metal ion] = 1 μM in 10 mM MOPS buffer.
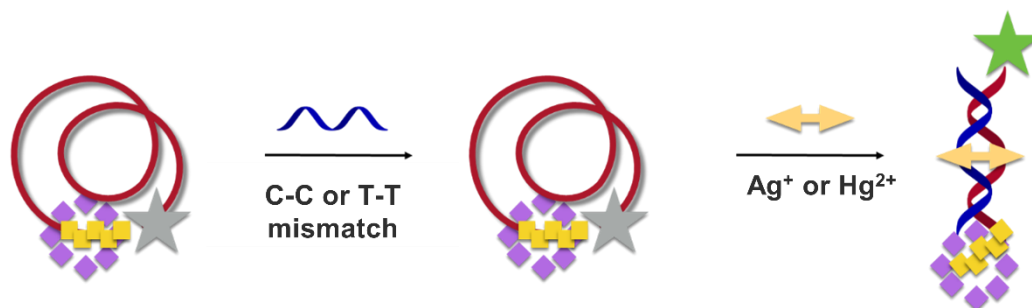
Figure 3.42 A principle of metal detection by using the quenching platform

Experiments were performed to assess the possibility of applying the previously developed PNA-dGX DNA sensing system for the detection of metal ions. **Figure 3.42** presents the hypothesis that the mismatch DNA target would not restore the fluorescence intensity of the dGx-quenched PNA probe until the correct metal ion was added to stabilize the C-C or T-T mismatched hybrids.
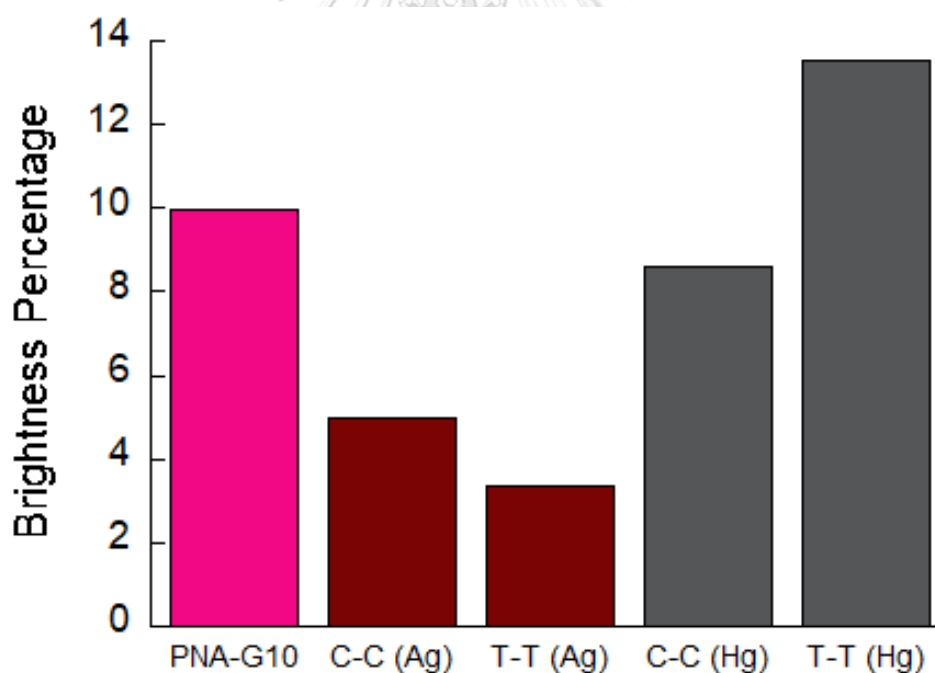
Figure 3.43 Selectivity of metal detection by using oligodeoxyguanosine quenching platform Conditions: [FluK5] = 0.1 µM, [DNAmisX] = 0.12 µM, [Metal ion] = 1 µM in 10 mM MOPS buffer, excitation wavelength at 490 nm

Unfortunately, in the case of Ag^+ detection, the fluorescence results after the addition of the metal ion were not consistent with the hypothesis (**Figure 3.43**). There was no restoration after the addition of silver ion, and the fluorescent actually decreased further to 0.6 times when compared to the dG10-quenched PNA probe. The same quenching was observed in the T-T mismatched duplex. This might be due to the quenching effect of Ag^+ on the fluorescein label as had been reported in previous studies.[131, 132] For the detection of Hg^{2+} by the T-T mismatched PNA-DNA duplex, the results revealed some selectivities between Ag^+ and Hg^{2+} since the signal of the T-T mismatch duplex increased around 1.3 folds after the addition of Hg^{2+} when compared to the dG10-quenched PNA probe. On the other hand, addition of Hg^{2+} to the C-C mismatch duplex decreased the fluorescence signal further. Although the experiments were partially successful to demonstrate the metal ion detection (Hg^{2+}) by the PNA-dGX sensing platform, the efficiency was not yet satisfactory. Hence, additional experiments were next performed in order to develop a more efficient metal ion sensing system.

According to the detection of Hg^{2+} by using DNA aptamers from Ms. Duangkamol Tiarpattaradilok's senior project,[133] the duplex should be incubated with the metal ion before the addition of other reagents. The metal detection experiments were thus repeated accordingly. When the order of the addition was PNA, DNA, Hg^{2+} and dG10, respectively, it was found that the PNA-dGX platform could detect Hg^{2+} more clearly. To make sure that the fluorescence change observed is specific to the T-T mispairing, the experiments were performed with the duplexes of the PNA and three DNA targets bearing different base mismatched (misC, misG and misT) as shown in **Figure 3.44.**
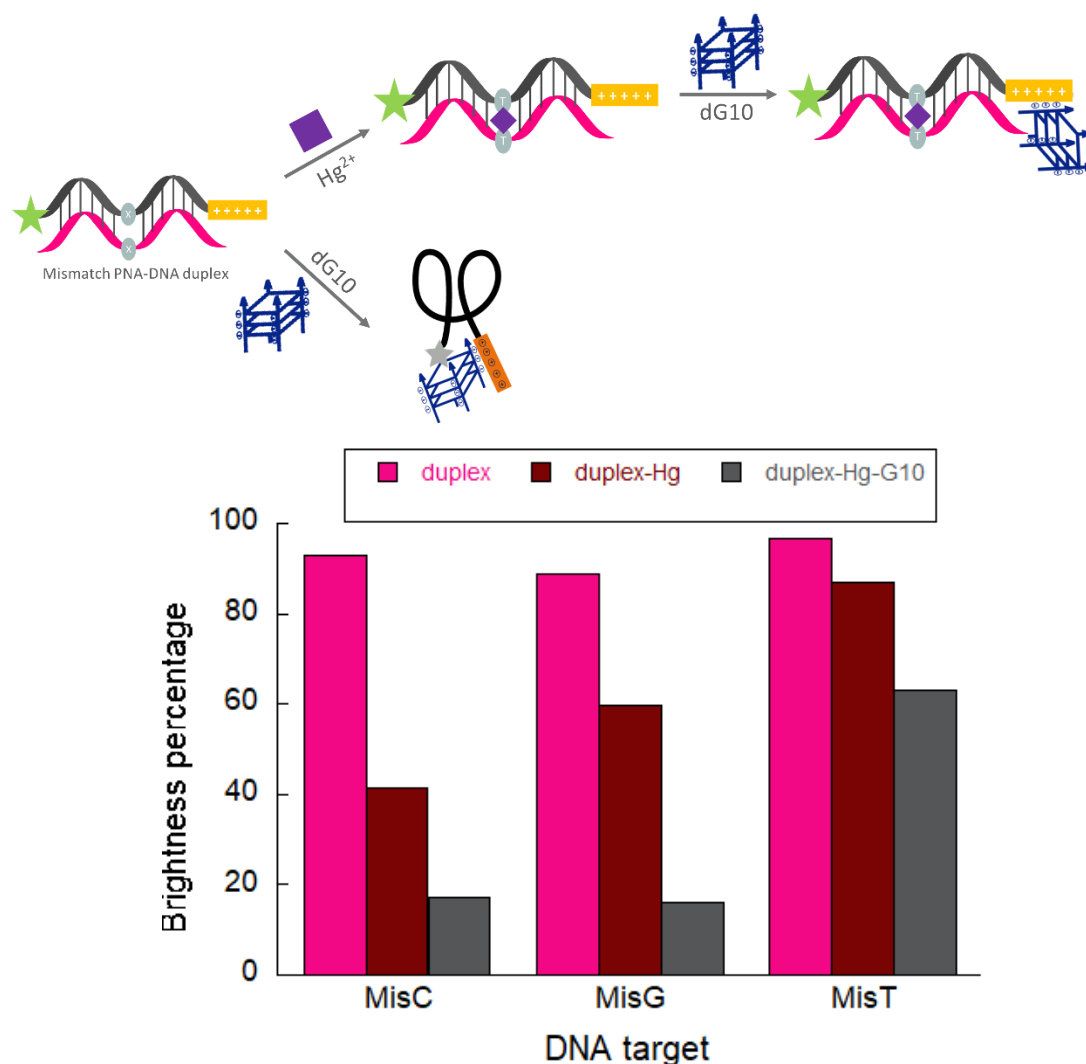
Figure 3.44 Selectivity of mercury (II) ion detection by using PNA and various type of DNA targets Conditions: [PNA] = 0.1 µM, [DNA] = 0.12 µM, [Metal ion] = 1 µM, FluK5: Flu-GTAGATCACT-KKKKKNH$_2$, Mis:5'-AGTGAXCTAC-3' [X=C, G, T] µM in phosphate buffer pH 7.0, excitation wavelength at 490 nm

After the addition of DNA targets (**Figure 3.44**), the fluorescence of all duplexes slightly decreased to around 90% of the single-stranded PNA probe. After the addition of Hg^{2+}, the fluorescence signals of the probe hybrids with the misT DNA remained high (around 80% of the original fluorescence of the PNA probe), while those of the misC and misG DNAs were much lower. The experiment suggested that the Hg^{2+} was able to quench the fluorescence of the duplexes which could not be

stabilized by the metal ion, leading to the observed fluorescence quenching in the cases of misC and misG DNA. After the addition of dG10, the fluorescence intensity decreased further in all cases. However, the PNA hybrid with misT gave the highest signal than other DNA targets (around 60% of the original PNA probe). The remaining mismatched PNA-DNA duplexes which were not stabilized by the Hg^{2+} (misC and misG) were dramatically quenched. In these cases, the PNA probe might exist in the single-stranded form and would therefore interact with the dG10 leading to the strong fluorescence quenching observed. On the other hand, in the case of misT DNA, the mismatched T-T duplex was stabilized by the Hg^{2+} causing the probe to exist in the duplex form. Thus, the addition of dG10 could not quench this T-T mismatch duplex much further.
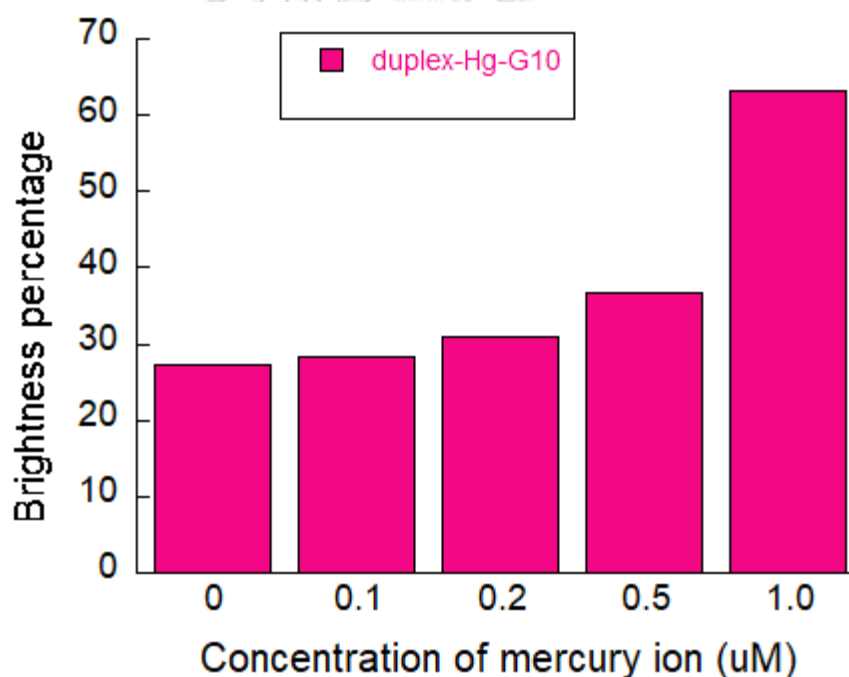
Figure 3.45 The sensitivity of the FluK5-dG10 platform for mercury detection. Conditions: [PNA] = 0.1 μM, [DNA] = 0.12 μM, [Metal ion] = 1 μM, FluK5: Flu-GTAGATCACT-KKKKKNH$_2$, DNA:5'-AGTGATCTAC-3' μM in phosphate buffer pH 7.0, excitation wavelength at 490 nm

The experiments above successfully demonstrated the applicability of the PNA-dGX system for the detection of Hg^{2+}. Next, an experiment was performed

to evaluate the concentration range of Hg^{2+} that can be detected by this sensing system. **Figure 3.45** revealed the detection of mercury by fixing the concentration of the probe and the misT DNA at 0.1 µM and 0.12 µM, respectively. Then, various concentrations of Hg^{2+} in the range of 0 – 1 µM were added (pink bars). After being incubated for 30 min, 0.1 µM of dG10 was added (red bars). The results showed that the signal decrease in response to the Hg^{2+} concentration level. Nevertheless, the lowest detectable concentration of Hg^{2+} were in the range of 200 nM or higher, which still require further improvements for practical applications.

3.3.3.4 Click reaction detection

Due to the limitation of the manual synthesis of acpcPNA, the yield from the synthesis of PNA would greatly depend on the length of the PNA sequences. The longer sequences, the smaller yield. Typically, manual synthesis of acpcPNA carried out in this laboratory gives acceptable yield and purity up to 16 bases in length. Therefore, the ligation of two PNA sequences was considered as another alternative method to make longer PNA probes.[134-136] In this part, we applied the oligodeoxyguanosine quenching to report the progress of the ligation between two PNA strands via click chemistry.
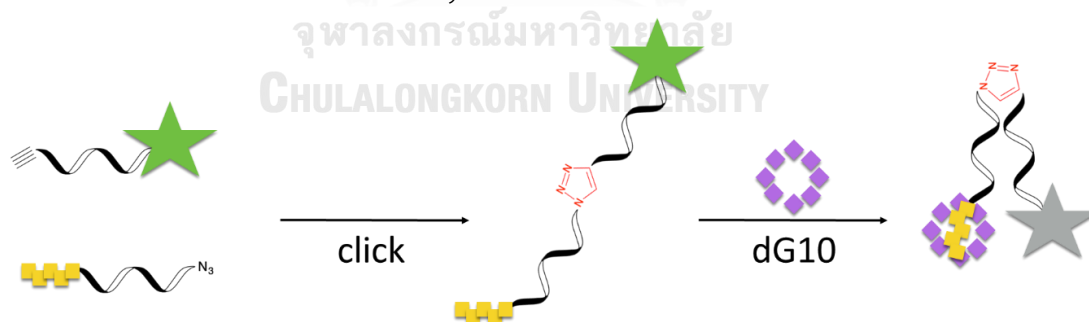
Figure 3.46 Concept of the detection of PNA ligation by using oligodeoxyguanosine

The concept of this work is shown in **Figure 3.46**, whereby dG10 could not quench the fluorescence of the fluorescein-labeled acpcPNA that does not contain the multiple lysine modification. The fluorescein-labeled PNA contains an alkyne group connected to the C-terminal tyrosine modification. After clicking with

another PNA bearing an azide group and a multiple lysine modification, the signal would be quenched as a result of favorable electrostatic interaction between the dye-labeled click product and the dG10.
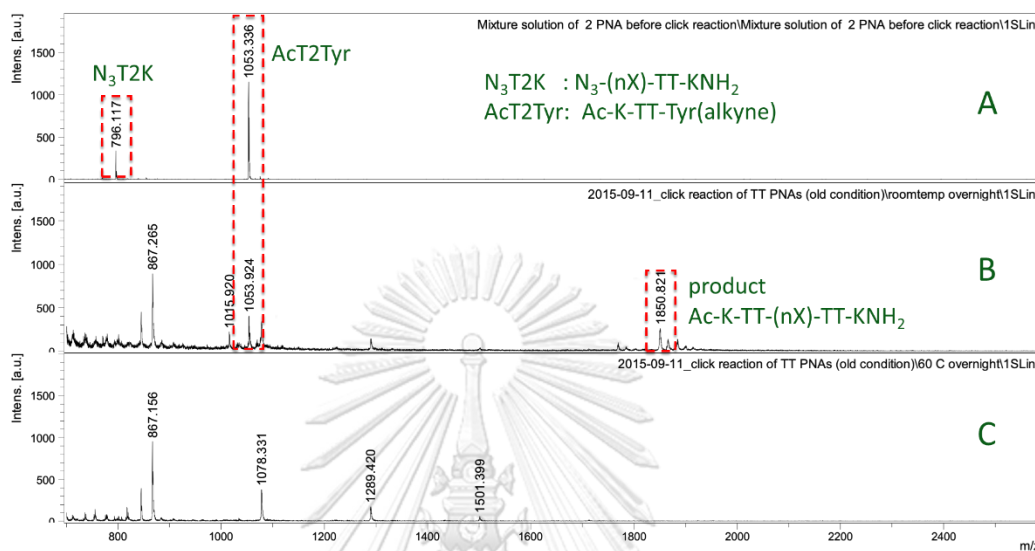
Figure 3.47 old condition for click reaction of N_3T2K and AcT2Tyr ; Conditions: [N_3T2K] = 100 µM, [AcT2Tyr] = 100 µM, [$CuSO_4$] = 10 mM, [SA] = 40 mM in 100 µL of H_2O

This study started with the optimization of the click chemistry reaction. The azide PNA without the final ACPC spacer (N_3T2K:N_3-(nX)-TT-LysNH$_2$) (*m/z* = 796.1) and the alkyne PNA [AcT2Tyr:Ac-Lys-TT-Tyr(alkyne)] (*m/z* = 1053.3) were used as the model PNA sequences for the click reaction. A mixture of 100 µM of N_3T2K and AcT2Tyr was treated with 10 mM of $CuSO_4$, and 40 mM of sodium ascorbate (SA) in water (100 µL). The results in **Figure 3.47** (panel B) showed only small peak of the product (*m/z* = 1850.8). However, the reaction was not clean and starting materials (*m/z* = 1053.3) remained in the reaction. Heating was attempted to drive the reaction to completion. Unfortunately, the product was decomposed (panel C) when the reaction was heated up to 60 °C.
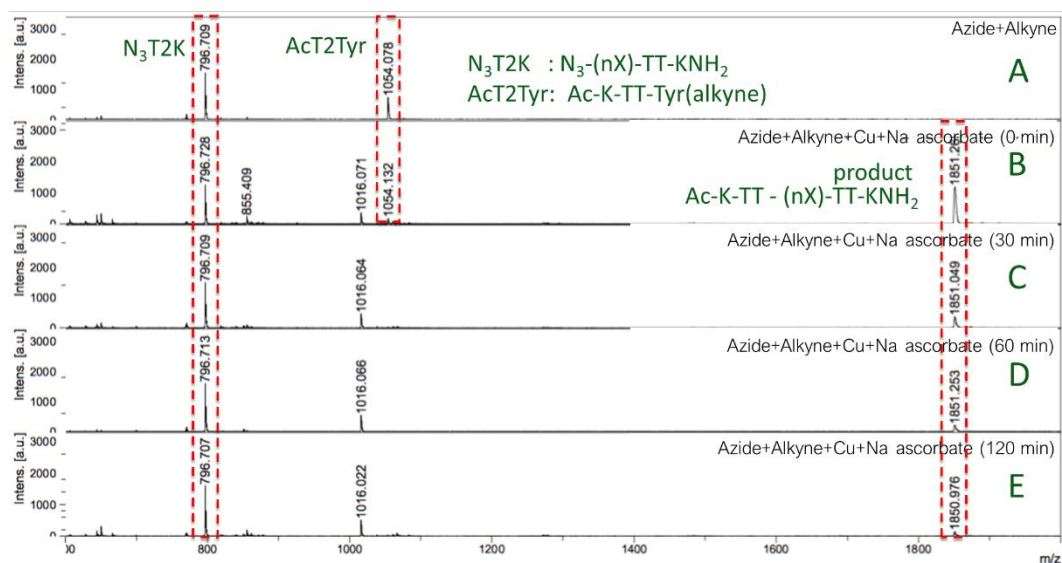
Figure 3.48 Click reaction of N$_3$T2K and AcT2Tyr with co-solvent; Conditions: [N$_3$T2K] = 100 µM, [AcT2Tyr] = 100 µM, [CuSO$_4$] = 10 mM, [SA] = 40 mM in 100 µM of H$_2$O:^{t}BuOH (1:1)

Next, the H$_2$O:^{t}BuOH (1:1) as a co-solvent was adapted to the investigation. The results in **Figure 3.48** showed that the product (m/z = 1851.2) could occur immediately after all reagents were mixed. Moreover, this reaction appeared cleaner than the previous one that use only water as the solvent. Thus, it could be concluded the *tert*-butanol co-solvent play an important role in the click reaction. However, the product's peak was decreased comparing to starting material when the reaction was allowed to proceed for longer time. Moreover, the m/z of the starting materials were changed from 796.7 to 855.4 and 1054.1 to 1016.0. This suggested that the product and starting materials might not be stable under the reaction conditions. Then, the *tris*-hydroxypropyltriazolylmethylamine (THPTA) ligand, which is reported as a very effective accelerating ligand for click reactions,[137] was then applied into the reaction. The results in **Figure 3.49** revealed that the product was now stable after 2 hour or overnight reactions, and there were no starting materials decomposition peaks at m/z = 855.4 and 1016.0, but the reaction was still not complete.
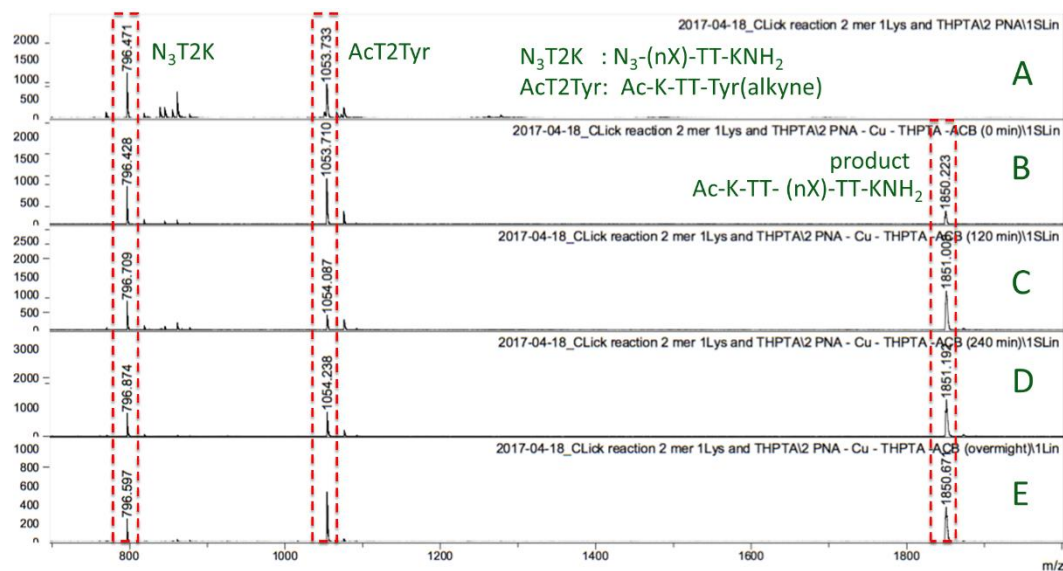
Figure 3.49 Click reaction of N₃T2K and AcT2Tyr with THPTA; Conditions: [N$_3$T2K] = 100 μM, [AcT2Tyr] = 100 μM, [CuSO$_4$] = 10 mM, [SA] = 40 mM, [THPTA] = 10 mM in 100 μM of H$_2$O:^{t}BuOH (1:1)

Since both the starting PNAs were still present in the reaction even though the reaction was left overnight, the reaction in **Figure 3.50** was next performed with the concentration of the starting materials increased from 100 μM to 500 μM, both in the absence and presence of the THPTA ligand. The results showed that there was no remaining AcT2Tyr observed in all cases but there was an unknown peak at m/z = 1015 in the conditions without THPTA. From this evidence, it might be concluded that the high concentration of PNA could force the reaction to get a complete conversion and that the addition of THPTA was beneficial to the reaction. Next, the experiment was performed with a fluorescein-labeled alkyne PNA FluT2Tyr [Flu-K-TT-Tyr(alkyne), m/z = 1259.6] to examine the impact of the availability of fluorescein on alkyne PNA with the optimized condition.
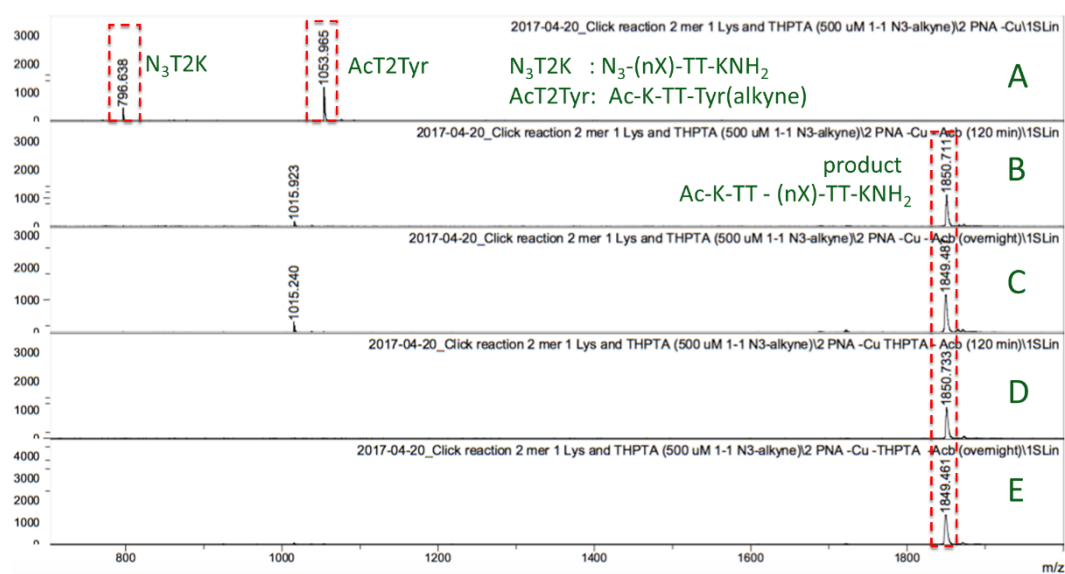
Figure 3.50 Click reaction of N_3T2K and AcT2Tyr at 500 µM; Conditions: $[N_3T2K]$ = 500 µM, [AcT2Tyr] = 500 µM , $[CuSO_4]$ = 10 mM, [SA] = 40 mM, [THPTA] = 0 mM (panel B and C) , 10 mM (panel D and E) in 100 µM of H_2O:^{t}BuOH (1:1)
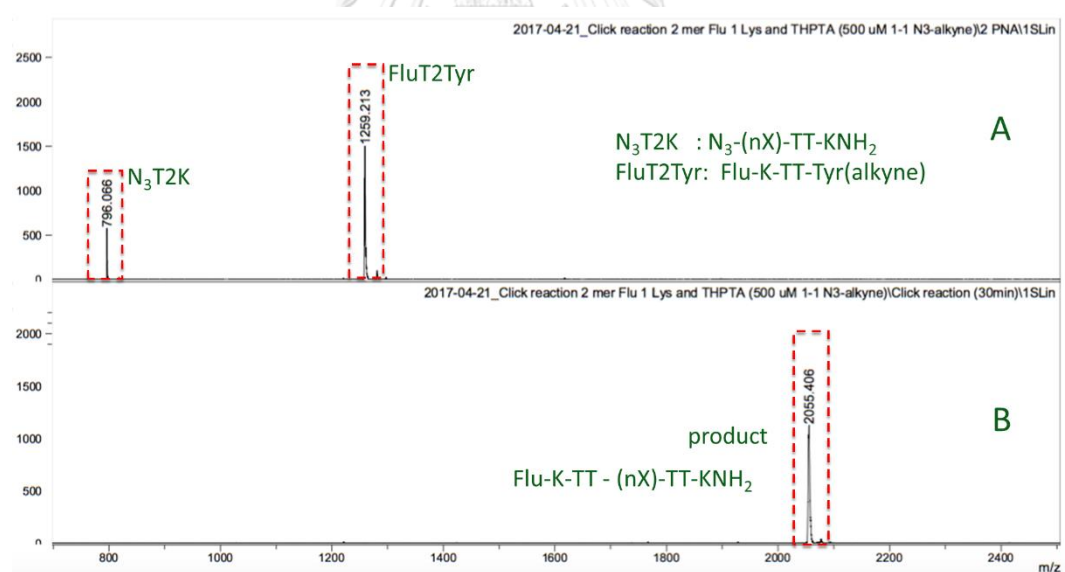
Figure 3.51 Click reaction of N_3T2K and FluT2Tyr; Conditions: [azide] = 500 µM, [alkyne] = 500 µM, $[CuSO_4]$ = 10 mM, [SA] = 40 mM, [THPTA] = 10 mM in 100 µM of H_2O:^{t}BuOH (1:1)

The result in **Figure 3.51** showed that the reaction cleanly proceeded to completion under the same condition to give the ligated product with

the expected *m/z* at 2055.4. Thus, fluorescein-labeled alkyne PNA was compatible with the click reaction. Next, the relationship between the success of the ligation reaction and the quenching by oligodeoxyguanosine was investigated. According to our hypothesis, when the ligation was successful, the fluorescence signal of the ligation product should be quenched by the oligodeoxyguanosine. **Figure 3.52** revealed that the ligation between a five lysine-modified azide PNA (N₃T2K5) (*m/z* = 1309.0) and the fluorescein-labeled alkyne PNA (FluT2Tyr) (*m/z* = 1259.6.0) in the presence of 10 mM of CuSO₄, 40 mM of SA, 10 mM of THPTA in 100 μM of H₂O:ᵗBuOH (1:1) proceeded efficiently as with other PNAs in the model reactions. After 2 hours for incubation, the reaction mixture was sampled and diluted to 10 μM in phosphate buffer pH 7. Next, dG10 was added to the diluted sample to give a final concentration of 12 μM and incubated for 10 min.
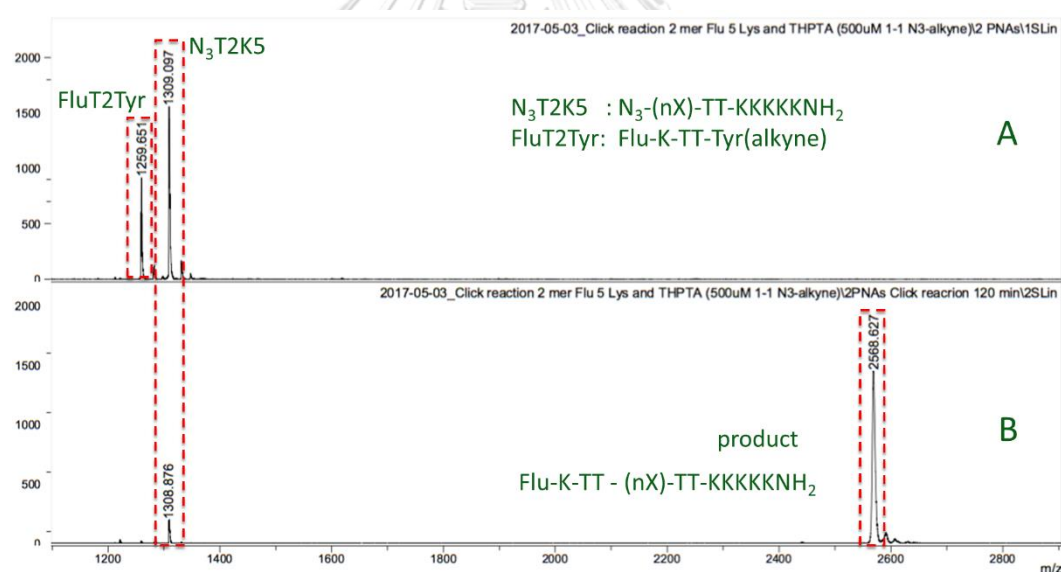
Figure 3.52 Click reaction of N₃T2K5 and FluT2Tyr Conditions: [N₃T2K5] = 500 μM, [FluT2Tyr] = 400 μM, [CuSO₄] = 10 mM, [SA] = 40 mM, [THPTA] = 10 mM in 100 μM of H₂O:ᵗBuOH (1:1)
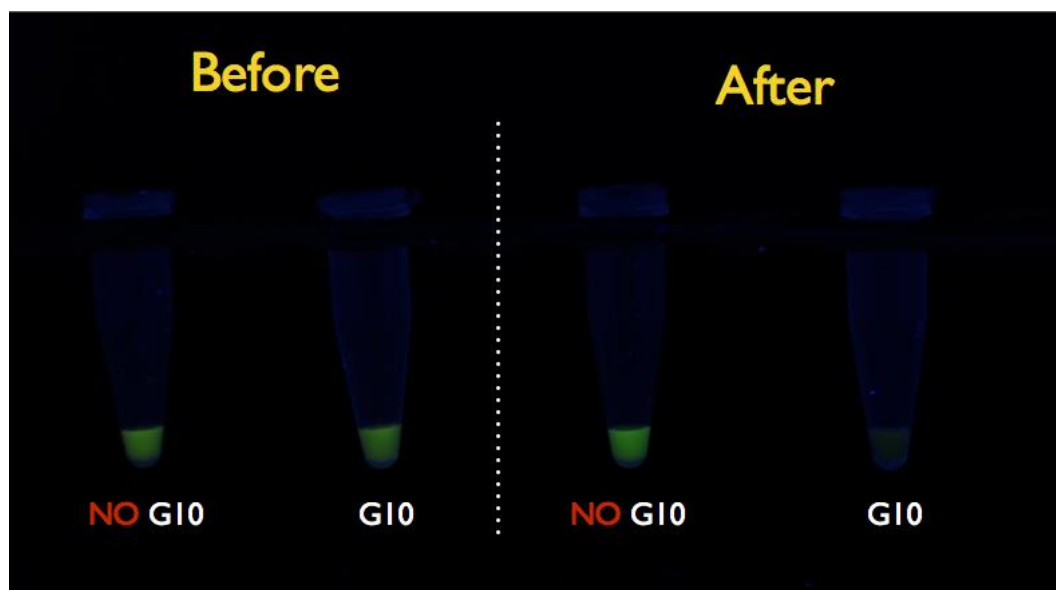
Figure 3.53 Detection of PNA ligation by using oligodeoxyguanosine; Conditions: [PNA] = 10 μM, [dG10] = 12 μM in 10 mM phosphate buffer pH 7

The results in **Figure 3.53** showed that the fluorescence after the ligation was quenched after adding dG10, while the fluorescence before the ligation remained the same. These preliminary experiments confirmed the hypothesis that oligodeoxyguanosine can be used to detect the click ligation between two PNA strands.

The ligation of longer PNA sequences (5mer) without the fluorescein label was next investigated. In the previous studies, the PNA dimers were used without purification. In the case of 5mer PNAs, purification was required before use. Although low yields were obtained from the purification, the results in **Figure 3.54** displayed a successful ligation between the PNAs N$_3$M5K5 [N$_3$-(nX)-TCACT-KKKKKNH$_2$, m/z = 2287.8] and AcM5Tyr [Ac-K-GTAGA-Tyr(alkyne), m/z = 1993.7] under the same click conditions. However, there were unknown peaks at m/z = 2138.6 and 3918.7 started to appear after the reaction was allowed to proceed for 30 min. Since the azide PNA peak was already consumed, it was proposed that the unstable azide PNA might be easily decomposed. Thus, the new type of azide-modified acpcPNA was investigated next.
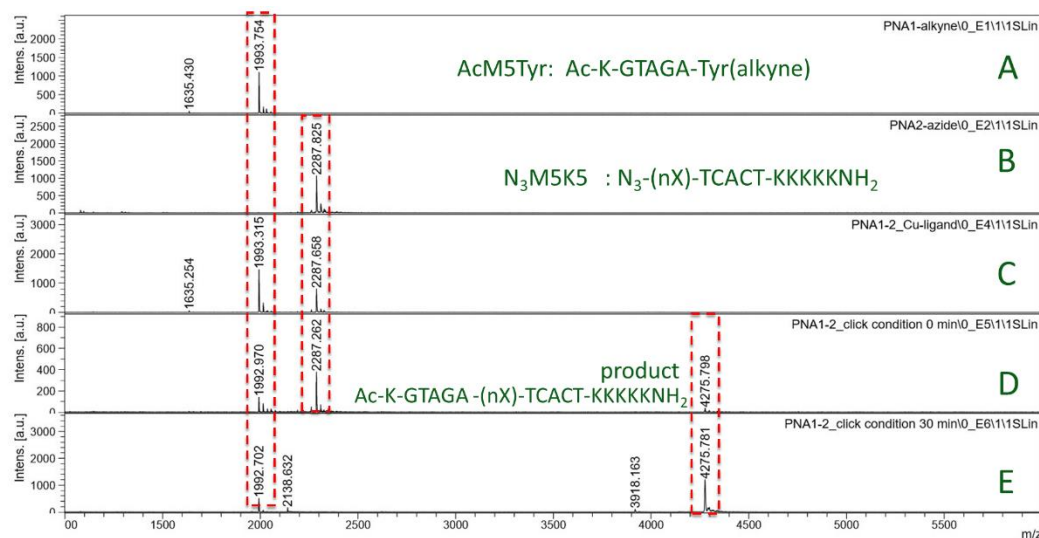
Figure 3.54 Click reaction of N_3M5K5 and AcM5Tyr ; Conditions: $[N_3M5K5]$ = 500 μM, $[AcM5Tyr]$ = 500 μM, $[CuSO_4]$ = 10 mM, $[SA]$ = 40 mM, $[THPTA]$ = 10 mM in 100 μM of H_2O:^{t}BuOH (1:1)

In 2012, there was a report that the use of 6-(azidometyl)nicotinic acid (PyrN$_3$) as a copper-chelating azide would accelerate the click chemistry reaction and reduce the cell toxicity.[97] The PyrN$_3$ modifier was synthesized following a literature procedure but the product could not crystallize and it was obtained as a yellow oil. However, the NMR data was in good agreement with the literature.[97] Then, 4 equiv. of this new azide modifier was attached to the N-terminus of a TT PNA (0.5 μmol) by using 3.9 equiv. of HATU in the presence of 7% of DIEA in DMF (30 μL) and the successful coupling was demonstrated by MALDI-TOF MS as shown in **Figure 3.55.**

After the successful coupling of the PyrN$_3$ modifier to the TT PNA was demonstrated, the azide modification reaction was attempted on a longer sequence (10mer) of acpcPNA: (nX)-GTAGATCACT-KKKKKNH$_2$. The successful attachment of the PyrN3 on the long PNA sequence was demonstrated in **Figure 3.56**. Panel A showed the Fmoc protected PNA at m/z = 3408.0. Then, the Fmoc group was deprotected and the PyrN$_3$ was attached onto the free amino group of the PNA by using the same condition. Panel B and C showed the reaction of the attachment at 2 and 3 hours, respectively. Due to the different chemistries used for the attachment (amide bond formation vs reductive alkylation), it was found that the PyrN3 attachment consumed

less time when compared to the azidobutyl modification commonly used in previous experiments. Then, the PyrN3-modified 10mer PNA was used in the ligation reaction with AcM5Tyr via click chemistry (500 µM of PNAs, 1 equiv. of Cu(I) and THPTA, and 4 equiv. of sodium ascorbate in 1:1 ^{t}BuOH:water).
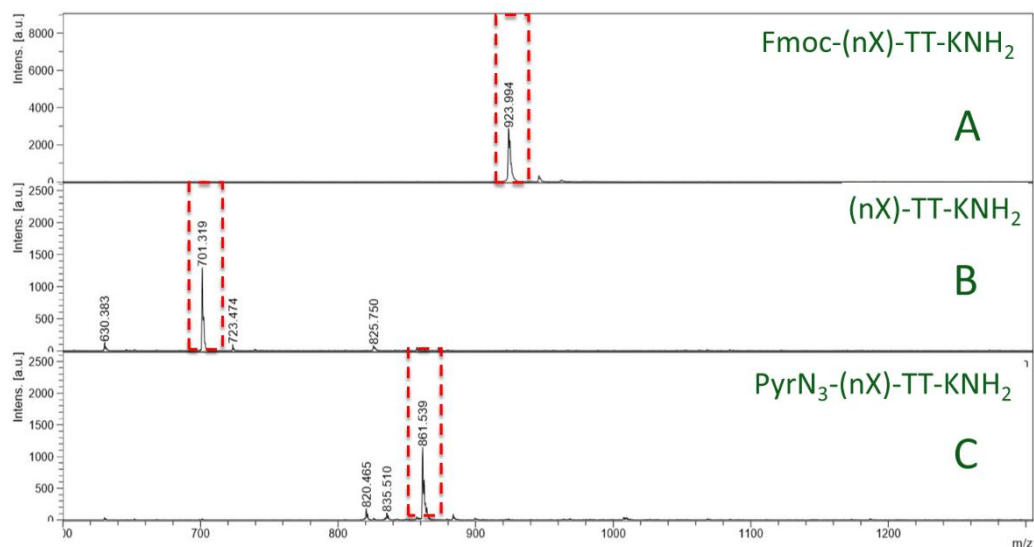
Figure 3.55 the attachment of 6-(azidometyl)nicotinic acid (PyrN$_3$) on PNA model
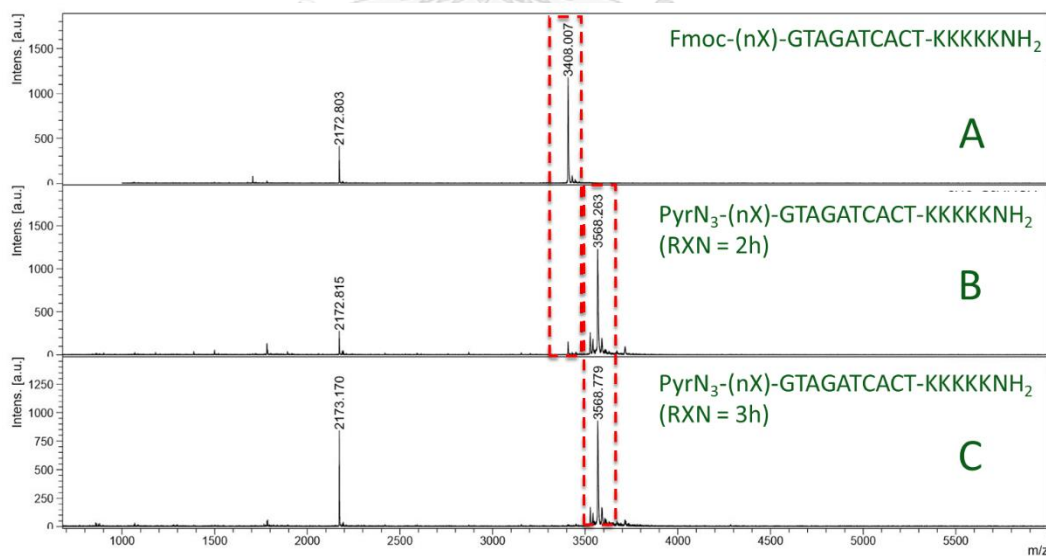
Figure 3.56 the attachment of 6-(azidometyl)nicotinic acid on the 10mer PNA: (nX)-GTAGATCACT-KKKKKNH$_2$

Disappointingly, the results in **Figure 3.57** showed that this reaction proceeded poorly. Only a small product peak was observed at *m/z* = 5555.5, but the reaction was not complete and a substantial signal of the alkyne PNA remained with complete disappearance of the azide PNA. Since the signal of the azide PNA at *m/z* = 3567.7 was small to begin with, it was suspected that the same issue about the stability of the azide PNA could not be solved with the new azide modifier.
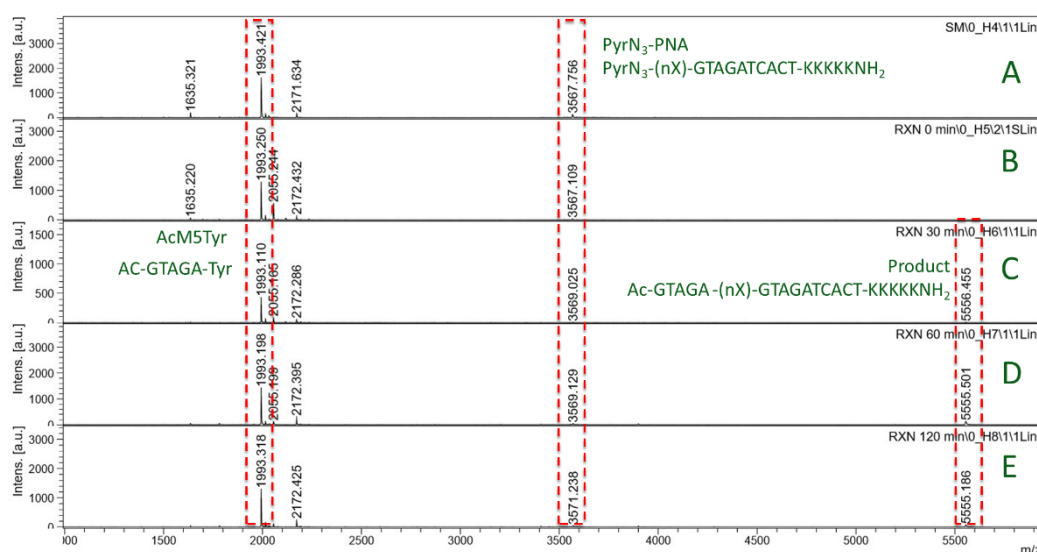
Figure 3.57 Click reaction of PyrN$_3$-PNA and AcM5Tyr; Conditions: [PyrN$_3$-PNA] = 500 μM, [AcM5Tyr] = 500 μM, [CuSO$_4$] = 100 μM, [SA] = 400 μM, [THPTA] = 100 μM in 100 μM of H$_2$O:^{t}BuOH (1:1)

Although the expected click reaction was likely to occur under this condition, the reaction was still not efficient, and the click reaction should still require further optimization to allow efficient synthesis of longer PNA sequences. Nevertheless, the experiments demonstrated at the proof-of-concept level that the dG10 quenching can be used to monitor the progress of the click reaction.

3.4 PNA and hemin/G-quadruplex DNAzyme

In the previous section, oligodeoxyguanosine was proven to be an effective quencher for DNA sensing applications when used in combination with fluorescently labeled acpcPNA probes. However, the signal was generated in a one-to-one fashion.

If a catalytic function could be incorporated into the DNA sensing system, it should be possible to improve the performance of the sensor by signal amplification. Since G-quadruplexes were reported to be catalytically active as a DNAzyme that exhibits peroxidase activities when combined with hemin as a cofactor,[138, 139] the G-rich DNA sequence was potentially useful for the proposed signal amplification assay. Thus, the objective of this study was to develop a PNA-based DNA sensing platform with signal amplification employing G-quarduplex DNAzymes.

3.4.1. Comparison of substrates

The study began with comparison of two different chromogenic substrates (CS) for peroxidase that have been frequently used in the literature, namely Amplex Red (AR) and 3,3′,5,5′-tetramethylbenzidine (TMB). A combination of decadeoxyguanosine (dG10) and hemin was used as the DNAzyme. The concentration of the DNAzyme, substrate, and buffer was taken from the literature[140] which was 100 µM of substrate, 0.125 µM of hemin, and 1 µM of dG10 in the presence of 20 µM of HEPES buffer, 1 mM of H_2O_2 and 200 mM of NH_4OAc. The results in **Figure 3.58** showed that the catalytic oxidation of both substrates readily occurred in the presence of both hemin and dG10 (**Tube4**) as shown by the appearance of pink and blue color for the AR and TMB, respectively. However, a pale pink color was also observed in the case of AR+hemin+H_2O_2 (**Tube2**), indicating that some uncatalyzed reaction was also significant for the AR as substrate. Thus, TMB was chosen as a more selective substrate for the dG10-hemin catalyzed oxidation.
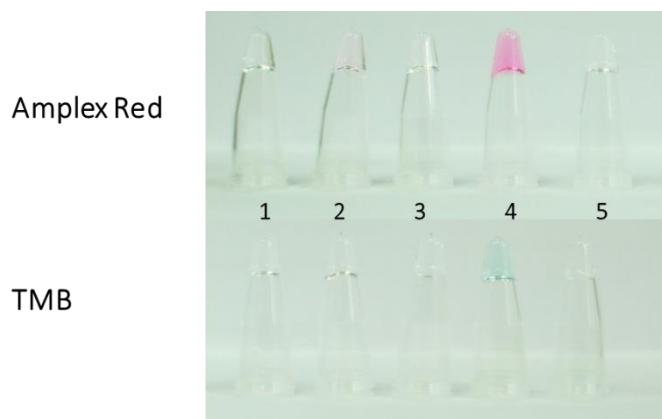
Figure 3.58 Comparison of chromogenic substrate; **Tube1**: CS+H$_2$O$_2$, **Tube2**: CS+hemin+H$_2$O$_2$, **Tube3**: CS+dG10+H$_2$O$_2$, **Tube4**: CS+hemin+dG10+H$_2$O$_2$, **Tube5**: CS+hemin+dG10 Conditions: [CS]= 100 μM, [hemin] = 0.125 μM, [dG10] = 1 μM, [H$_2$O$_2$] = 1 mM in 20 μM of HEPES buffer and 200 mM of NH$_4$OAc

3.4.2 Effect of oligodeoxyguanosine

After TMB was selected as the substrate in the dG10-hemin catalyzed oxidation, the effect of the oxidant (H$_2$O$_2$) in the reaction was examined by varying the concentration of H$_2$O$_2$ from 0 – 4 mM. The results showed that higher concentrations of H$_2$O$_2$ gave higher color intensity of the oxidized substrate (**Figure 3.59**). Importantly, if the dG10 was omitted from the reaction, no color change was observed at all concentrations of H$_2$O$_2$ tested. Thus, it could be concluded that the more hydrogen peroxide added, the faster the reaction, and that dG10 was an important component of the DNAzyme activities. The results in **Figure 3.60** revealed the effect of concentration of dG10 in the range of 0.5 – 3 μM, which showed the same blue color, suggesting that the lowest concentration of the dG10 employed at 0.5 μM was already sufficient for the maximum catalytic activity. Thus, the concentrations of dG10 and H$_2$O$_2$ were chosen at 1 μM and 100 mM in the next experiments.
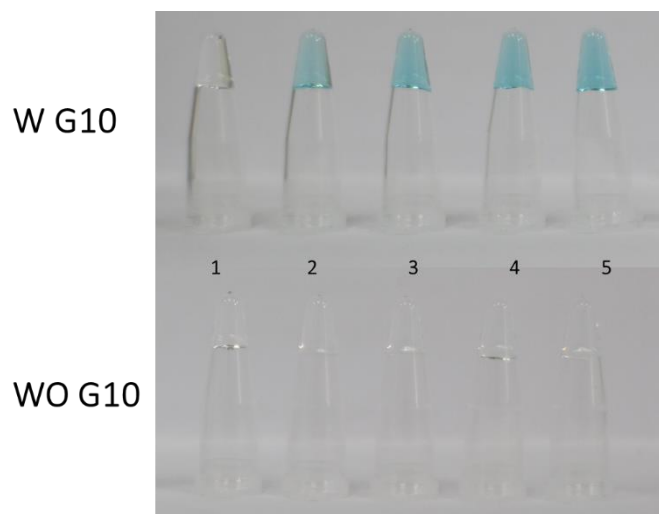
Figure 3.59 Comparison of hydrogen peroxide concentration in the condition with or without dG10; **Tube1**: 0 mM, **Tube2**: 1 mM, **Tube3**: 2 mM, **Tube4**: 3 mM, **Tube5**: 4 mM. Conditions: [TMB]= 100 μM, [hemin] = 0.125 μM, [dG10] = 1 μM, [H_2O_2] = 0 - 4 mM in 20 μM of HEPES buffer and 200 mM of NH_4OAc
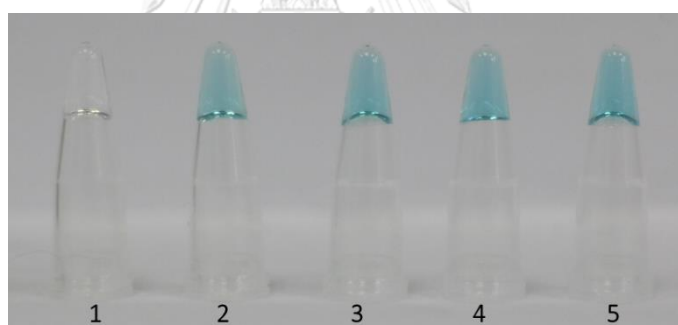
Figure 3.60 Comparison the effect of dG10 concentration; **Tube1:** 0 μM, **Tube2:** 0.5 μM, **Tube3**: 1 μM, **Tube4**: 2 μM, **Tube5**: 3 μM. Conditions: [TMB]= 100 μM, [hemin] = 0.125 μM, [dG10] = 0 – 3 μM, [H_2O_2] = 100 mM in 20 μM of HEPES buffer and 200 mM of NH_4OAc

3.4.3 The catalytic activity of dG10-hemin in the presence of PNA
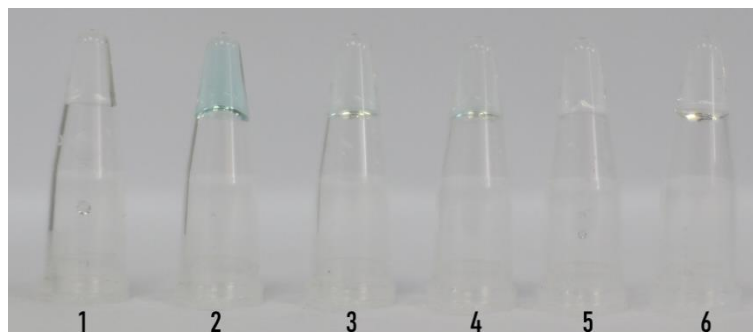
Figure 3.61 The reactivity of dG10-hemin in the presence of PNA and its complementary DNA; **Tube1**: PNA, **Tube2**: dG10, **Tube3**: PNA+dG10, **Tube4**: PNA+dG10+dcom, **Tube5**: PNA+dcom **Tube6**: dcom Conditions: [PNA = Ac-GTAGATCACT-KKKKKNH$_2$] = 3 µM, [dcom = 3'-CATCTAGTGC-5'] = 4 µM, [TMB]= 100 µM, [hemin] = 0.125 µM, [dG10] = 1 µM, [H$_2$O$_2$] = 100 mM in 20 µM of HEPES buffer and 200 mM of NH$_4$OAc

Our original hypothesis was that when the dG10 was bound to the positively charged lysine-modified PNA, its catalytic activity (in the presence of hemin) should be lower. It was proposed that when dG10 was bound to the PNA via the electrostatic interaction, the G-quadruplex structure might be distorted so that it cannot accommodate the stacking of the hemin, leading to the inability to catalyze the reaction. The reactivity was expected to restore once the complementary DNA target was bound to the PNA due to the displacement of the bound DNAzyme. Indeed, the results in **Figure 3.61** demonstrated that the PNA complexation does inhibit the catalytic activity of the dG10, as shown by the absence of color change in **Tube3**. Unfortunately, no color change was observed when the complementary DNA was added (**Tube 4**). This suggests that the PNA-bound dG10 could not participate in the formation of an active DNAzyme regardless of the status of the PNA probe (free or DNA-bound). This experiment supported our previous finding (**section 3.3.3.2**) that the PNA and dG10 remained complexed after the DNA hybridization. Thus, it was impossible to use a simple combination of dG10-hemin and PNA to indicate the presence of the correct DNA target.

3.4.4 The catalytic activity of hemin/overhang DNA

a   b
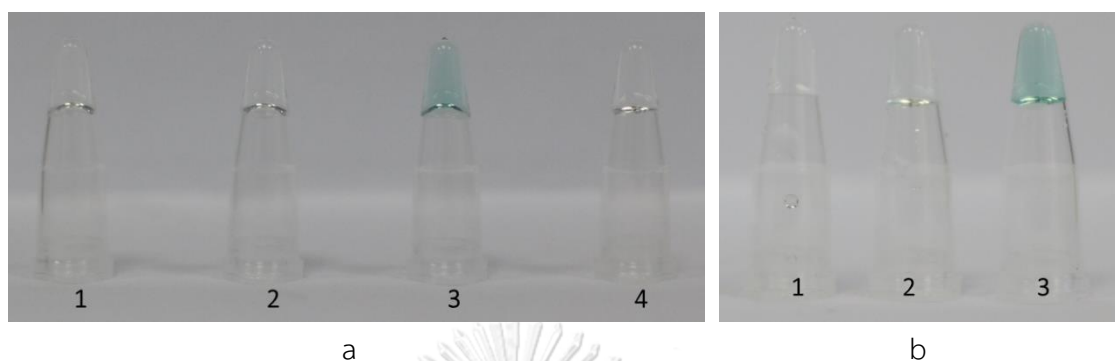
Figure 3.62 reactivity of (a) dHX/hemin; **Tube1:** dHA, **Tube2**: dHC, **Tube3**: dHG, **Tube4**: dHT and (b) dHG/hemin in the presence of PNA and its complementary DNA; **Tube1:** PNA, **Tube2**: PNA+dHG, **Tube3**: dHG Conditions: [PNA = Ac-GTAGATCACT-KKKKKNH$_2$] = 3 µM, [dHX = 3'-XXXXXCATCTAGTGC-5'] = 1 µM, [TMB]= 100 µM, [hemin] = 0.125 µM, [H$_2$O$_2$] = 100 mM in 20 µM of HEPES buffer and 200 mM of NH$_4$OAc

Since the combination of simple dG10-hemin and PNA alone could not be used to identify the correct DNA target, presumably due to the direct electrostatic interaction of the G-quadruplex with the PNA probe that impaired its ability to form a catalytically active DNAzyme with hemin, alternative designs of the sensing systems were explored. Next, the DNA targets with a complementary sequence to the PNA probe, but with different 3'-overhangs consisting of five repeating dX units (dHX) was examined. It was proposed that in this case, the complementary DNA part would bind to the PNA, forming a PNA-DNA hybrid. This would leave a free oligodeoxyguanosine overhang that would be prevented from forming a proper G-quadruplex by the PNA. The results in **Figure 3.62a** showed that only the dHG-hemin combination without the PNA (positive control) could act as DNAzyme (**Tube3**) as shown by the color change of the TMB substrate from colorless to blue. This confirms the previous results that the oligodeoxyguanosine tract was necessary for the catalytic activity. Next, the addition of PNA completely inhibited the catalytic

activity as shown by the absence of color change in **Figure 3.62b**. It could be concluded that the free dHG could form the quadruplex structure that can bind with hemin and led to the catalytic activity. The presence of bound PNA probe to the complementary region might block or destabilize the quadruplex formation leading to the observed absence of catalytic activity.
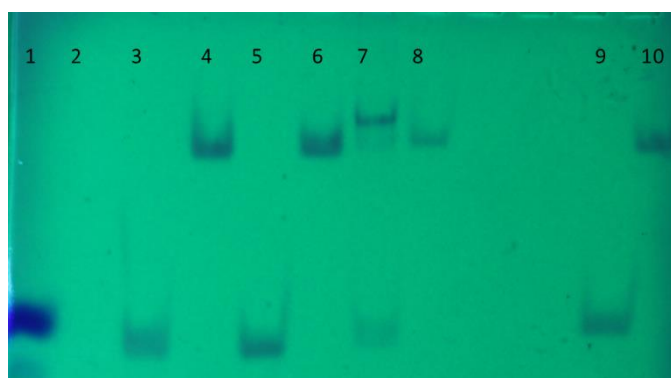
Figure 3.63 Gel electrophoresis of PNA and dHX; **lane1:** loading dye, **lane3:** dHA, **lane4:** PNA+dHA, **lane5:** dHC, **lane6:** PNA+dHC, **lane7:** dHG, **lane8:** PNA+dHG, **lane9:** dHT, **lane10:** PNA+dHT. Conditions: 0.5 nmol of PNA, 0.6 nmol of DNA in each lane and 150V was applied for 2.5 hours.

Moreover, the gel electrophoresis experiments in **Figure 3.63** confirmed that the binding between PNA and dHG would destroy the quadruplex structure as evidenced by the disappearance of the slow-moving bands due to the G-quadruplex (lane 7) upon hybridization with the PNA with concomitant formation of the PNA-DNA duplex band (lane 8).

Next, the effect of other G-quadruplex forming sequences were tested whereby they were attached to the 3'-end of the DNA with a sequence complementary to the PNA probe similar to dHG. The results are shown in **Figure 3.64**, whereby the catalytic activities were compared in the absence and presence of the PNA probe. **Tube2** was the exact complementary DNA sequence, **Tubes3** to **6** were complementary DNA containing various number of deoxyguanosine units (1, 3, 5 and 6), and **Tube7** to **9** contain overhangs that can form intramolecular parallel G-quadruplexes.[139] In the absence of the PNA, the color change was observed in

Tube5 to **9**. It was concluded that the quadruplex structures could form and lead to the catalytic activity in the presence of hemin only when the DNA contained at least 5 adjacent deoxyguanosine overhang (**Tube5** and **6**) or when an intramolecular G-quadruplex formation was possible (**Tube7**, **8** and **9**). When the PNA was added, the catalytic activity was reduced in the cases of DNAs that form intermolecular G-quadruplexes (**Tube5** and **6**). Interestingly, the DNA that does not contain the PNA binding site (**Tube7**) also gave a reduced catalytic activity, which could be explained by the non-specific electrostatic interaction with the FluK5 PNA probe that inhibited the formation of the catalytically active DNAzyme. In contrast, the hybridization to the PNA did not affect the catalytic activity of the complementary DNAs carrying the overhangs that can form intramolecular G-quadruplexes (**Tube8** and **9**).
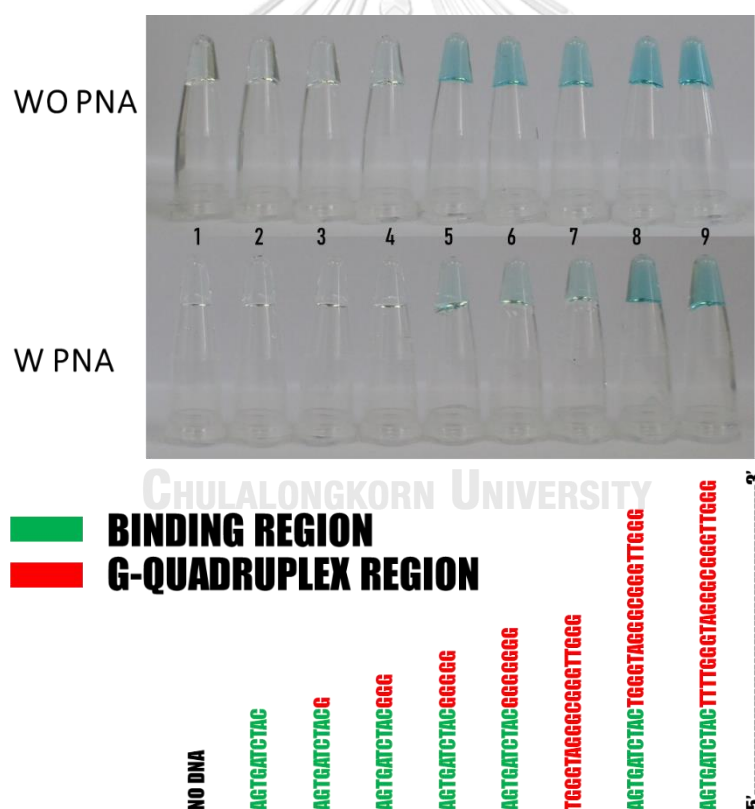
Figure 3.64 The reactivity of hemin and complementary DNA containing G-quadruplex sequences in the presence or absence of PNA Conditions: [PNA = Ac-GTAGATCACT-KKKKKNH$_2$] = 3 μM, [DNA] = 1 μM, [TMB]= 100 μM, [hemin] = 0.125 μM, [H$_2$O$_2$] = 100 mM in 20 μM of HEPES buffer and 200 mM of NH$_4$OAc

Thus, the experiments not only confirmed the previously proposed model that the binding of PNA to the DNA target bearing a G-quadruplex forming sequence could inhibit the formation of G-quadruplex, but also give additional information that the G-quadruplex destabilization occurred only in the case of intermolecular G-quadruplexes. Hence, these intermolecular G-quadruplex forming sequences are potentially useful as a catalytic label for the DNAzyme-PNA based DNA detection being developed.

3.4.5 Detection of DNA by strand displacement reaction

In previous experiments, it was shown that the binding of PNA probe to the DNA target with an oligodeoxyguanosine overhang inhibited the G-quadruplex formation and thus decreasing the catalytic activity of the DNAzyme. It was further proposed that if the DNAzyme was released from the PNA probe by another DNA strand that can bind more strongly to the PNA probe, the displaced DNAzyme would be free to catalyze the substrate oxidation again. Such strand displacement reaction would require that the PNA-DNAzyme complex must be less stable than the PNA-DNA target duplex. To develop the proposed strand displacement assay, the sequence of the DNAzyme was shortened to 7mer to decrease the stability of the PNA-DNAzyme duplex. In addition to the short complementary DNA target, two single-base mismatch sequences, and a double-base mismatch sequence were included for comparison. The three DNAzymes contained five deoxyguanosine overhang at the 3'-end. These DNAzymes were first hybridized with the PNA probe Ac-GTAGATCACT-KKKKKNH$_2$. Next, the 10mers perfectly complementary DNA target was added and incubated for 30 min. Control experiments without the DNA target were also included for comparison. After that, the reagents (hemin, H$_2$O$_2$) and the substrate (TMB) for the catalytic oxidation were added.

DNAG : 3'-G₅CATCTAG-5'   3'-G₅CTTCTAG-5'   3'-G₅CATCTTG-5'   3'-G₅CTTCTTG-5'
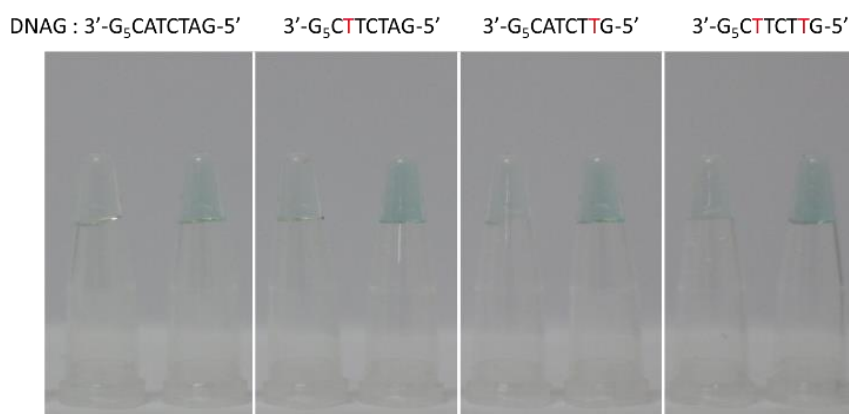
Figure 3.65 Detection of DNA displacement process by using hemin/G-quadruplex PNA; [PNA = Ac-GTAGATCACT-KKKKKNH₂] = 3 µM, [DNA with guanosine overhang] = 1 µM, [10mers DNA: 5'-AGTGATCTAC-3'] = 3 µM [TMB]= 100 µM, [hemin] = 0.125 µM, [H₂O₂] = 100 mM in 20 µM of HEPES buffer and 200 mM of NH₄OAc

The results are shown in **Figure 3.65**. In the absence of the DNA target (PNA with DNAzymes only), there was no color change observed in the case of complementary or single-base mismatched DNAs but some blue coloration was observed in the double-base mismatched DNA. This suggested that the binding between the PNA and the short complementary DNA or single-base mismatch DNA was strong enough to block the G-quadruplex formation and thus diminishing the catalytic activities of the DNAzyme. The duplex formed from the PNA and the double-base mismatched DNA was not stable and thus less effective in inhibiting the G-quadruplex formation, resulting in the observed catalytic activities. When the complementary DNA target was added, the catalytic activity was restored in all cases. But the weakest activity was observed with the DNAzyme attached to the fully complementary DNA sequence, which was not unexpected because of the strength of the hybridization between PNA and the fully complementary DNAzyme counterstrand. The more stable PNA-DNAzyme hybrid would be less likely to be displaced by the fully complementary DNA target due to the small free energy difference. This suggests that there need to be some fine-tuning the system to find a balance point at which the stability of the PNA-DNAzyme duplex is high enough to prevent the G-quadruplex formation but not too high to allow the strand

displacement to occur prematurely that would restore the catalytic activity of the DNAzyme even before the addition of the DNA target. Nevertheless, these preliminary studies demonstrated the proof-of-concept of a new PNA-based strand displacement process that could be further developed into a DNA sensing platform. The potential advantage of this system would be the catalytic nature of the DNAzyme that should generate more signal than conventional fluorescence-based assay and thus improving the sensitivity of the detection.

3.4.6 UV-vis studies

After the preliminary study had been completed, the study of hemin-G-quadruplex as a DNAzyme for DNA detection was performed using the UV-visible spectrometry. First, we aimed to detect the displacement of the guanosine-modified DNA counterstrand (5'-GATCTTC-G_5-3') from the PNA probe by the DNA target. The concentrations of the PNA and the DNA used were 1.2 µM and 0.4 µM, which was the ratio between the PNA and dG overhang DNA from the previous study. TMB substrate showed the 4 regions of absorption in this catalytic system,[141] and the absorption at 652 nm was selected for the first optimization.

Figure 3.66 Optimization of DNAzyme-based DNA detection by varying the concentrations of hemin. Conditions: [G] = 0.4 µM, [Hemin] = 0.06 b-0.4 µM, [TMB] = 10 µM, [H_2O_2] = 100 µM in 20 µM of HEPES buffer and 200 mM of NH_4OAc. (X axis is time (min) and Y axis is absorbance)

Figure 3.66 showed the optimization by varying the concentration of hemin ranging from 0.06 – 0.4 µM with and without G-quadruplex sequence. The absorbance at 652 nm was measured every 2 min following the addition of 0.4 µM of the DNA counterstrand with the G5 overhang, 10 µM of TMB, and 100 µM of H_2O_2 in 20 µM of HEPES buffer and 200 mM of NH_4OAc. The results showed that the catalytic reaction occurred only in the presence of G-rich DNA (green, orange, red, and yellow lines). This confirmed that G-quadruplex structure was the key component for the catalytic reactivity. From the experiment, 0.08 µM of hemin which showed the most obvious and long-lasting signal change was chosen for the next experiment.

The next experiment was performed to optimize the amount of TMB and H_2O_2 through the detection at other absorption wavelengths of TMB every 5 min. Figure 3.67 showed the experiments at different ratios of TMB and H_2O_2 at 20:200 (blue), 20:1000 (orange), 100:200 (grey), and 100:1000 (yellow). The data indicated that 20 µM of TMB and 1000 µM of hydrogen peroxide performed better than others. It should be noted that the high concentration of TMB as shown by the grey and yellow line was not suitable for the catalytic reactivity. The absorbance change was most pronounced at 280 nm, but the signal was negative (i.e, the signal gets smaller after the reaction). The second most prominent signal change was observed at 370 nm, followed by 652 nm. The signal change at 450 nm was low and the maximum change was observed at a lower amount of H_2O2 (200 µM). In all cases, the maximum signal was observed at around 10 min, after that the signal started to decay at all wavelengths indicated that the oxidation product of TMB was not stable.
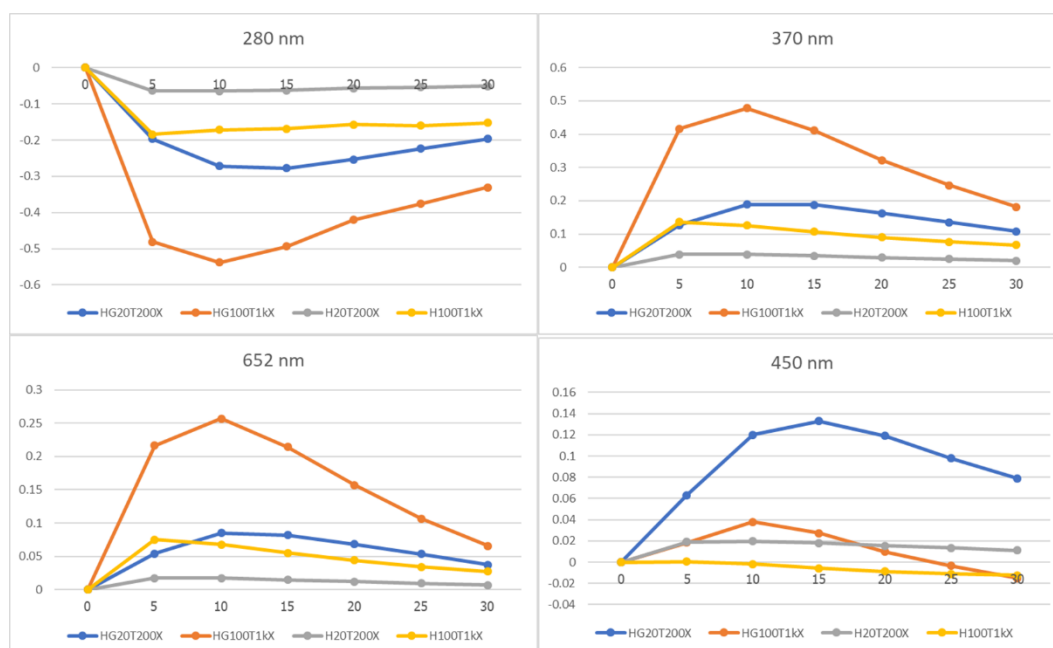
Figure 3.67 Optimization of DNAzyme-based DNA detection by varying the ratios of TMB and hydrogen peroxide. Conditions: [G] = 0.4 µM, [Hemin] = 0.08 µM, [TMB] = 20, 100 µM, [H$_2$O$_2$] = 200, 1000 µM in 20 µM of HEPES buffer and 200 mM of NH$_4$OAc. (X axis is time (min) and Y axis is absorbance)

The experiments in **Figure 3.68** showed the reactivity at lower TMB concentrations. The concentration of TMB was varied from 10-100 µM at a fixed concentrations of G-quadruplex, hemin and hydrogen peroxide of 0.4, 0.08 and 1000 µM, respectively. The results revealed that 100 µM of TMB gave the highest absorption up to 0.5 unit at 652 nm. However, the change of the absorption was not stable and started to decrease after 5-10 min.

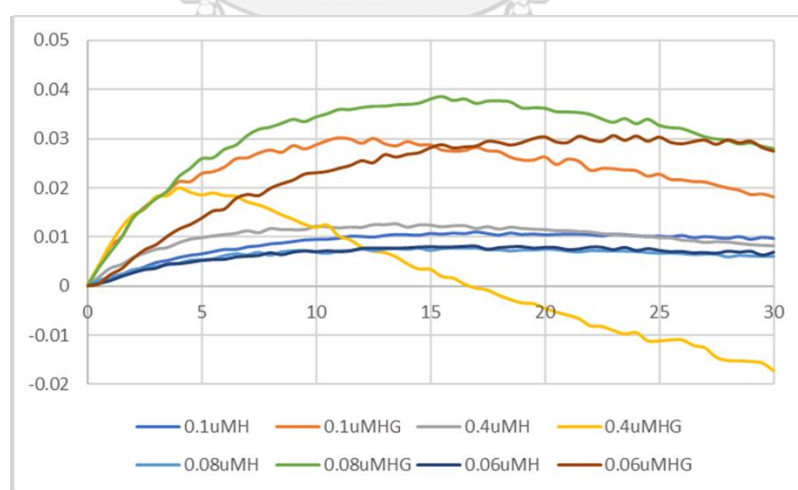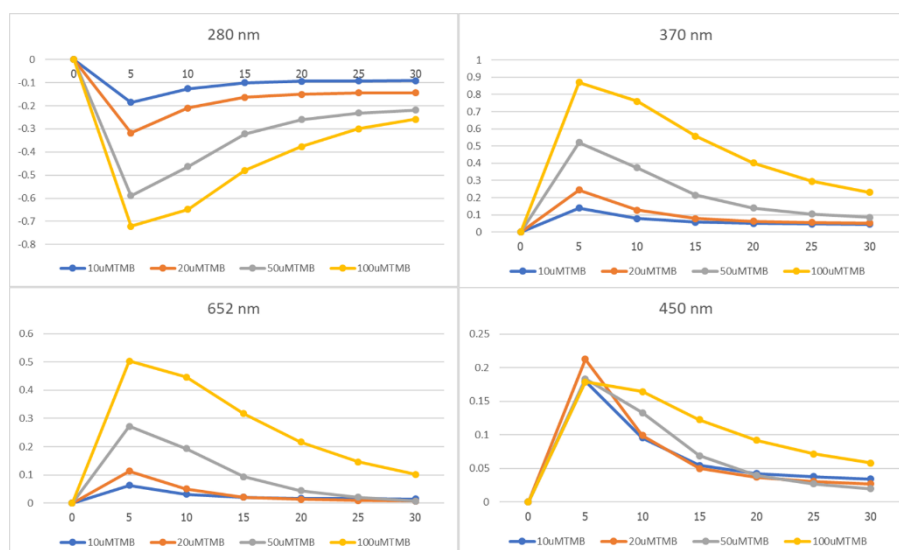**Figure 3.68** Optimization of DNAzyme-based DNA detection by varying the concentration of TMB. Conditions: [G] = 0.4 µM, [Hemin] = 0.08 µM, [TMB] = 10-100 µM, [H_2O_2] = 1000 µM in 20 µM of HEPES buffer and 200 mM of NH_4OAc. (X axis is time (min) and Y axis is absorbance)
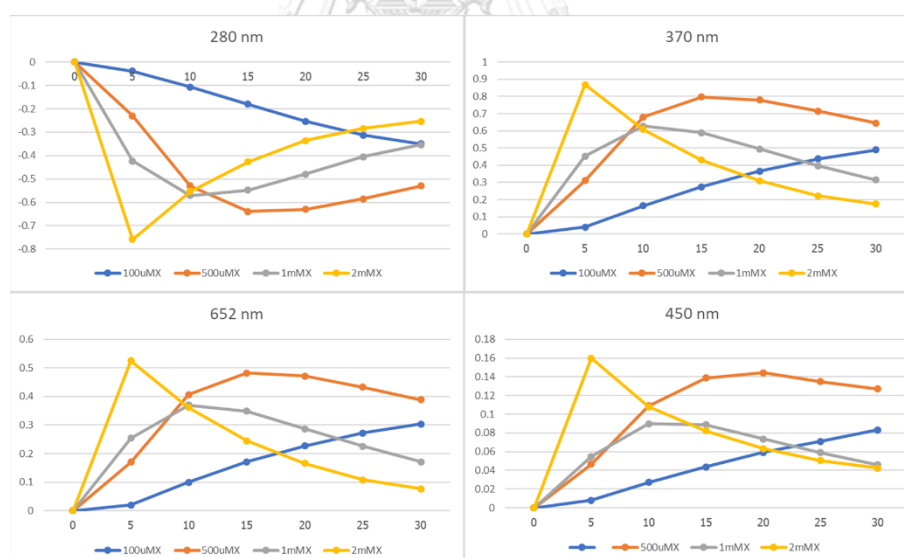
Figure 3.69 Optimization of DNAzyme-based DNA detection by varying of hydrogen peroxide concentrations. Conditions: [G] = 0.4 µM, [Hemin] = 0.08 µM, [TMB] = 100 µM, [H_2O_2] = 100-2000 µM in 20 µM of HEPES buffer and 200 mM of NH_4OAc. (X axis is time (min) and Y axis is absorbance)

The experiments in **Figure 3.69** further confirmed that increasing the hydrogen peroxide in the system resulted in a more rapid reaction as shown by the higher maximum signal obtained, but the signal lifetime was short. Finally, the condition of the peroxidase activity with 0.4 µM of G-quadruplex and 0.08 µM of hemin as a DNAzyme, 100 µM of TMB, and 500 µM of hydrogen peroxide which seems to give a good balance between the signal intensity and stability will be selected for further studies of the DNA sensing using PNA probe.

CHAPTER IV

CONCLUSION

The study began with the development of new DNA sensing platforms based on a combination of fluorescently labeled pyrrolidinyl peptide nucleic acid (acpcPNA) probes and two universal external quenchers, namely graphene oxide (GO) and oligodeoxyguanosine. In the first part, graphene oxide was investigated as a potential external quencher. It showed the excellent capability to quench the fluorescein-labeled PNA probes. Moreover, the signal was rapidly and selectively restored after the addition of a complementary DNA target at room temperature. Compared with other reports on PNA-GO sensors, our developed acpcPNA-GO DNA sensing system gave a rapid and better signal restoration and did not require heating. Moreover, it could be applied to detect the strand-invasion of DNA duplexes by acpcPNA. Finally, the ability to simultaneously detect two DNA targets in a multiplex, multicolor detection format was demonstrated.

Applying oligodeoxyguanosine as an external quencher was the main focus of this dissertation. The detection principle relies on the electrostatic interaction between the positively-charged multiple lysine-modified fluorescein-labeled acpcPNA probe and negatively-charged oligodeoxyguanosine, which resulted in a significant quenching of the fluorescein label on the PNA probe via photoinduced electron transfer (PET). The addition of DNA complementary in stoichiometric quantities rapidly and completely restored the fluorescence. It was proven that the quencher still adhered to the PNA probe following the DNA hybridization and the fluorescence restoration was explained by the separation of the fluorophore and the quencher as a result of the rigidification of the PNA-DNA duplex structure. The fluorescence restoration could distinguish single-base mismatched DNA from complementary DNA targets with the same length. However, discrimination among long DNA targets was less efficient and required heating to increase the selectivity.

The general applicability of the acpcPNA-dGX platform for the sensing of other DNA sequences was demonstrated in three other PNA probe sequences. The

application of the sensing system for multiplex detection of two DNA targets was achieved when the TAMRA-labeled probe was used in combination with the fluorescein-labeled PNA probe. The applications of the acpcPNA-dGX platform for other purposes including the detections of metal ions and PNA ligation were also investigated. For the metal ion detection – specifically Hg^{2+} via the formation of T-Hg^{2+}-T complex - the concept had been proven although the performance of this sensing platform still required further improvement. It can, at least, be considered as a starting point in the use of acpcPNA in the detection of Hg^{2+}. In terms of the detection of PNA ligation, this platform could be used to detect the ligation of short PNA sequences via click chemistry. However, due to the difficulty in achieving the ligation of longer PNA sequences, it was not yet possible to test the performance of this acpcPNA-dGX system in such cases.

Apart from using oligodeoxyguanosine as a quencher when combined with PNA probes, its role as a DNAzyme was also explored. The oligodeoxyguanosine formed a G-quadruplex that upon association with hemin can exhibit a peroxidase-like activity. In the presence of tetramethylbenzidine as a chromogenic substrate, a blue coloration was observed. In this study, we used the DNAzyme in combination with acpcPNA probes for DNA sensing applications. The association of the oligodeoxyguanosine to the acpcPNA probes via electrostatic attraction diminished the DNAzyme activities, presumably by the interference of the hemin binding. Disappointingly, the addition of DNA did not restore the DNAzyme activity as expected. Next, a strand displacement probe concept was employed, whereby the G-quadruplex forming DNA sequence was associated with the PNA probe by hybridization. The preliminary results revealed the hybridization of the PNA probe and the G-quadruplex forming sequence also diminished the activity of the DNAzyme. However, when the target DNA with a sequence complementary to the PNA probe was added, the binding of the PNA probe and the DNA target caused a displacement of the DNAzyme from the PNA probe and restored its peroxidase activity. This is a promising result that should be elaborated further to develop another new DNA sensing system based on the central theme of acpcPNA-dGX combination.

APPENDIX

a
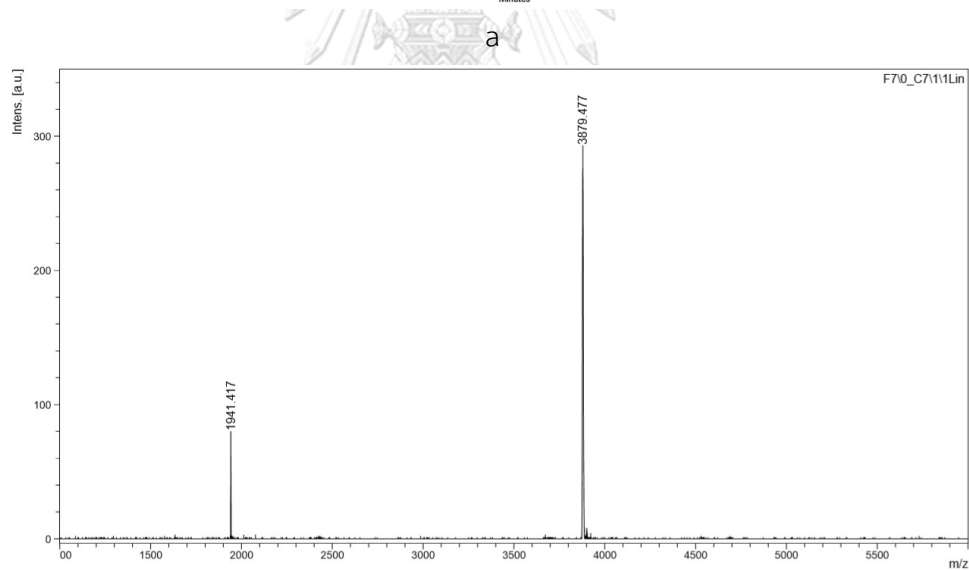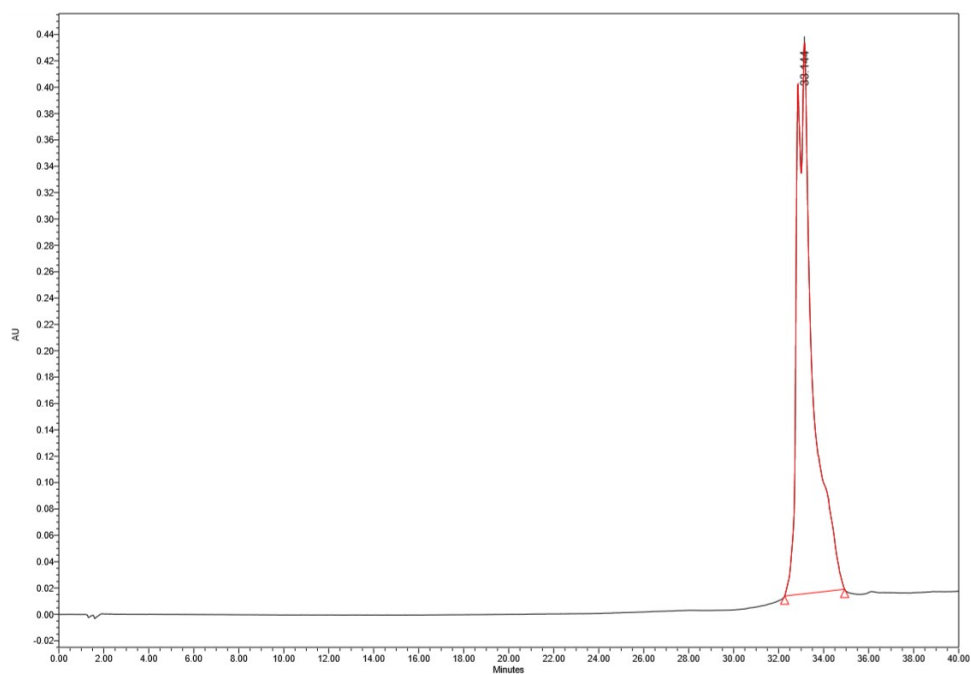
b

Figure S1: (a) Analytical HPLC chromatogram and (b) MALDI-TOF mass spectrum of Flu-GTAATCACT-KNH$_2$ (calcd for [M·H]$^+$ = 3875.101)
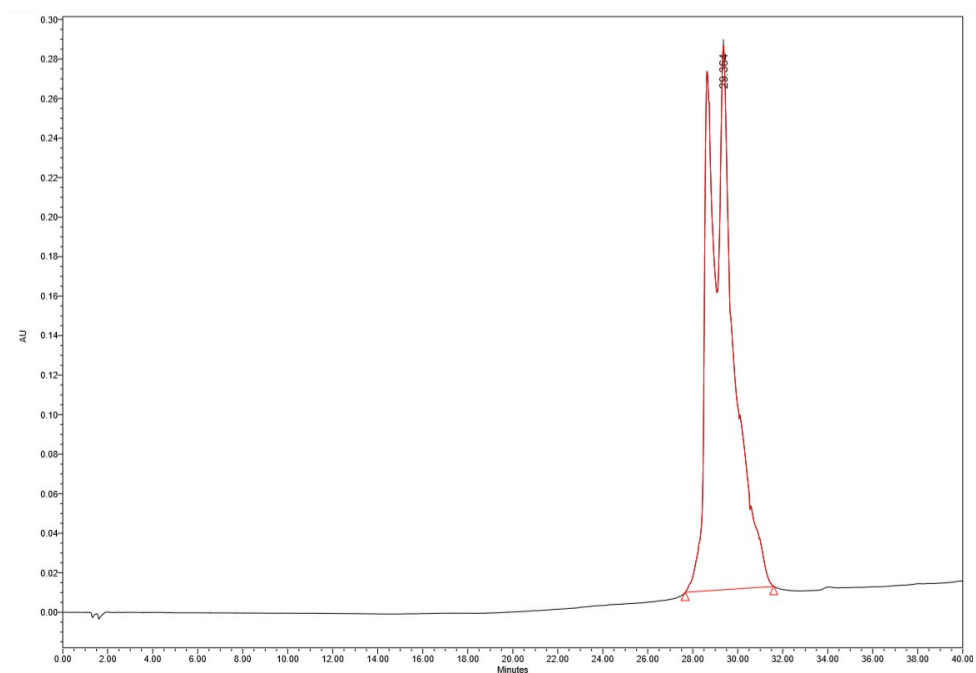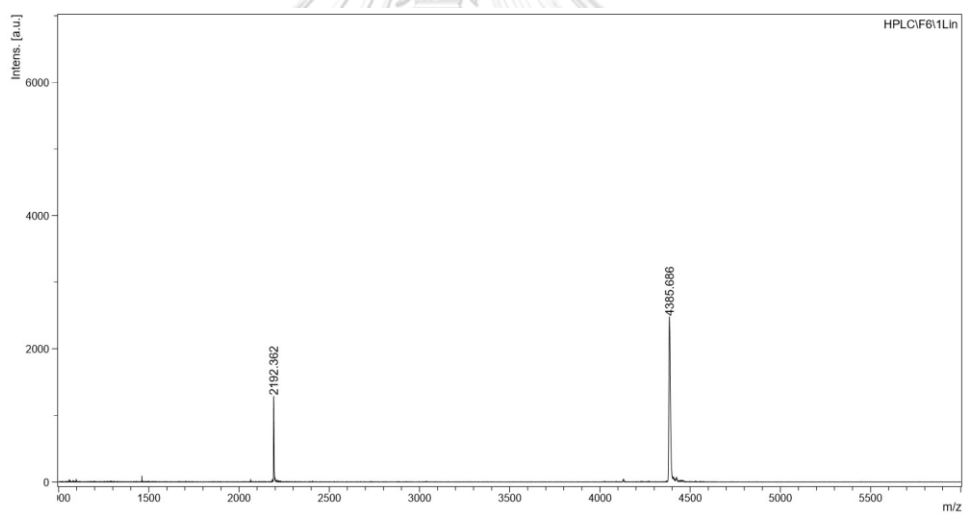
Figure S2: (a) Analytical HPLC chromatogram and (b) MALDI-TOF mass spectrum of Flu-GTAGATCACT-KKKKKNH$_2$ (calcd for [M·H]$^+$ = 4387.790)
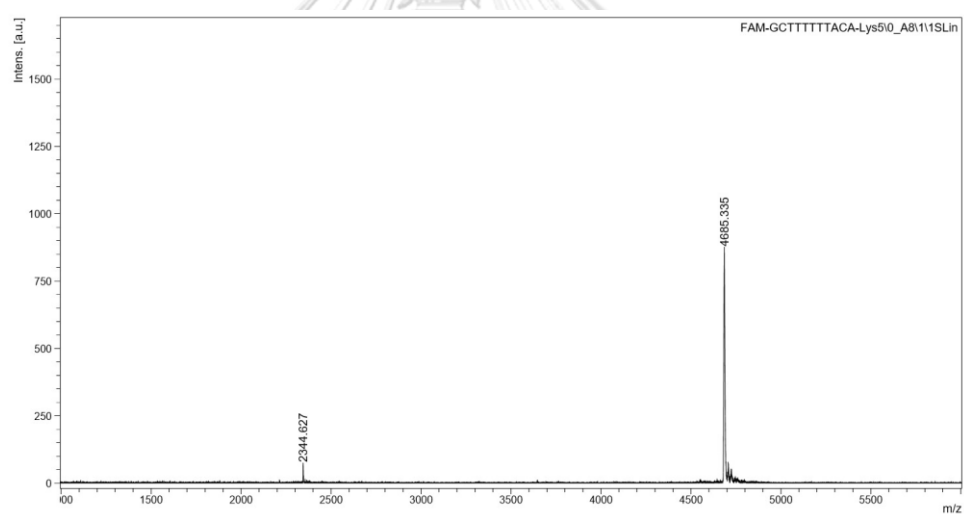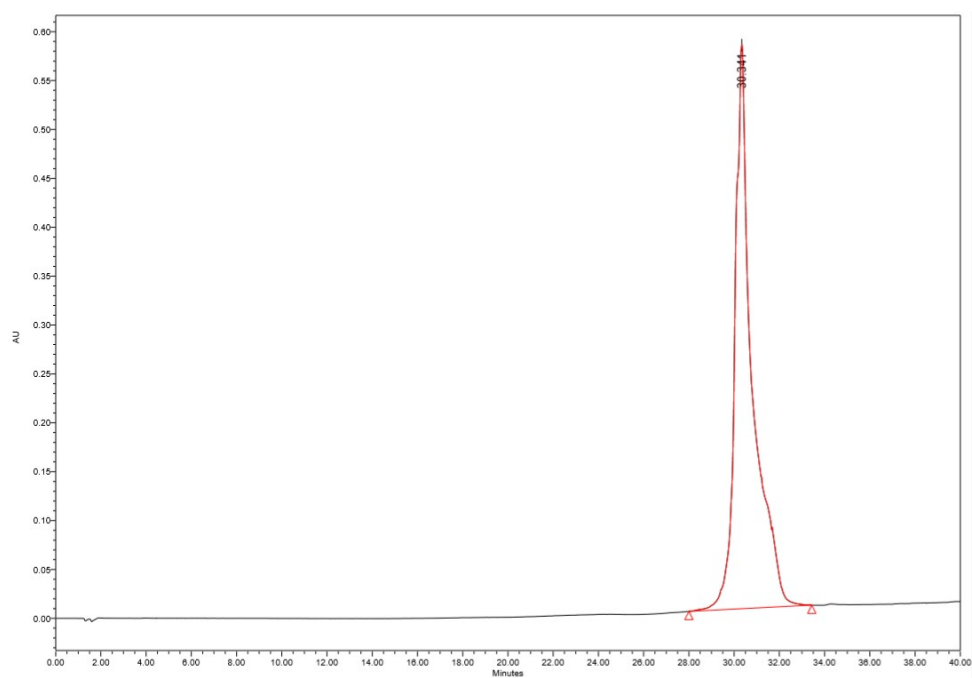
Figure S3: (a) Analytical HPLC chromatogram and (b) MALDI-TOF mass spectrum of Flu-GCTTTTTTACA-KKKKKNH$_2$ (calcd for [M·H]$^+$ = 4686.119)
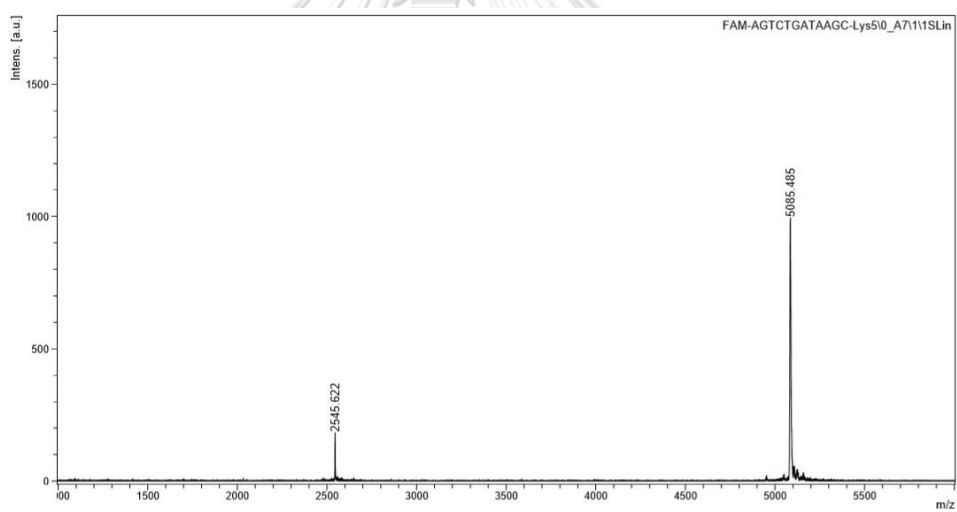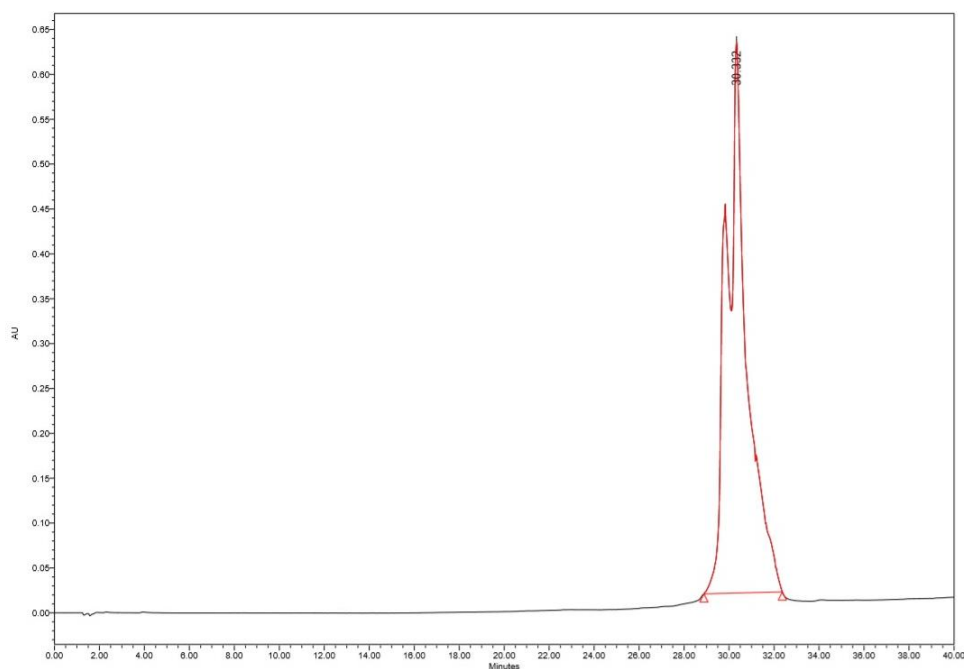
Figure S4: (a) Analytical HPLC chromatogram and (b) MALDI-TOF mass spectrum of Flu-AGTCTGATAAGC-KKKKKNH$_2$ (calcd for [M·H]$^+$ = 5086.526)
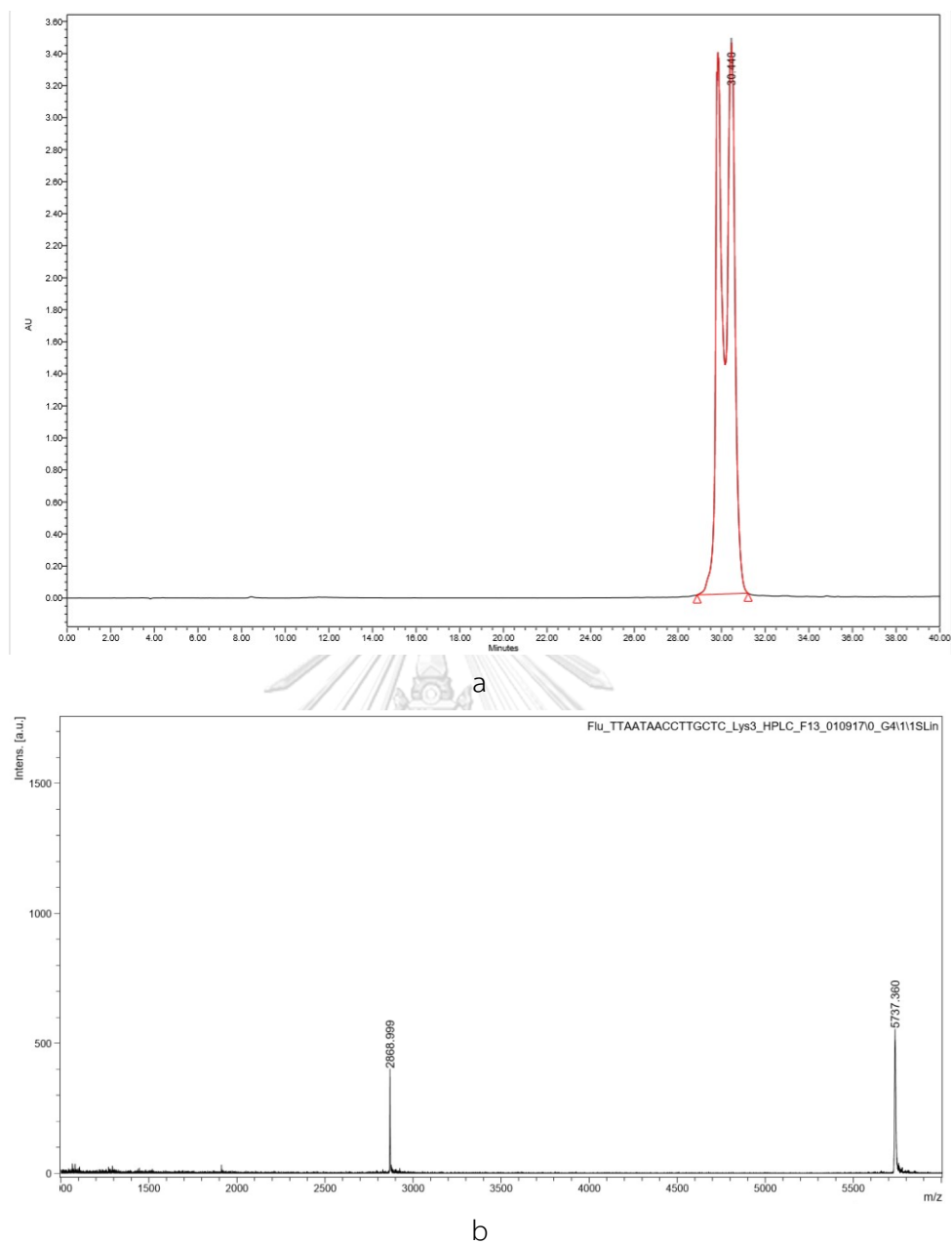
Figure S5: (a) Analytical HPLC chromatogram and (b) MALDI-TOF mass spectrum of Flu-TTAATACCTTTGCTC-KKKNH$_2$ (calcd for [M·H]$^+$ = 5738.183)
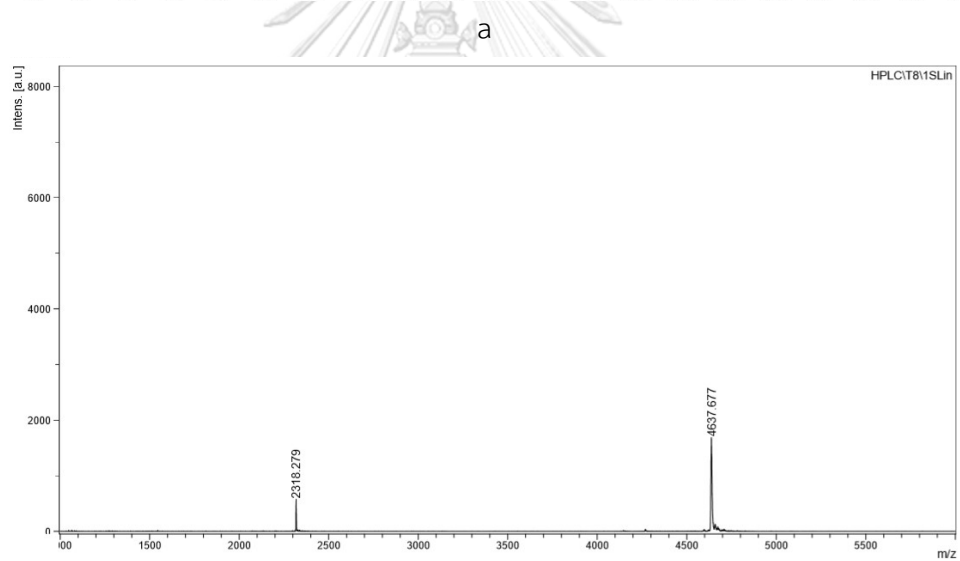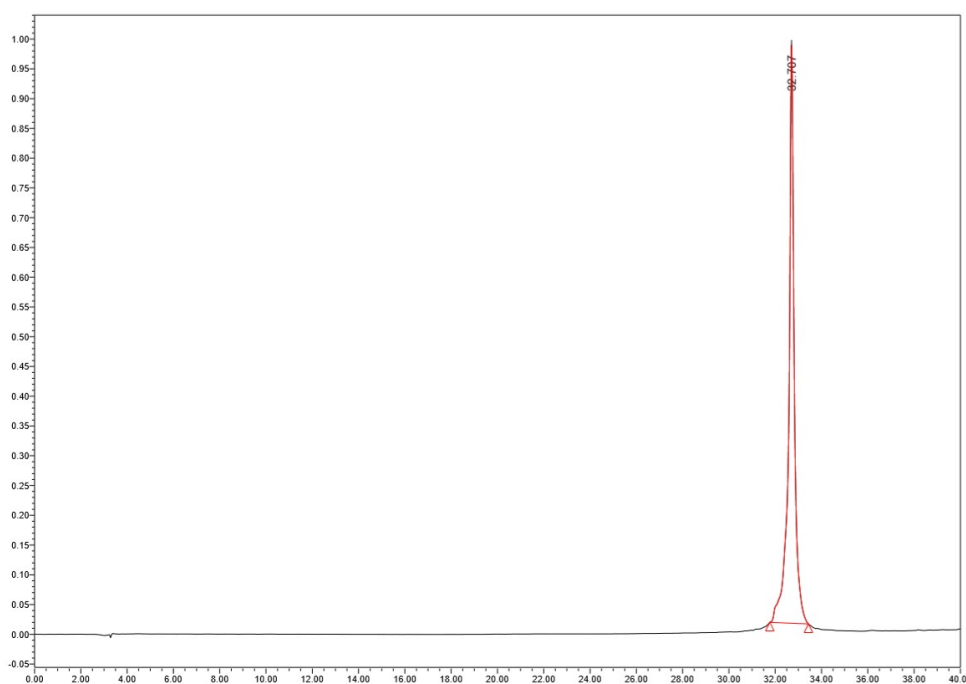
Figure S6: (a) Analytical HPLC chromatogram and (b) MALDI-TOF mass spectrum of TMR-CTAAATTCAGA-KKKK (calcd for [M·H]$^+$ = 4640.131)

129
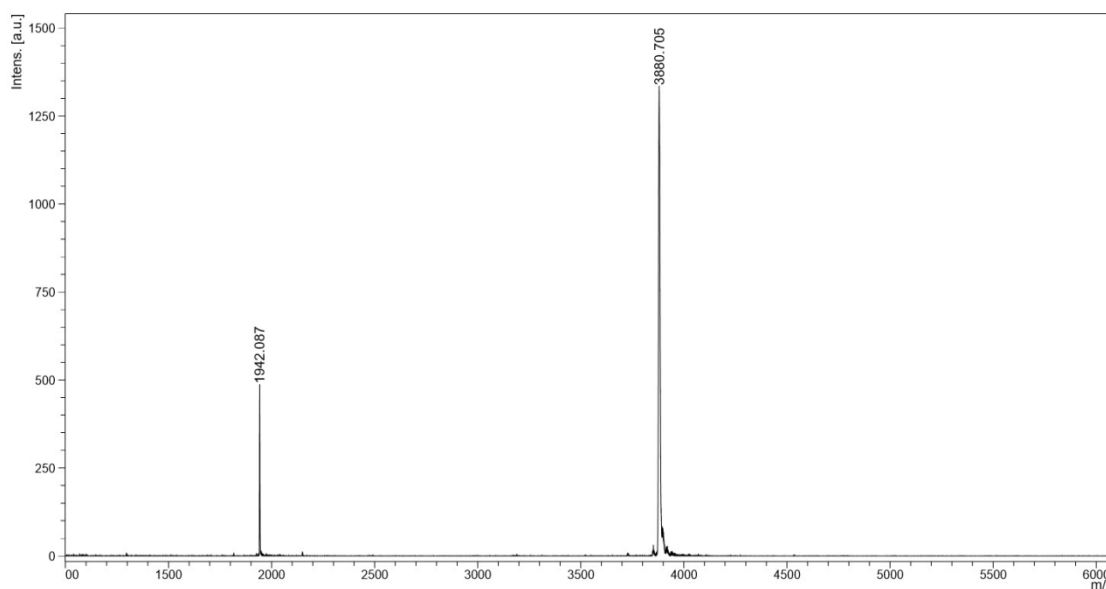
Figure S7: MALDI-TOF mass spectrum of Nr-GTAGATCACT-K (calcd for [M·H]⁺ = 3878.642)
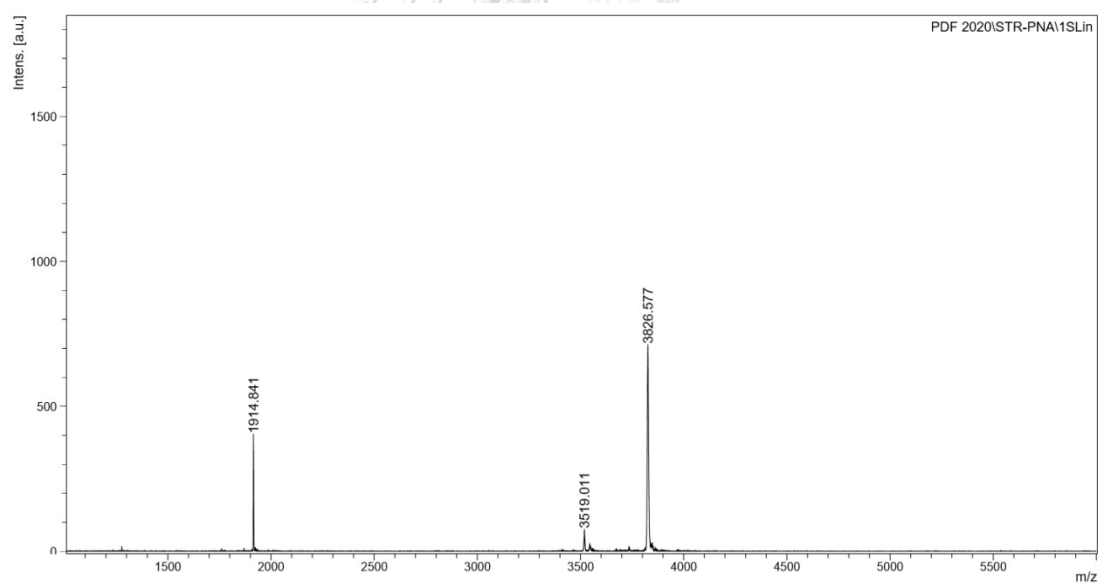
Figure S8: MALDI-TOF mass spectrum of STR-GTAGATCACT-K (calcd for [M·H]⁺ = 3824.452)
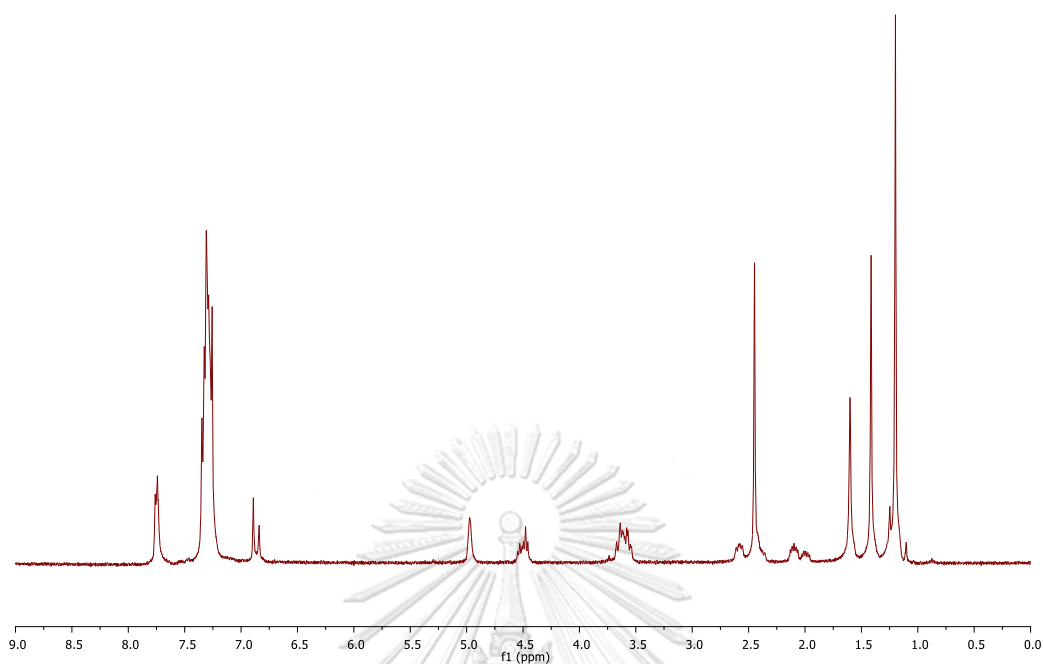
Figure S9: ^{1}H NMR of *N*-Boc-*trans*-4-tosyloxy-D-proline diphenylmethyl ester
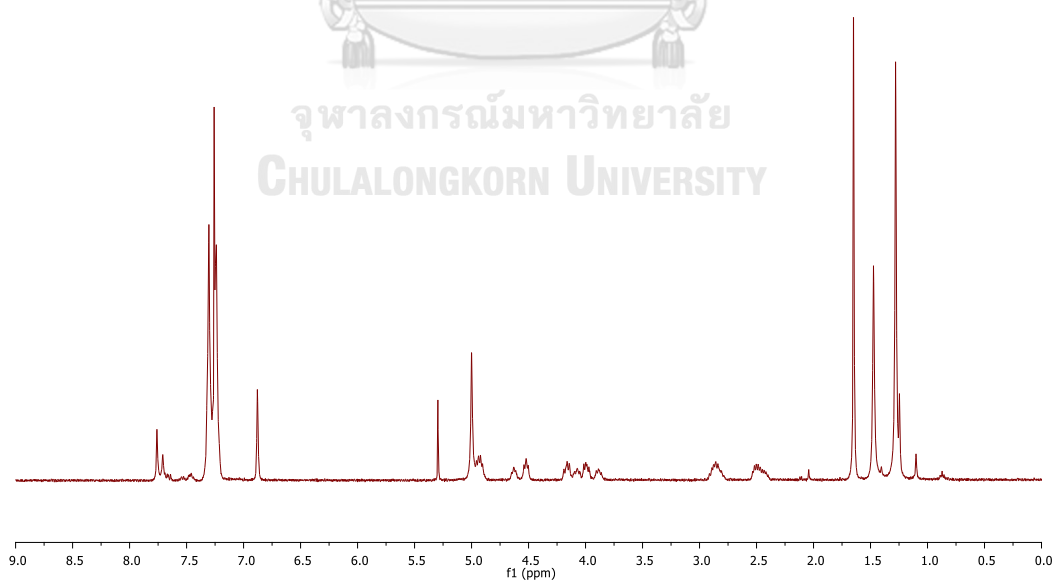
Figure S10: ^{1}H NMR of *N*-Boc-*cis*-4-G^{Cl}-D-proline diphenylmethyl ester
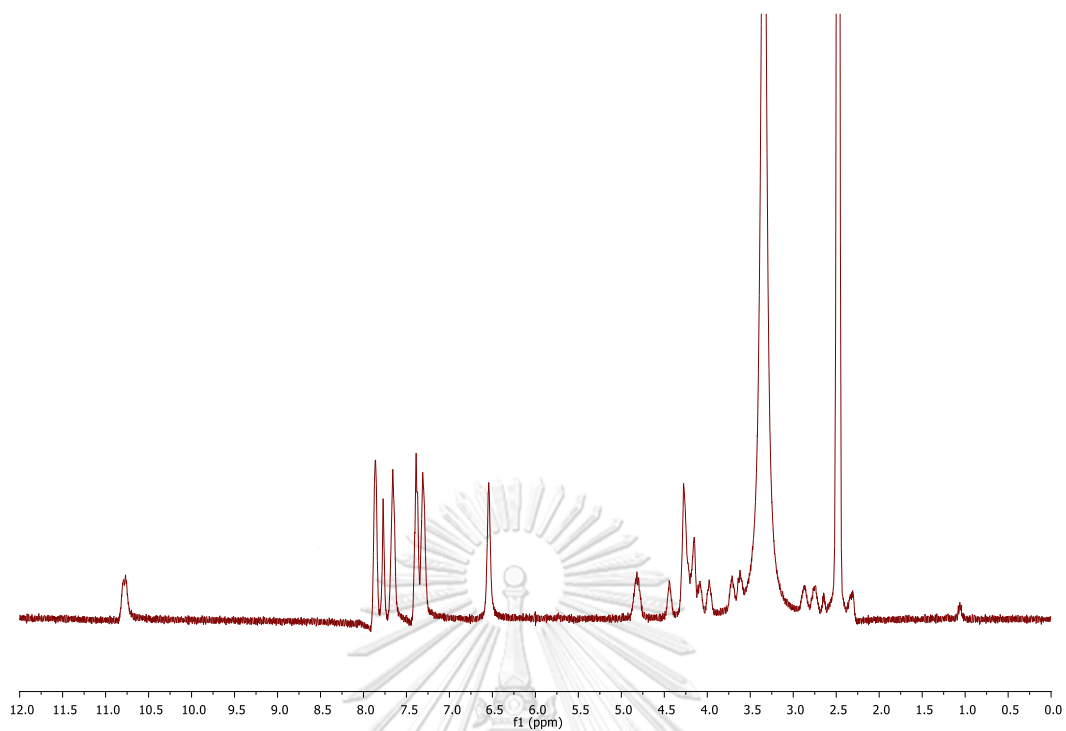
Figure S11: ^{1}H NMR of *N*-Fmoc-*cis*-4-guanine-D-proline (G monomer)
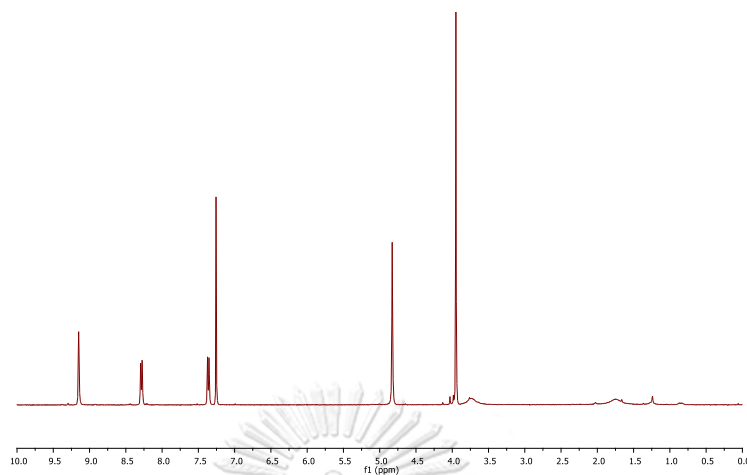
Figure S12: ^{1}H NMR of 6-hydroxymethyl-nicotinic acid methyl ester
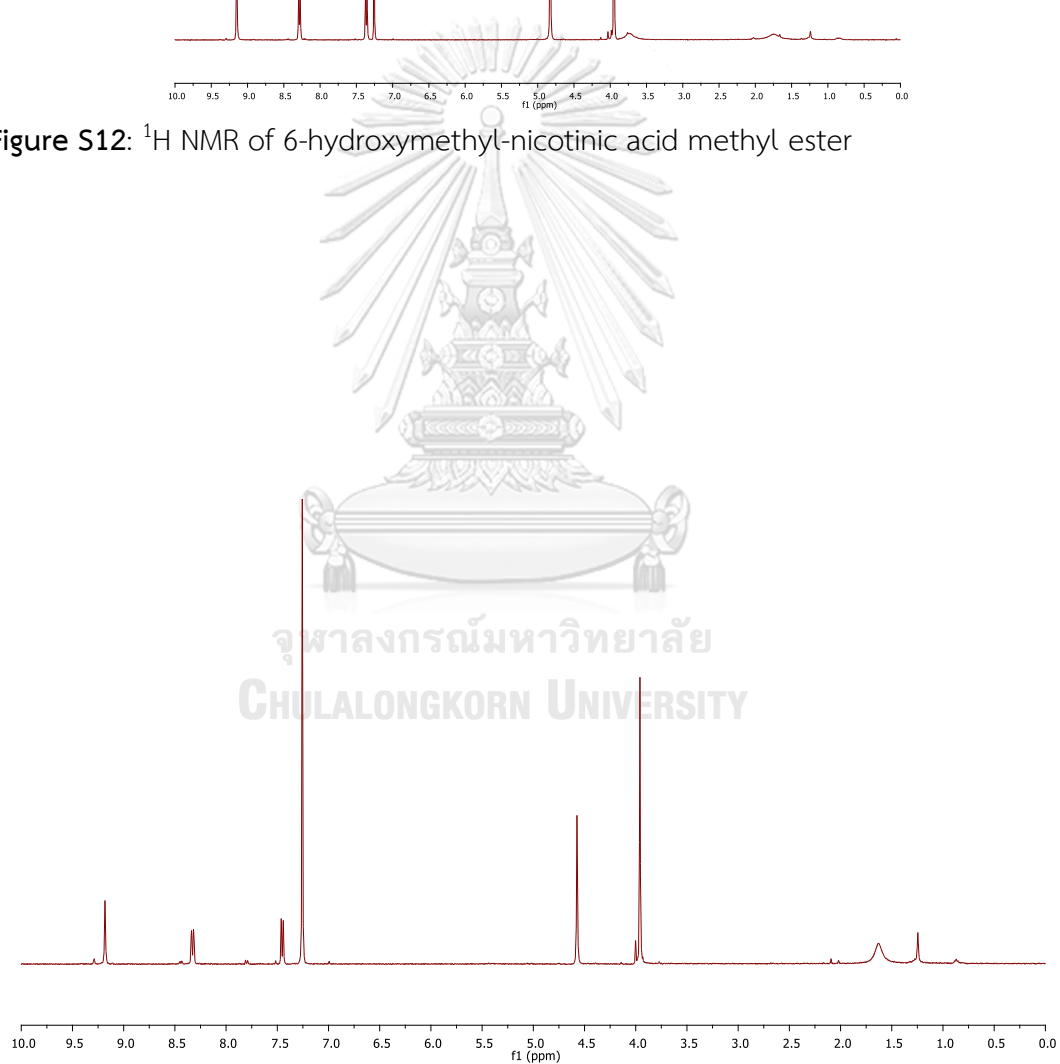
Figure S13: ^{1}H NMR of methyl 5-(azidomethyl)nicotinate

REFERENCES

1.   Perumal, V.; Hashim, U., Advances in biosensors: principle, architecture and applications. *J. Appl. Biomed.* **2014,** *12,* 1-15.

2.   Du, Y.; Dong, S., Nucleic acid biosensors: recent advances and perspectives. *Anal. Chem.* **2017,** *89,* 189-215.

3.   Sassolas, A.; Leca-Bouvier, B. D.; Blum, L. J., DNA biosensors and microarrays. *Chem. Rev.* **2008,** *108,* 109-139.

4.   Yáñez-Sedeňo, P.; Agüí, L.; Villalonga, R.; Pingarrón, J. M., Biosensors in forensic analysis. A review. *Anal. Chim. Acta* **2014,** *823,* 1-19.

5.   Liu, J.; Cao, Z.; Lu, Y., Functional nucleic acid sensors. *Chem. Rev.* **2009,** *109,* 1948-1998.

6.   Chambers, J. P.; Arulanandam, B. P.; Matta, L. L.; Weis, A.; Valdés, J. J., Biosensor recognition elements. *Curr. Issues Mol. Biol.* **2008,** *10,* 1-12.

7.   Shorte, S. L.; Bolsover, S., CHAPTER SEVEN - imaging reality: understanding maps of physiological cell signals measured by fluorescence microscopy and digital imaging. in *fluorescent and luminescent probes for biological activity (second edition),* Mason, W. T., Ed. Academic Press: London, 1999; pp 94-107.

8.   Boutorine, S. A.; Novopashina, S. D.; Krasheninina, A. O.; Nozeret, K.; Venyaminova, G. A., Fluorescent probes for nucleic acid visualization in fixed and live cells. *Molecules* **2013,** *18.*

9.   Ranasinghe, R. T.; Brown, T., Fluorescence based strategies for genetic analysis. *Chem. Commun.* **2005,** 5487-5502.

10.   Yuan, L.; Lin, W.; Zheng, K.; Zhu, S., FRET-based small-molecule fluorescent probes: rational design and bioimaging applications. *Acc. Chem. Res.* **2013,** *46,* 1462-1473.

11.   Jothikumar, N.; Hill, V. R., A novel photoinduced electron transfer (PET) primer technique for rapid real-time PCR detection of Cryptosporidium spp. *Biochem. Biophys. Res. Commun.* **2013,** *436,* 134-139.

12.   Lu, S.; Wang, S.; Zhao, J.; Sun, J.; Yang, X., Fluorescence light-up biosensor for

microRNA based on the distance-dependent photoinduced electron transfer. *Anal. Chem.* **2017,** *89,* 8429-8436.

13.   Goel, G.; Kumar, A.; Puniya, A. K.; Chen, W.; Singh, K., Molecular beacon: a multitask probe. *J. Appl. Microbiol.* **2005,** *99,* 435-442.

14.   Tyagi, S.; Kramer, F. R., Molecular beacons: probes that fluoresce upon hybridization. *Nat. Biotechnol.* **1996,** *14,* 303-308.

15.   Ma, H.; Li, Z.; Xue, N.; Cheng, Z.; Miao, X., A gold nanoparticle based fluorescent probe for simultaneous recognition of single-stranded DNA and double-stranded DNA. *Microchim. Acta* **2018,** *185*, 93.

16.   Yang, Y.; Zhong, S.; Wang, K.; Huang, J., Gold nanoparticle based fluorescent oligonucleotide probes for imaging and therapy in living systems. *Analyst* **2019,** *144*, 1052-1072.

17.   Lu, C.-H.; Yang, H.-H.; Zhu, C.-L.; Chen, X.; Chen, G.-N., A graphene platform for sensing biomolecules. *Angew. Chem. Int. Ed.* **2009,** *48*, 4785-4787.

18.   Guo, S.; Du, D.; Tang, L.; Ning, Y.; Yao, Q.; Zhang, G.-J., PNA-assembled graphene oxide for sensitive and selective detection of DNA. *Analyst* **2013,** *138,* 3216-3220.

19.   Roh, K.; Kim, D.-M.; Lee, E. H.; Kim, H.; Park, H. S.; Jang, J.-H.; Hwang, S.-H.; Kim, D.-E., A simple PCR-based fluorometric system for detection of mutant fusion DNAs using a quencher-free fluorescent DNA probe and graphene oxide. *Chem. Commun.* **2015,** *51,* 6960-6963.

20.   Khalil, I.; Yehye, W. A.; Julkapli, N. M.; Rahmati, S.; Sina, A. A. I.; Basirun, W. J.; Johan, M. R., Graphene oxide and gold nanoparticle based dual platform with short DNA probe for the PCR free DNA biosensing using surface-enhanced Raman scattering. *Biosens. Bioelectron.* **2019,** *131*, 214-223.

21.   Bülbül, G.; Hayat, A.; Mustafa, F.; Andreescu, S., DNA assay based on nanoceria as fluorescence quenchers (NanoCeracQ DNA assay). *Sci. Rep.* **2018,** *8,* 2426.

22.   Hu, R.; Liu, T.; Zhang, X.-B.; Huan, S.-Y.; Wu, C.; Fu, T.; Tan, W., Multicolor fluorescent biosensor for multiplexed detection of DNA. *Anal. Chem.* **2014,** *86,* 5009-5016.

23.   Kong, R.-M.; Sun, N.-N.; Qu, F.; Wu, H.; Wang, H.; You, J., Sensitive

fluorescence "turn-on" detection of bleomycin based on a superquenched perylene–DNA complex. *RSC adv.* **2015,** *5*, 86849-86854.

24.   Zheng, J.; Yang, R.; Shi, M.; Wu, C.; Fang, X.; Li, Y.; Li, J.; Tan, W., Rationally designed molecular beacons for bioanalytical and biomedical applications. *Chem. Soc. Rev.* **2015,** *44*, 3036-3055.

25.   Wang, K.; Tang, Z.; Yang, C. J.; Kim, Y.; Fang, X.; Li, W.; Wu, Y.; Medley, C. D.; Cao, Z.; Li, J.; Colon, P.; Lin, H.; Tan, W., Molecular engineering of dna: molecular beacons. *Angew. Chem. Int. Ed.* **2009,** *48*, 856-870.

26.   Wei, C.; Lipton, J. H.; Kamel-Reid, S., Chapter 14 - monitoring of minimal residual hematologic disease. in *cell and tissue based molecular pathology*, Tubbs, R. R.; Stoler, M. H., Eds. Churchill Livingstone: Philadelphia, 2009; pp 135-144.

27.   Venkatesan, N.; Seo, Y. J.; Kim, B. H., Quencher-free molecular beacons: a new strategy in fluorescence based nucleic acid analysis. *Chem. Soc. Rev.* **2008,** *37*, 648-663.

28.   Klimkowski, P.; De Ornellas, S.; Singleton, D.; El-Sagheer, A. H.; Brown, T., Design of thiazole orange oligonucleotide probes for detection of DNA and RNA by fluorescence and duplex melting. *Org. Biomol. Chem.* **2019,** *17*, 5943-5950.

29.   Wu, P.; Tu, Y.; Qian, Y.; Zhang, H.; Cai, C., DNA strand-displacement-induced fluorescence enhancement for highly sensitive and selective assay of multiple microRNA in cancer cells. *Chem. Commun.* **2014,** *50*, 1012-1014.

30.   Pinheiro, V. B.; Taylor, A. I.; Cozens, C.; Abramov, M.; Renders, M.; Zhang, S.; Chaput, J. C.; Wengel, J.; Peak-Chew, S.-Y.; McLaughlin, S. H.; Herdewijn, P.; Holliger, P., Synthetic genetic polymers capable of heredity and evolution. *Science* **2012,** *336*, 341.

31.   Schmidt, M., Xenobiology: a new form of life as the ultimate biosafety tool. *Bioessays* **2010,** *32*, 322-331.

32.   Nielsen, P. E.; Egholm, M.; Berg, R. H.; Buchardt, O., Sequence-selective recognition of DNA by strand displacement with a thymine-substituted polyamide. *Science* **1991,** *254*, 1497.

33.   Nielsen, P. E.; Egholm, M., An introduction to peptide nucleic acid. *Curr. Issues Mol. Biol.* **1999,** *1*, 89-104.

34.   Egholm, M.; Buchardt, O.; Christensen, L.; Behrens, C.; Freier, S. M.; Driver, D.

A.; Berg, R. H.; Kim, S. K.; Norden, B.; Nielsen, P. E., PNA hybridizes to complementary oligonucleotides obeying the Watson–Crick hydrogen-bonding rules. *Nature* **1993,** *365,* 566-568.

35.   Nielsen, P. E.; Haaima, G., Peptide nucleic acid (PNA). A DNA mimic with a pseudopeptide backbone. *Chem. Soc. Rev.* **1997,** *26,* 73-78.

36.   Nielsen, P. E., Peptide nucleic acid: a versatile tool in genetic diagnostics and molecular biology. *Curr. Opin. Biotechnol.* **2001,** *12,* 16-20.

37.   Gupta, A.; Mishra, A.; Puri, N., Peptide nucleic acids: advanced tools for biomedical applications. *J. Biotechnol.* **2017,** *259,* 148-159.

38.   Sugiyama, T.; Kittaka, A., Chiral peptide nucleic acids with a substituent in the *N*-(2-aminoethy)glycine backbone. *Molecules* **2013,** *18*.

39.   Vilaivan, T.; Suparpprom, C.; Harnyuttanakorn, P.; Lowe, G., Synthesis and properties of novel pyrrolidinyl PNA carrying β-amino acid spacers. *Tetrahedron Lett.* **2001,** *42,* 5533-5536.

40.   Vilaivan, T.; Lowe, G., A Novel pyrrolidinyl pna showing high sequence specificity and preferential binding to DNA over RNA. *J. Am. Chem. Soc.* **2002,** *124,* 9326-9327.

41.   Suparpprom, C.; Srisuwannaket, C.; Sangvanich, P.; Vilaivan, T., Synthesis and oligodeoxynucleotide binding properties of pyrrolidinyl peptide nucleic acids bearing prolyl-2-aminocyclopentanecarboxylic acid (ACPC) backbones. *Tetrahedron Lett.* **2005,** *46,* 2833-2837.

42.   Vilaivan, T., Pyrrolidinyl PNA with α/β-dipeptide backbone: from development to applications. *Acc. Chem. Res.* **2015,** *48,* 1645-1656.

43.   Ananthanawat, C.; Vilaivan, T.; Hoven, V. P., Synthesis and immobilization of thiolated pyrrolidinyl peptide nucleic acids on gold-coated piezoelectric quartz crystals for the detection of DNA hybridization. *Sens. Actuators, B* **2009,** *137,* 215-221.

44.   Boonlua, C.; Vilaivan, C.; Wagenknecht, H.-A.; Vilaivan, T., 5-(Pyren-1-yl)uracil as a base-discriminating fluorescent nucleobase in pyrrolidinyl peptide nucleic acids. *Chem. - Asian J.* **2011,** *6,* 3251-3259.

45.   Reenabthue, N.; Boonlua, C.; Vilaivan, C.; Vilaivan, T.; Suparpprom, C., 3-aminopyrrolidine-4-carboxylic acid as versatile handle for internal labeling of pyrrolidinyl PNA. *Bioorg. Med. Chem. Lett.* **2011,** *21,* 6465-6469.

46.   Yotapan, N.; Charoenpakdee, C.; Wathanathavorn, P.; Ditmangklo, B.; Wagenknecht, H.-A.; Vilaivan, T., Synthesis and optical properties of pyrrolidinyl peptide nucleic acid carrying a clicked Nile red label. *Beilstein J. Org. Chem.* **2014,** *10,* 2166-2174.

47.   Theppaleak, T.; Rutnakornpituk, B.; Wichai, U.; Vilaivan, T.; Rutnakornpituk, M., Magnetite nanoparticle with positively charged surface for immobilization of peptide nucleic acid and deoxyribonucleic acid. *J. Biomed. Nanotechnol.* **2013,** *9,* 1509-1520.

48.   Ortiz, E.; Estrada, G.; Lizardi, P. M., PNA molecular beacons for rapid detection of PCR amplicons. *Mol. Cell. Probes* **1998,** *12,* 219-226.

49.   Vilaivan, T., Fluorogenic PNA probes. *Beilstein J. Org. Chem.* **2018,** *14,* 253-281.

50.   Boonlua, C.; Charoenpakdee, C.; Vilaivan, T.; Praneenararat, T., Preparation and performance evaluation of a pyrrolidinyl peptide nucleic-acid-based displacement probe as a DNA sensor. *ChemistrySelect* **2016,** *1,* 5691-5697.

51.   Yotapan, N.; Nim-anussornkul, D.; Vilaivan, T., Pyrrolidinyl peptide nucleic acid terminally labeled with fluorophore and end-stacking quencher as a probe for highly specific DNA sequence discrimination. *Tetrahedron* **2016,** *72,* 7992-7999.

52.   Ditmangklo, B.; Taechalertpaisarn, J.; Siriwong, K.; Vilaivan, T., Clickable styryl dyes for fluorescence labeling of pyrrolidinyl PNA probes for the detection of base mutations in DNA. *Org. Biomol. Chem.* **2019,** *17,* 9712-9725.

53.   Maxwell, D. J.; Taylor, J. R.; Nie, S., Self-assembled nanoparticle probes for recognition and detection of biomolecules. *J. Am. Chem. Soc.* **2002,** *124,* 9606-9612.

54.   Mo, Z. H.; Yang, X. C.; Guo, K. P.; Wen, Z. Y., A nanogold-quenched fluorescence duplex probe for homogeneous DNA detection based on strand displacement. *Anal. Bioanal. Chem.* **2007,** *389,* 493-497.

55.   Varghese, N.; Mogera, U.; Govindaraj, A.; Das, A.; Maiti, P. K.; Sood, A. K.; Rao, C. N. R., Binding of DNA nucleobases and nucleosides with graphene. *ChemPhysChem* **2009,** *10,* 206-210.

56.   Shi, J.; Tian, F.; Lyu, J.; Yang, M., Nanoparticle based fluorescence resonance energy transfer (FRET) for biosensing applications. *J. Mater. Chem. B* **2015,** *3,* 6989-7005.

57.   Woo, Y. C.; Kim, S.-H.; Shon, H. K.; Tijing, L. D., Introduction: membrane desalination today, past, and future. in *current trends and future developments on*

(bio-) membranes, Basile, A.; Curcio, E.; Inamuddin, Eds. Elsevier: 2019; pp xxv-xlvi.

58.   Liu, B.; Salgado, S.; Maheshwari, V.; Liu, J., DNA adsorbed on graphene and graphene oxide: fundamental interactions, desorption and applications. *Curr. Opin. Colloid Interface Sci.* **2016,** *26*, 41-49.

59.   Wu, M.; Kempaiah, R.; Huang, P.-J. J.; Maheshwari, V.; Liu, J., Adsorption and desorption of DNA on graphene oxide studied by fluorescently labeled oligonucleotides. *Langmuir* **2011,** *27*, 2731-2738.

60.   Liu, B.; Sun, Z.; Zhang, X.; Liu, J., Mechanisms of DNA sensing on graphene oxide. *Anal. Chem.* **2013,** *85*, 7987-7993.

61.   Ryoo, S.-R.; Lee, J.; Yeo, J.; Na, H.-K.; Kim, Y.-K.; Jang, H.; Lee, J. H.; Han, S. W.; Lee, Y.; Kim, V. N.; Min, D.-H., Quantitative and multiplexed microRNA sensing in living cells based on peptide nucleic acid and nano graphene oxide (PANGO). *ACS Nano* **2013,** *7*, 5882-5891.

62.   Lee, J.; Park, I.-S.; Jung, E.; Lee, Y.; Min, D.-H., Direct, sequence-specific detection of dsDNA based on peptide nucleic acid and graphene oxide without requiring denaturation. *Biosens. Bioelectron.* **2014,** *62*, 140-144.

63.   Chen, R. F.; Knutson, J. R., Mechanism of fluorescence concentration quenching of carboxyfluorescein in liposomes: energy transfer to nonfluorescent dimers. *Anal. Biochem.* **1988,** *172*, 61-77.

64.   Seidel, C. A. M.; Schulz, A.; Sauer, M. H. M., Nucleobase-specific quenching of fluorescent dyes. 1. nucleobase one-electron redox potentials and their correlation with static and dynamic quenching efficiencies. *J. Phys. Chem.* **1996,** *100*, 5541-5553.

65.   Sauer, M.; Drexhage, K. H.; Lieberwirth, U.; Müller, R.; Nord, S.; Zander, C., Dynamics of the electron transfer reaction between an oxazine dye and DNA oligonucleotides monitored on the single-molecule level. *Chem. Phys. Lett.* **1998,** *284*, 153-163.

66.   Torimura, M.; Kurata, S.; Yamada, K.; Yokomaku, T.; Kamagata, Y.; Kanagawa, T.; Kurane, R., Fluorescence-quenching phenomenon by photoinduced electron transfer between a fluorescent dye and a nucleotide base. *Anal. Sci.* **2001,** *17*, 155-160.

67.   Piotrowiak, P., Photoinduced electron transfer in molecular systems: recent developments. *Chem. Soc. Rev.* **1999,** *28*, 143-150.

68.   Doose, S.; Neuweiler, H.; Sauer, M., Fluorescence quenching by photoinduced electron transfer: a reporter for conformational dynamics of macromolecules. *ChemPhysChem* **2009,** *10,* 1389-1398.

69.   Thongyod, W.; Buranachai, C.; Pengpan, T.; Punwong, C., Fluorescence quenching by photoinduced electron transfer between 7-methoxycoumarin and guanine base facilitated by hydrogen bonds: an in silico study. *Physical Chemistry Chemical Physics* **2019,** *21,* 16258-16269.

70.   Ziarani, G. M.; Moradi, R.; Lashgari, N.; Kruger, H. G., Chapter 10 - Fluorescein *dyes. in metal-free synthetic organic dyes,* Ziarani, G. M.; Moradi, R.; Lashgari, N.; Kruger, H. G., Eds. Elsevier: 2018; pp 165-170.

71.   Noble, J. E.; Wang, L.; Cole, K. D.; Gaigalas, A. K., The effect of overhanging nucleotides on fluorescence properties of hybridising oligonucleotides labelled with Alexa-488 and FAM fluorophores. *Biophys. Chem.* **2005,** *113,* 255-263.

72.   Qu, P.; Chen, X.; Zhou, X.; Li, X.; Zhao, X., Fluorescence quenching of TMR by guanosine in oligonucleotides. *Sci. China, Ser. B: Chem.* **2009,** *52,* 1653-1659.

73.   Heinlein, T.; Knemeyer, J.-P.; Piestert, O.; Sauer, M., Photoinduced electron transfer between fluorescent dyes and guanosine residues in DNA-hairpins. *J. Phys. Chem. B* **2003,** *107,* 7957-7964.

74.   Misra, A.; Kumar, P.; Gupta, K. C., Synthesis of hairpin probe using deoxyguanosine as a quencher: fluorescence and hybridization studies. *Anal. Biochem.* **2007,** *364,* 86-88.

75.   Hu, P.; Jin, L.; Zhu, C.; Dong, S., A simple and sensitive fluorescent sensing platform for Hg^{2+} ions assay based on G-quenching. *Talanta* **2011,** *85,* 713-717.

76.   Zhou, F.; Meng, R.; Liu, Q.; Jin, Y.; Li, B., Photoinduced electron transfer-based fluorescence quenching combined with rolling circle amplification for sensitive detection of microRNA. *ChemistrySelect* **2016,** *1,* 6422-6428.

77.   Rhodes, D.; Lipps, H. J., G-quadruplexes and their regulatory roles in biology. *Nucleic Acids Res.* **2015,** *43,* 8627-8637.

78.   Davis, J. T., G-Quartets 40 Years Later: From 5′-GMP to Molecular Biology and Supramolecular Chemistry. *Angew. Chem. Int. Ed.* **2004,** *43,* 668-698.

79.   Hänsel-Hertsch, R.; Di Antonio, M.; Balasubramanian, S., DNA G-quadruplexes in

the human genome: detection, functions and therapeutic potential. *Nat. Rev. Mol. Cell Biol.* **2017,** *18,* 279-284.

80.   Yang, X.; Zhu, Y.; Liu, P.; He, L.; Li, Q.; Wang, Q.; Wang, K.; Huang, J.; Liu, J., G-quadruplex fluorescence quenching ability: a simple and efficient strategy to design a single-labeled DNA probe. *Anal. Methods* **2012,** *4,* 895-897.

81.   Miyake, Y.; Togashi, H.; Tashiro, M.; Yamaguchi, H.; Oda, S.; Kudo, M.; Tanaka, Y.; Kondo, Y.; Sawa, R.; Fujimoto, T.; Machinami, T.; Ono, A., MercuryII-Mediated Formation of Thymine–HgII–Thymine Base Pairs in DNA Duplexes. *J. Am. Chem. Soc.* **2006,** *128,* 2172-2173.

82.   Zhou, X.-H.; Kong, D.-M.; Shen, H.-X., G-quadruplex–hemin DNAzyme-amplified colorimetric detection of Ag+ ion. *Anal. Chim. Acta* **2010,** *678,* 124-127.

83.   Wang, F.; Lu, C.-H.; Willner, I., From cascaded catalytic nucleic acids to enzyme–DNA nanostructures: controlling reactivity, sensing, logic operations, and assembly of complex structures. *Chem. Rev.* **2014,** *114,* 2881-2941.

84.   Fu, S.; Sun, L.-Q., DNAzyme-based therapeutics for cancer treatment. *Future Med. Chem.* **2015,** *7,* 1701-1707.

85.   Xiang, Y.; Lu, Y., DNA as sensors and imaging agents for metal ions. *Inorg. Chem.* **2014,** *53,* 1925-1942.

86.   Yang, Z.; Loh, K. Y.; Chu, Y.-T.; Feng, R.; Satyavolu, N. S. R.; Xiong, M.; Nakamata Huynh, S. M.; Hwang, K.; Li, L.; Xing, H.; Zhang, X.; Chemla, Y. R.; Gruebele, M.; Lu, Y., Optical control of metal ion probes in cells and zebrafish using highly selective DNAzymes conjugated to upconversion nanoparticles. *J. Am. Chem. Soc.* **2018,** *140,* 17656-17665.

87.   Travascio, P.; Li, Y.; Sen, D., DNA-enhanced peroxidase activity of a DNA aptamer-hemin complex. *Chem. Biol.* **1998,** *5,* 505-517.

88.   Cao, Y.; Ding, P.; Yang, L.; Li, W.; Luo, Y.; Wang, J.; Pei, R., Investigation and improvement of catalytic activity of G-quadruplex/hemin DNAzymes using designed terminal G-tetrads with deoxyadenosine caps. *Chem. Sci.* **2020,** *11,* 6896-6906.

89.   Travascio, P.; Bennet, A. J.; Wang, D. Y.; Sen, D., A ribozyme and a catalytic DNA with peroxidase activity: active sites versus cofactor-binding sites. *Chem. Biol.* **1999,** *6,* 779-787.

90. Xiao, Y.; Pavlov, V.; Niazov, T.; Dishon, A.; Kotler, M.; Willner, I., Catalytic beacons for the detection of dna and telomerase activity. *J. Am. Chem. Soc.* **2004,** *126,* 7430-7431.

91. Shao, C.; Lu, N.; Sun, D., A G-quadruplex/hemin complex with switchable peroxidase activity by DNA hybridization. *Chin. J. Chem .* **2012,** *30,* 1575-1581.

92. Childs, R. E.; Bardsley, W. G., The steady-state kinetics of peroxidase with 2,2'-azino-di-(3-ethyl-benzthiazoline-6-sulphonic acid) as chromogen. *Biochem. J* **1975,** *145,* 93-103.

93. Zhang, L.; Zhu, J.; Li, T.; Wang, E., Bifunctional colorimetric oligonucleotide probe based on a G-quadruplex dnazyme molecular beacon. *Anal. Chem.* **2011,** *83,* 8871-8876.

94. Ditmangklo, B.; Muangkaew, P.; Supabowornsathit, K.; Vilaivan, T., Synthesis of Pyrrolidinyl PNA and its site-specific labeling at internal positions by click chemistry. In *Peptide Nucleic Acids: Methods and Protocols*, Nielsen, P. E., Ed. Springer US: New York, NY, 2020; pp 35-60.

95. Vilaivan, C.; Srisuwannaket, C.; Ananthanawat, C.; Suparpprom, C.; Kawakami, J.; Yamaguchi, Y.; Tanaka, Y.; Vilaivan, T., Pyrrolidinyl peptide nucleic acid with α/β-peptide backbone: a conformationally constrained pna with unusual hybridization properties. *Artif DNA PNA XNA* **2011,** *2,* 50-59.

96. Lowe, G.; Vilaivan, T., Dipeptides bearing nucleobases for the synthesis of novel peptide nucleic acids. *J. Chem. Soc., Perkin Trans. 1* **1997**, 547-554.

97. Uttamapinant, C.; Tangpeerachaikul, A.; Grecian, S.; Clarke, S.; Singh, U.; Slade, P.; Gee, K. R.; Ting, A. Y., Fast, cell-compatible click chemistry with copper-chelating azides for biomolecular labeling. *Angew. Chem. Int. Ed.* **2012,** *51,* 5852-5856.

98. Ditmangklo, B.; Boonlua, C.; Suparpprom, C.; Vilaivan, T., Reductive alkylation and sequential reductive alkylation-click chemistry for on-solid-support modification of pyrrolidinyl peptide nucleic acid. *Bioconjugate Chem.* **2013,** *24,* 614-625.

99. Presolski, S. I.; Hong, V. P.; Finn, M. G., Copper-catalyzed azide-alkyne click chemistry for bioconjugation. *Curr Protoc Chem Biol* **2011,** *3,* 153-162.

100. Zanardi, C.; Terzi, F.; Seeber, R.; Baldoli, C.; Licandro, E.; Maiorana, S., Peptide nucleic acids tagged with four lysine residues for amperometric genosensors. *Artif. DNA*

2012, *3,* 80-87.

101.   Ray, S. C., Chapter 1 - Application and Uses of Graphene. In *applications of graphene and graphene-oxide based nanomaterials*, Ray, S. C., Ed. William Andrew Publishing: Oxford, 2015; pp 1-38.

102.   He, S.; Song, B.; Li, D.; Zhu, C.; Qi, W.; Wen, Y.; Wang, L.; Song, S.; Fang, H.; Fan, C., A graphene nanoprobe for rapid, sensitive, and multicolor fluorescent DNA analysis. *Adv. Funct. Mater.* **2010,** *20,* 453-459.

103.   Zhang, H.; Zhang, H.; Aldalbahi, A.; Zuo, X.; Fan, C.; Mi, X., Fluorescent biosensors enabled by graphene and graphene oxide. *Biosens. Bioelectron.* **2017,** *89,* 96-106.

104.   Li, F.; Huang, Y.; Yang, Q.; Zhong, Z.; Li, D.; Wang, L.; Song, S.; Fan, C., A graphene-enhanced molecular beacon for homogeneous DNA detection. *Nanoscale* **2010,** *2,* 1021-1026.

105.   Yi, J. W.; Park, J.; Singh, N. J.; Lee, I. J.; Kim, K. S.; Kim, B. H., Quencher-free molecular beacon: enhancement of the signal-to-background ratio with graphene oxide. *Bioorg. Med. Chem. Lett.* **2011,** *21,* 704-706.

106.   Zhao, X.-H.; Ma, Q.-J.; Wu, X.-X.; Zhu, X., Graphene oxide-based biosensor for sensitive fluorescence detection of DNA based on exonuclease III-aided signal amplification. *Anal. Chim. Acta* **2012,** *727,* 67-70.

107.   Hong, C.; Baek, A.; Hah, S. S.; Jung, W.; Kim, D.-E., Fluorometric Detection of MicroRNA Using Isothermal Gene Amplification and Graphene Oxide. *Anal. Chem.* **2016,** *88,* 2999-3003.

108.   Baek, A.; Baek, Y. M.; Kim, H.-M.; Jun, B.-H.; Kim, D.-E., Polyethylene glycol-engrafted graphene oxide as biocompatible materials for peptide nucleic acid delivery into cells. *Bioconjugate Chem.* **2018,** *29,* 528-537.

109.   Lee, J.; Park, I.-S.; Jung, E.; Lee, Y.; Min, D.-H., Direct, sequence-specific detection of dsDNA based on peptide nucleic acid and graphene oxide without requiring denaturation. *Biosens. Bioelectron.* **2014,** *62,* 140-144.

110.   Sabale, P. M.; George, J. T.; Srivatsan, S. G., A base-modified PNA–graphene oxide platform as a turn-on fluorescence sensor for the detection of human telomeric repeats. *Nanoscale* **2014,** *6,* 10460-10469.

111. Hwang, D. W.; Choi, Y.; Kim, D.; Park, H. Y.; Kim, K. W.; Kim, M. Y.; Park, C.-K.; Lee, D. S., Graphene oxide-quenching-based fluorescence in situ hybridization (G-FISH) to detect RNA in tissue: Simple and fast tissue RNA diagnostics. *Nanomedicine* **2019,** *16*, 162-172.

112. Deligeorgiev, T.; Vasilev, A.; Kaloyanova, S.; Vaquero, J. J., Styryl dyes – synthesis and applications during the last 15 years. *Color. Technol.* **2010,** *126*, 55-80.

113. Kovalska, V. B.; Kryvorotenko, D. V.; Balanda, A. O.; Losytskyy, M. Y.; Tokar, V. P.; Yarmoluk, S. M., Fluorescent homodimer styrylcyanines: synthesis and spectral-luminescent studies in nucleic acids and protein complexes. *Dyes Pigm.* **2005,** *67*, 47-54.

114. Liu, Y.; Liu, C.-y.; Liu, Y., Investigation on fluorescence quenching of dyes by graphite oxide and graphene. *Appl. Surf. Sci.* **2011,** *257*, 5513-5518.

115. Peffer, N. J.; Hanvey, J. C.; Bisi, J. E.; Thomson, S. A.; Hassman, C. F.; Noble, S. A.; Babiss, L. E., Strand-invasion of duplex DNA by peptide nucleic acid oligomers. *Proc. Natl. Acad. Sci.* **1993,** *90*, 10648.

116. Rapireddy, S.; He, G.; Roy, S.; Armitage, B. A.; Ly, D. H., Strand invasion of mixed-sequence B-DNA by Acridine-Linked, γ-peptide nucleic acid (γ-PNA). *J. Am. Chem. Soc.* **2007,** *129*, 15596-15600.

117. Demidov, V. V.; Protozanova, E.; Izvolsky, K. I.; Price, C.; Nielsen, P. E.; Frank-Kamenetskii, M. D., Kinetics and mechanism of the DNA double helix invasion by pseudocomplementary peptide nucleic acids. *Proc. Natl. Acad. Sci. U. S. A.* **2002,** *99*, 5953-5958.

118. Lohse, J.; Dahl, O.; Nielsen, P. E., Double duplex invasion by peptide nucleic acid: a general principle for sequence-specific targeting of double-stranded DNA. *Proc. Natl. Acad. Sci. U. S. A.* **1999,** *96*, 11804-11808.

119. Mao, H.; Luo, G.; Zhan, Y.; Zhang, J.; Yao, S.; Yu, Y., The mechanism and regularity of quenching the effect of bases on fluorophores: the base-quenched probe method. *Analyst* **2018,** *143*, 3292-3301.

120. Zhang, Y.; Tian, J.; Li, H.; Wang, L.; Sun, X., A novel single fluorophore-labeled double-stranded oligonucleotide probe for fluorescence-enhanced nucleic acid detection based on the inherent quenching ability of deoxyguanosine bases and

competitive strand-displacement reaction. *J. Fluoresc.* **2012,** *22*, 43-46.

121.   Thapa, B.; Schlegel, H. B., Calculations of pKa's and redox potentials of nucleobases with explicit waters and polarizable continuum solvation. *J. Phys. Chem. A* **2015,** *119*, 5134-5144.

122.   Paramasivan, S.; Rujan, I.; Bolton, P. H., Circular dichroism of quadruplex DNAs: Applications to structure, cation effects and ligand binding. *Methods* **2007,** *43*, 324-331.

123.   Carvalho, J.; Queiroz, J. A.; Cruz, C., Circular dichroism of G-Quadruplex: a laboratory experiment for the study of topology and ligand binding. *J. Chem. Educ.* **2017,** *94*, 1547-1551.

124.   Park, J. S.; Goo, N.-I.; Kim, D.-E., Mechanism of DNA adsorption and desorption on graphene oxide. *Langmuir* **2014,** *30*, 12587-12595.

125.   Lu, C.; Huang, P.-J. J.; Liu, B.; Ying, Y.; Liu, J., Comparison of graphene oxide and reduced graphene oxide for DNA adsorption and sensing. *Langmuir* **2016,** *32*, 10776-10783.

126.   Tang, W.; Zhou, H.; Li, W., Silver and cyanine staining of oligonucleotides in polyacrylamide gel. *PLoS One* **2015,** *10*, e0144422.

127.   Habl, G.; Böhm, H.; Marmé, N.; Knemeyer, J.-P., A new assay for single nucleotide polymorphism analysis based on displacement reactions in PNA–DNA double helices. *Int. J. Environ. Anal. Chem.* **2005,** *85*, 613-623.

128.   Zeng, P.; Hou, P.; Jing, C. J.; Huang, C. Z., Highly sensitive detection of hepatitis C virus DNA by using a one-donor-four-acceptors FRET probe. *Talanta* **2018,** *185*, 118-122.

129.   Balaji, A.; Yang, S.; Wang, J.; Zhang, J., Graphene oxide-based nanostructured DNA sensor. *Biosensors* **2019,** *9*, 74.

130.   Liu, Q.; Pu, Z.; Asiri, A. M.; Al-Youbi, A. O.; Sun, X., Polydopamine nanospheres: A biopolymer-based fluorescent sensing platform for DNA detection. *Sens. Actuators, B* **2014,** *191*, 567-571.

131.   Xie, W. Y.; Huang, W. T.; Li, N. B.; Luo, H. Q., Silver(i) ions and cysteine detection based on photoinduced electron transfer mediated by cytosine–Ag+–cytosine base pairs. *Analyst* **2011,** *136*, 4130-4133.

132.   Zhao, C.; Qu, K.; Song, Y.; Xu, C.; Ren, J.; Qu, X., A reusable dna single-walled

carbon-nanotube-based fluorescent sensor for highly sensitive and selective detection of Ag$^+$ and cysteine in aqueous solutions. *Chem. - Eur. J.* **2010,** *16,* 8147-8154.

133. Tiarpattaradilok, D. The detection of small molecule target by styryl dye and aptamer. Senior project, Chulalongkorn University, 2018.

134. Peng, X.; Li, H.; Seidman, M., A Template-mediated click-click reaction: PNA-DNA, PNA-PNA (or Peptide) ligation, and single nucleotide discrimination. *Eur. J. Org. Chem.* **2010**, 4194.

135. Ficht, S.; Mattes, A.; Seitz, O., Single-nucleotide-specific PNA-peptide ligation on synthetic and PCR DNA templates. *J. Am. Chem. Soc.* **2004,** *126,* 9970-9981.

136. Dose, C.; Seitz, O., Single nucleotide specific detection of DNA by native chemical ligation of fluorescence labeled PNA-probes. *Bioorg. Med. Chem.* **2008,** *16,* 65-77.

137. Hong, V.; Presolski, S. I.; Ma, C.; Finn, M. G., Analysis and optimization of copper-catalyzed azide-alkyne cycloaddition for bioconjugation. *Angew. Chem. Int. Ed.* **2009,** *48,* 9879-9883.

138. Liu, Y.; Lai, P.; Wang, J.; Xing, X.; Xu, L., A superior G-quadruplex DNAzyme through functionalized modification of the hemin cofactor. *Chem. Commun.* **2020,** *56,* 2427-2430.

139. Zhang, L.-M.; Cui, Y.-X.; Zhu, L.-N.; Chu, J.-Q.; Kong, D.-M., Cationic porphyrins with large side arm substituents as resonance light scattering ratiometric probes for specific recognition of nucleic acid G-quadruplexes. *Nucleic Acids Res.* **2019,** *47,* 2727-2738.

140. Wang, S.; Fu, B.; Wang, J.; Long, Y.; Zhang, X.; Peng, S.; Guo, P.; Tian, T.; Zhou, X., Novel amplex red oxidases based on noncanonical DNA structures: property studies and applications in microrna detection. *Anal. Chem.* **2014,** *86,* 2925-2930.

141. Josephy, P. D.; Eling, T.; Mason, R. P., The horseradish peroxidase-catalyzed oxidation of 3,5,3',5'-tetramethylbenzidine. free radical and charge-transfer complex intermediates. *J. Biol. Chem.* **1982,** *257,* 3669.

VITA

NAME   MR. CHAYAN CHAROENPAKDEE

DATE OF BIRTH   30 October 1990

PLACE OF BIRTH   Songkhla, Thailand

INSTITUTIONS ATTENDED   Bachelor's Degree of Science (Chemistry) in 2012

PUBLICATION

1. Yotapan, N.; Charoenpakdee, C.; Wathanathavorn, P.; Ditmangklo, B.; Wagenknecht, H.-A.; Vilaivan, T., Synthesis and optical properties of pyrrolidinyl peptide nucleic acid carrying a clicked Nile red label. Beilstein J Org Chem 2014, 10, 2166-2174.

2. Boonlua, C.; Charoenpakdee, C.; Vilaivan, T.; Praneenararat, T., Preparation and Performance Evaluation of a Pyrrolidinyl Peptide Nucleic-Acid-Based Displacement Probe as a DNA Sensor. ChemistrySelect 2016, 1, 5691-5697.

3. Suraritdechachai, S.; Charoenpakdee, C.; Young, I.; Maher, S.; Vilaivan, T.; Praneenararat, T., Rapid Detection of the Antibiotic Sulfamethazine in Pig Body Fluids by Paper Spray Mass Spectrometry. J. Agric. Food Chem. 2019, 67, 3055-3061.

4. Charoenpakdee, C.; Vilaivan, T. Quenching of fluorescently labeled pyrrolidinyl peptide nucleic acid by oligodeoxyguanosine and its application in DNA sensing. Org. Biomol. Chem., 2020,18, 5951-5962.